Determination of Mechanical Properties of Individual Living Cells

Marjan Molavi Zarandi

A Thesis

in

The Department

of

Mechanical and Industrial Engineering

Presented in Partial Fulfillment of the Requirements for
the Degree of Master of Applied Science (Mechanical Engineering) at
Concordia University
Montreal, Quebec, Canada

December 2007

Your file Votre référence
ISBN: 978-0-494-40915-2
Our file Notre référence
ISBN: 978-0-494-40915-2

ABSTRACT

Determination of Mechanical Properties of Individual Living Cells

Marjan Molavi Zarandi

In this thesis, a finite element and experimental modal analysis are employed to determine the mechanical properties of the living cells. Because the determination of mechanical properties of the living cells and particularly the natural frequencies are highly important to diagnose the health condition of cells, a comprehensive analysis is carried out to determine the natural frequencies of individual cells. Since many cells have a spherical shape, a spherical shape of the cell is considered for this analysis. The natural frequencies and corresponding mode shapes are determined for specific type of cell whose elastic properties of cell have been measured experimentally. To validate the numerical analysis, an experimental set up is designed to measure the natural frequencies of some scaled up models of cell. In parallel, the numerical method that was used for cell modal analysis is employed to determine the natural frequencies of scaled up models of cell to show the agreement between the finite element and experimental analyses. For then, the FEA model is extrapolated to the biological cell. The results obtained from the finite element modal analysis of cell are compared to the latest reports available on the values of natural frequencies of cell.

This thesis is dedicated to my parents for their love and to Ali for his endless supports and encouragements.

ACKNOWLEDGEMENTS

It is the most pleasant task where I have the opportunity to express my gratitude to all the people who have helped me in the path to a Master's degree.

I am deeply indebted to my supervisors, Professor Ion Stiharu and Professor Javad Dargahi for their invaluable supports. I could not have imagined having a better advisors and mentors for my Master and without their common sense, knowledge and perceptiveness, I would never have finished.

I would like to express my special and sincere thanks to my colleague at Concordia University, Dr. Ali Bonakdar for his assistance and friendly support during the length of my research work. In addition, I am thankful to Dr. Gino Rinaldi and Mr. Henry Szczawinski for their assistance during my experiments.

Finally, I would like to express my sincerest gratitude, love to my parents and my family for their continuous motivation and emotional support. I would like to thank my mother Mrs. Batool Hadizadeh and my father Mr. Abdolhamid Molavi Zarandi who taught me the value of patience, hard work and commitment without which I could not have completed my Master. I am thankful to my sisters Maryam and Mahsa for their love and being a great source of motivation and inspiration during my education.

TABLE OF CONTENTS

LIST OF FIGURES

LIST OF TABLES

LIST OF SYMBOLS

a	Inner radius of shell
a	Inner shell radius
α^2	Thickness parameter, is defined by $h^2/12a^2$
Ω	Dimensionless frequency, is defined by $\omega a/c$
α_n	Rate of their decay
λ	Constant, is defined by $\lambda = n(n+1)$
Ω_n	Frequency of oscillations
$j_n(\Omega)$	Spherical Bessel function of the first kind,
E	Young's modulus
h	Shell thickness
s	Speed ratio, is defined by c/c_s
c_s	Apparent wave speed in the shell
T	Kinetic energy of the fluid filled shell

t	Time
u	Meridional displacement
V	Potential energy of the fluid filled shell
w	Radial displacement
ν	Poisson's ratio

Chapter 1 - Introduction and literature review

1.1. Mechanics applied to biology

Biomechanics is referred to the mechanics of biological entities. A variety of biological processes involve mechanical phenomena like tension, compression, fracture, impact, bending and others, which ultimately effects on complex functions performed by organisms and biological materials. Biomechanics help us to understand the connection between the mechanical factors associated with these biological entities and the functions, which are performed by them.

Each living organism has a specific function and the performance is governed by a vast spectrum of biomechanical and biochemical processes. Proteins, cells, tissues, organs and organisms, are all based on the use of such processes to achieve the desired task. Locomotion in organisms is done with the help of alternate expansion and contraction of the cell membrane. Pumping function performed by the heart maintains the essential blood flow inside an organism. Mechanical strength of the tendons and ligament tissues is a key issue for trouble-free movement of joints. A fine force balance between the intracellular and extra cellular materials helps in cell shape regulation and signaling [1]. These and many such examples reveal the mechanical factors involved in biological functions. Proper functioning of these biological elements makes sure that the organism possesses adequate health condition, whereas their malfunctioning yields to risks to diseases or may lead to death. Since biological functions are governed by the mechanical properties of biological entities, it can be assumed that mechanical properties of these

entities, in turn, provide information about the health of the organism. Detailed understanding of mechanical properties of biological samples can thus provide insight into the causes of the diseases and possibly their remedies.

1.2. Measuring mechanical properties of biological samples

The mechanical behavior of biological materials has been studied extensively at the tissue, organ and systems levels. Emerging experimental tools, however, enable quantitative studies of deformation of individual cells and biomolecules.

Fundamental understanding of the basic cellular processes, and of the pathological responses of the cell, will be facilitated greatly by developments in the fields of cell and molecular biomechanics. Despite the sophistication of experimental and computational approaches in cell and molecular biology, the mechanisms by which cells sense and respond to mechanical stimuli are still poorly understood. Largely, the complicated coupling between the biochemical and mechanical processes of the cell needs further research efforts. Application of external mechanical stimuli can induce biochemical reactions and changes in chemical stimuli, temperature, and bimolecular activity, can alter the structure and mechanical integrity of the cell, even in the absence of mechanical stimuli[8].

In contrast with most material systems, the mechanical behavior of a living cell can not be characterized simply in terms of fixed properties, as the cell structure is a dynamic system that adapts to its local mechanochemical environment. Understanding the

relationships among extra cellular environment and intracellular structure and function, however, requires quantification of these closely coupled fields. To that end, researchers from such diverse disciplines as molecular biology, biophysics, materials science, chemical, mechanical and biomedical engineering have developed an impressive array of experimental tools that can measure and impose forces as small as a few fN (10^{-15} N) and displacements as small as a few Angstroms ($10^{-10}\,m$)[8].

Experimental tools are reviewed with the aim to identify opportunities and challenges in the field of experimental micro- and nano-mechanics of biological materials. There exist a variety of techniques to manipulate the mechanical aspects of individual living cells and individual biomolecules. Techniques in experimental mechanobiology, although varied, fall into two broad categories - passive characterization and active stimulation [2].

Passive characterization techniques are used to determine mechanical properties of the cellular structure while active stimulation seeks to apply mechanical forces and observe the biological response of the cell.

Passive characterization includes techniques such as micropipette aspiration, atomic force microscopy (AFM), laser optical trapping and magnetic bead measurement [2]. Membrane-based stretching, flow-induced shear stress and substrate stiffness are techniques belong to the active stimulation techniques [2].

1.2.1. Passive characterization techniques

Passive techniques for characterization of cells are described in the following subsections.

1.2.1.1. Micropipette aspiration

In micropipette aspiration, a glass pipette with an internal diameter of 1-10 μm is used to deform a cell. The micropipette is manipulated in the cell growth medium such that it is very close to the cell being studied. A vacuum is then applied through the micropipette to the cell that is partially aspirated into the micropipette, as shown in Figure1.1. The aspiration length varies with the applied pressure. The aspiration length is used to calculate the rigidity of the cellular membrane and cytoskeleton. This technique can be used to characterize both adherent and non-adherent cells [4]. Through application of a chosen viscoelastic model for the cell membrane, micropipette aspiration-induced deformation is used to calculate elastic modulus E, apparent viscosity μ for the cell membrane.

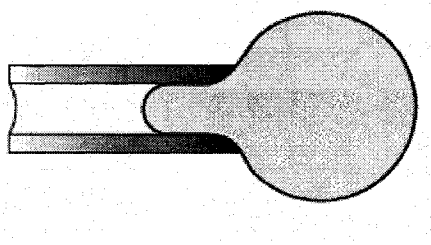

Figure 1.1 -- Micropipette aspiration for single cell [3]

With this method, experiments have been developed to measure the viscoelastic behavior of the cell. Cell is flown and deform in narrow channels during physiological function, including erythrocytes (red blood cells), and endothelial and neutrophils cells (two types of white blood cells) [5, 6, 7].

It is clear that micropipette aspiration is a useful approach for cell types that undergo large, general deformation that contributes critically to cell and/or tissue function. Although the applied stress state is relatively complex and based largely on fluid mechanics. Approximations have been used to extract the mechanical and functional characteristics of the cell deformed by micropipette aspiration.

1.2.1.2. Atomic force microscopy (AFM)

Due to the capacity of AFM to produce forces in nano-Newtons and measure displacements in nano-meters, it can be used to study micron level biological samples like cells, proteins and DNAs.

In AFM, an indenter attached to the free end of a cantilever beam is used. As the sample presses against the indenter tip, the cantilever beam deflects by an amount proportional to the force applied.

Imaging of a surface with AFM involves a micro fabricated cantilever beam with a very small tip with contact area of only a few square nanometers. That tip moves above the surface of a sample (see Figure 1.2).

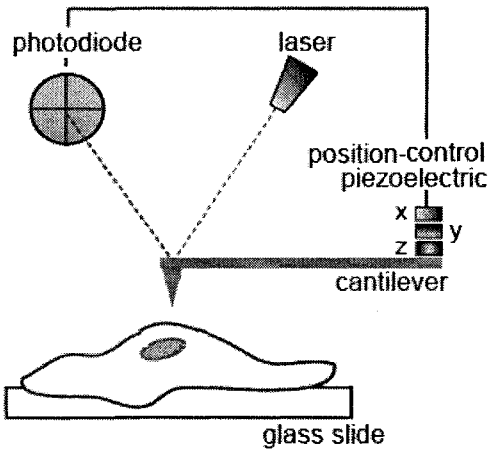

Figure1. 2 -- Schematic of atomic force microscope (AFM) [8]

The movement of the cantilever is controlled by a x, y, z-piezoelectric ceramic actuator that moves the cantilever, and a laser beam that is reflected off the back of the cantilever onto a photodiode that measures the cantilever deflection. A feedback loop linking the current applies the piezo and the detector enables precise control of the positioning of the cantilever and the force applied to the sample [9, 10].

A complete explanation of the basic working principle of an AFM can be found in the original work, have been done by Binnig and Quate [11].

The application of AFM for studying soft biological materials is reviewed by Radmacher et. al [12] and Bowen et. al [13]. In all the indentation techniques, the experimental data have to be processed in order to understand the properties of the specimen. Several different modes of operation have been developed for AFM and have been reviewed by Radmacher et. al [14]. Horton et. al and Lehenkari et. al [15, 16] have studied single

ligand-receptor binding forces by using AFM. In recent years, AFM has been increasingly used to deal with problems of biomedical applications. In another investigation, Pesen et. al have determined the material properties of endothelial cortex cells by AFM [17].

In another assessment, Lehenkari et. al [18] has determined the material properties of biological cell using AFM. Investigating the mechanical properties of biological materials has been used continuously to measuring the elastic properties of biological samples [19- 25]. AFM has the advantage of being able to operate in air and fluid under physiological conditions, which has allowed biologically relevant, force spectroscopy studies of single biomolecules [26] and a wide range of applications in cell biology, such as studying cell-surface morphology [27].

AFM has been used to study the mechanical properties of cells and organelles [28, 29] and cell-matrix or cell-cell interaction forces [30, 31].

Further, AFM has been used to determine the natural frequency if living cells. Andrew E. Pelling et. al [32] demonstrated that the cell wall of living Saccharomyces Cerevisiae (baker's yeast cell) exhibits local temperature-dependent nanomechanical motion at characteristic frequencies.

1.2.1.3. Laser optical trapping

Laser traps or laser tweezers, also commonly known as optical traps or optical tweezers, are finding widespread applications in the study of mechanical deformation of biological

cells and molecules. The instrument known as 'optical tweezers' makes use of laser to create a potential well, capable of trapping small objects within a defined region. Particles can be attached to the cellular membrane and be manipulated laterally across the substrate surface. The laser power required to constrain the particle is directly proportional to the forces being applied to that particle by the cell [8].

In this way, the stiffness of the cell can be measured. Recently, Guck et. al [33] developed an innovative technique, in which dual optical tweezers stretch the entire cell. A schematic of optical tweezers is shown in Figure 1.3.

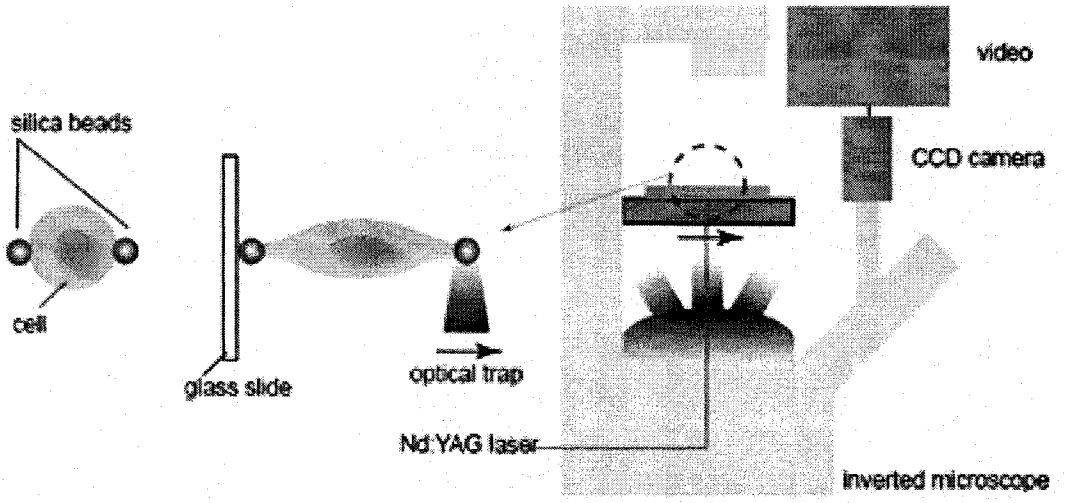

Figure1. 3 -- Schematic showing optical tweezers [8]

1.2.1.4. Magnetic bead measurement

In this technique, a 4-5 μm diameter paramagnetic bead is bound to a live cell. This is one by coating the bead with an extracellular matrix protein or an antibody, which then binds

to receptors or other proteins on the cell membrane. An external magnetic field is applied to twist the bead (magnetic bead twisting cytometry), or to apply a displacement to the bead (magnetic bead microrheometry). This is usually done under an optical microscope to observe displacements of the beads [34]. In a single cell, the observed displacement can be used to characterize cellular mechanical properties. Additionally, because beads can be bound to specific cell surface proteins, the biological response induced by tugging on these proteins can be studied with this technique.

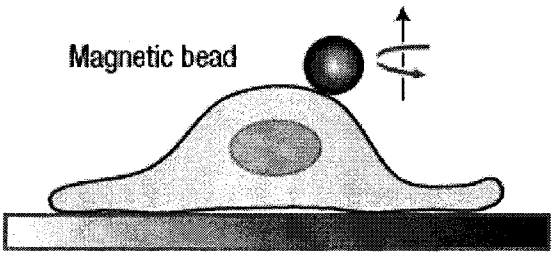

Figure 1.4 -- Magnetic twisting cytometry (MTC) [3]

1.2.2. Active stimulation techniques

Active techniques for characterization of cells are described in the following subsections.

1.2.2.1. Membrane-based stretching

In membrane-based stretching methods, cells are grown on a flexible substrate. The substrate is cyclically deformed in some manner. Each of the focal contact points stretches the cells, which is bound to the substrate.

There are two types of stress fields, which are currently used for testing cellular response. One is uniaxial stretching, in which the cells are stretched longitudinally [8]. This is conducted either by stretching an elastomeric substrate in one direction, or by flexing the substrate to create a tensile strain on the convex side. The other type of stress field is biaxial stretching, in which the outer edges of a circular membrane are constrained, and a pressure differential is applied across the membrane [35].

1.2.2.2. Flow-induced shear stress

In vivo and in the real condition, fluid flow applies shear stress to cells in several situations. For example, the blood flow shear forces on the endothelial cells that line blood vessels. Because of their physiological relevance, experiments aimed at determining the biological effects of flow-induced shear stress on cells are particularly useful. There are a large number of experimental devices applying various kinds of fluid flow to cells. Flow can be unsteady or steady, and flow chamber geometries are designed to create flow disturbances that simulate complex flow profiles in the vasculature [36]. Microfluidic devices have recently received much attention in this area, due to their ability to apply precise uniform stresses across a specified region. Such microfluidic devices can be used to determine the effect of applied shear on protein expression, or to determine adhesion strength between cells and the substrate [37, 38].

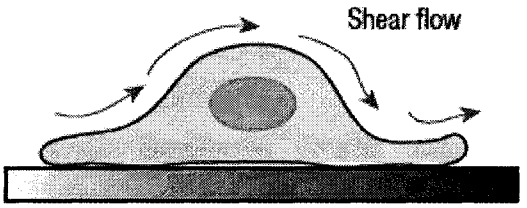

Figure 1.5 -- Flow-induced shear stress [3]

1.2.2.3. Substrate stretching

Cells are exquisitely sensitive to the stiffness of the substrate to which they are attached. Adherent cells sense the local elasticity of their matrix by pulling on the substrate via cytoskeleton-based contraction. These forces are tuned by the cell to balance the resistance provided by the substrate. To a certain limit, it appears as though the cell attempts to match its stiffness with that of the underlying substrate by altering the organization of its cytoskeleton [39].

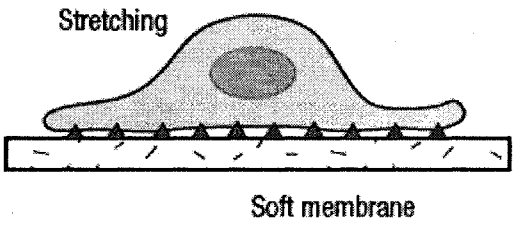

Figure 1.6 -- Substrate stretching [3]

1.3. Introduction to cell oscillation

In some diseases, the mechanical properties of individual cells are altered. In blood cells, changes in cell mechanical properties can have profound effects on the cell's ability to normally flow through the blood vessels, since increased stiffness impedes progress of cells through small capillaries [40]. Actually, changing the stiffness of cells changes the natural frequencies of cells.

Ackerman [41] investigated the question of resonance in mechanical oscillations of cells. Ackerman found out the resonance frequencies of the red blood cells by modeling the cells as spherical, isotropic elastic shells filled with and surrounded by viscous fluids [41, 42].

Natural frequencies of biological cells based the elasticity properties of cellular materials were subsequently developed by P.V. Zinin et. al [43]. The results obtained by P.V. Zinin et. al has complex forms and only simple approximations were obtained for red blood cells (RBC).

Following this observations P. V. Zinin et. al [44] have modeled and numerically analyzed the spectra of the natural oscillations of different types of bacteria.

Later investigation on the mechanical properties of cell lead to the cell walls vibration by Andrew E. Pelling et. al [45]. They have detected the vibrations of the cells with an atomic force microscope. The instrument, used to analyze this structure, was a microscopic cantilever with a down-pointing needle sharpened to just a few atoms wide.

They placed the cantilever in contact with yeast cell. The tip of the cantilever is rejected by atomic force created between the tip of the cantilever and the atoms on the surface of the cell. By using this method, it has been measured distinct periodic nanomechanical motion of yeast cells. The periodic motions in the range of 0.8 to 1.6 *kHz* with amplitudes of 1-7 *nm* have been reported by Andrew E. Pelling et. al [45] using a very low stiffness cantilever with atomic force microscope.

Amirouche et. al [46] at the biomechanic and research laboratory at university of Illinois have modeled a spherical cell using finite element method (FEM). The cell model is composed of two structural elements: cytoplasm and nucleus and material properties are assumed continuous, homogeneous, incompressible, isotropic, and hyperelastic. The natural frequencies of cell for this approach have been reported from 16.199 to 60.962 *Hz* respectively.

1.4. Oscillations of fluid filled elastic spheres

Free oscillations of spheres have been the area of interest for a long time. Lamb [47] has obtained the equations governing the free vibration of the solid sphere and Chree [48] subsequently obtained these equations rather than in Cartesian co-ordinates in the more convenient spherical co-ordinates. More recently, Sato and Usami have studied the vibrations of solid spheres and provided extensive numerical results [49, 50].

Jiang et. al have studied the free vibration behavior of multi-layered hollow spheres and provided tabular results for a number of cases [51]. Lampwood and Usami [52] also have treat solid and hollow spheres in the book on oscillations of the Earth.

Engin has developed a model of the human head consisting of a spherical shell filled with in viscid fluid using a thin-shell theory [53]. Advani and Lee have investigated the vibration of a fluid-filled shell [54]. Free vibration spectra and mode shapes have obtained based on moderate thick shell theory. They have reported the value of 1200 *Hz* for the first resonance frequency for human head while it was experimentally determined in the range from 650-900 *Hz*. More recently, Guarino and Elgar [55] have looked at the frequency spectra of a fluid-filled sphere, both with and without a central solid sphere [55]. Mode shapes of elastic fluid filled sphere that were proposed by Grarino and Elger are shown in Figure 1.7 to 1.10.

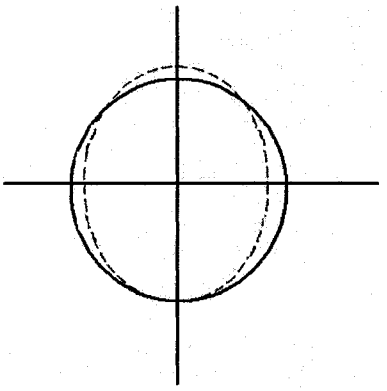

Figure 1.7 -- Mode shapes of elastic spherical shell, first mode [55]

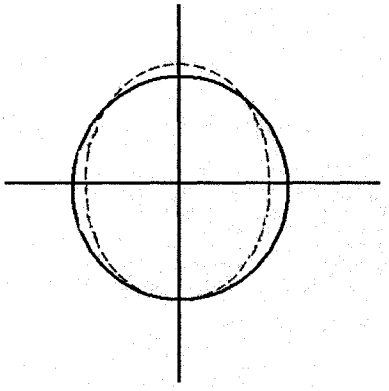

Figure 1.8 -- Mode shapes of elastic spherical shell, second mode [55]

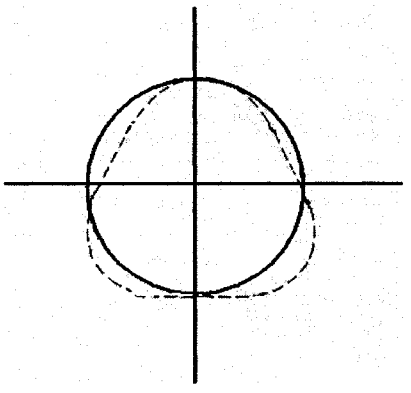

Figure 1.9 -- Mode shapes of elastic spherical shell, third mode [55]

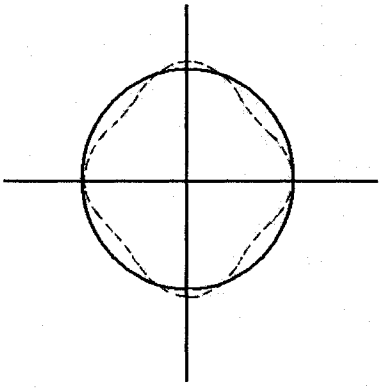

Figure 1.10 -- Mode shapes of elastic spherical shell, forth mode [55]

For the head impact modeling, the multi-layered spherical shells with liquid core of relevance to head impact has been modeled by Young [56]. He found the free vibration of spheres composed of inviscid compressible liquid cores surrounded by spherical layers. Spheroidal modes of vibration of spheres composed of inviscid compressible liquid cores surrounded by spherical layers of elastic fluid filled sphere were proposed by Young are shown in Figure 1.11.

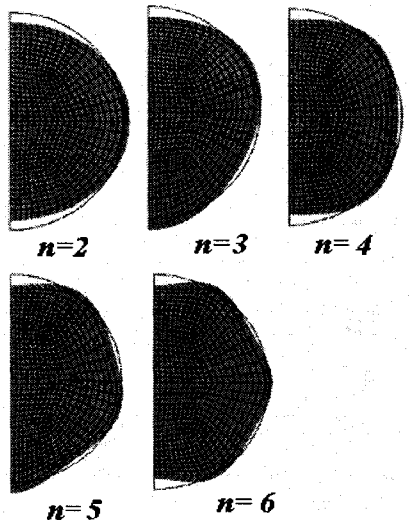

Figure 1.11 -- Mode shapes for the n=2 to n= 6 spheroidal modes of vibration for a fluid-filled sphere [56].

1.5. Objective and scope of this research

For a specific cell, different reports on elastic modulus and particularly natural frequencies raised serious questions, which motivated the following research. The aim of this research is to determine the natural frequency of spherical cells. To this end, a comprehensive finite element along with an experimental analysis on the scaled up models of cell is carried out and then the FEA is extrapolated to the biological cell and the results are compared with the results obtained form literatures.

1.6. Thesis overview

The thesis is organized in six chapters. Chapter one gives an overview of variety of techniques to manipulate the mechanical aspects of individual living cells and individual biomolecules, various contributions by different people in the field of characterizing various kinds of cells, attempts on obtaining natural frequencies of spherical shells and some investigations on natural frequencies of micro scale cells numerically and experimentally.

Chapter two gives an overview of cell biology, cell kingdoms and structural parts of cell.

In Chapter three, a specific spherical cell with various mechanical properties is described. Three-dimensional model of cell for characterization in this thesis is introduced.

In Chapter four, three-dimensional finite element modal analysis for empty and fluid filled spherical cells are carried out using ANSYS and COMSOL (FEMLAB) and the results are compared.

In Chapter five, to fine-tuning the results obtained form FEA, some scaled up models of cell are considered for modal analysis using both FEA and experimental methods.

Numerous figures, plots, and Tables substantiate the results wherever required. Finally, some concluding remarks and suggestions for future works to follow.

Chapter 2 - Introduction to cells and models of living cells

2.1. Introduction

Cell is a fantastic representation of biology. It literally encapsulates life in its elemental form. By understanding the components of a cell, one is able to discern and decipher many of the complexities of living organisms. Each component of a cell has larger-scale counterparts, which can be examined in multi-cellular organisms such as humans.

The number of cells in the human body is literally astronomical, about three orders of magnitude more than the number of stars in the Milky Way. Yet, for their immense number, the variety of cells is much smaller: only about 200 different cell types are represented in the collection of about 10^{14} cells that make up our bodies [57]. These cells have diverse capabilities and, superficially, have remarkably different shapes.

Some cells, like certain varieties of bacteria, are not much more than inflated bags, shaped like the hot-air or gas balloons invented more than two centuries ago. Others, such as nerve cells, may have branched structures at each end connected by an arm that is more than a thousand times long as it is wide. The basic structural elements of most cells, however, are the same: fluid sheets enclose the cell and its compartments, while networks of filaments maintain the cell's shape and help organize its contents [57].

The operative length of scale of the cell is the micron, a millionth of a meter. The smallest cells are a third of a micron in diameter while the largest ones maybe more than hundred micron across.

2.2. Different types of cells

There are two main groups of cells, prokaryotic and eukaryotic cells. Prokaryote cells do not have a membrane-bound nucleus while eukaryotic cells can be easily distinguished through a membrane-bound nucleus. The difference in cells is in their appearance and their structure, reproduction, and metabolism. All of the cells belong to one of the five life kingdoms. The greatest difference lies between cells of different kingdoms. There are five kingdoms for the cells. The following figure shows the five kingdoms: Monera, Protista, Plantae, Fungi and Animalia [58].

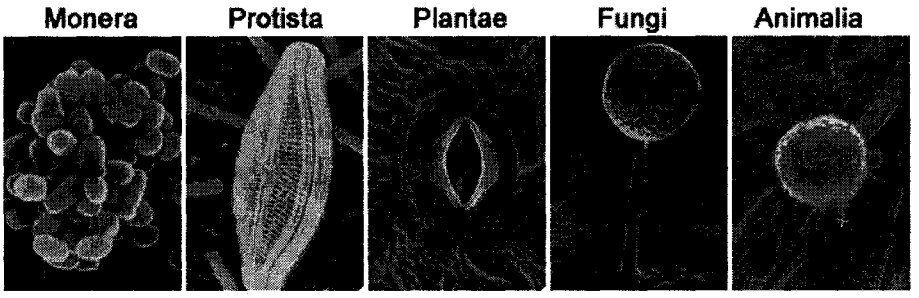

Figure 2.1 -- Five kingdoms of cells [59]

2.2.1. Kingdom Monera

This kingdom consists entirely of the bacteria - very small one-celled organisms. Thousand bacteria can sit side by side in just one tiny millimeter. Despite their small size, bacteria are the most abundant of any organism on Earth. They can be found in the air, soil, water and inside the body. In fact, there are more bacterial cells inside the body and on the skin than there are cells in entire body [60]. The cells of all bacteria, Monerans are

from prokaryotic, the simplest and most ancient type of the cell types. Bacteria often get a bad reputation because certain types are responsible for causing a variety of illnesses, including many types of food poisoning. However, most bacteria are completely harmless and many even perform beneficial functions, such as turning milk into yogurt or cheese and helping scientists produce drugs to fight disease. Bacteria were among the first life forms on earth [58].

2.2.2. Kingdom Protista

Members of the kingdom Protista are the simplest of the eukaryotes. Protistas are an unusual group of organisms. Some Protistas perform photosynthesis like plants while others move around and act like animals, but Protistas are neither plants nor animals. They are not Fungi either. In some ways, the kingdom Protista is home for the leftover organisms that could not be classified elsewhere [61].

2.2.3. Kingdom Plantae

The kingdom Plantae is familiar to everyone. This kingdom encompasses all of the plants, from the simplest mosses to the incredible complexity of the flowering plants.

All plants have a eukaryotic cell type. Kingdom Plantae are multi-cellular and they are autotrophic, meaning they can make their own food via photosynthesis and they surround their cells with a cell wall. The cell wall in kingdom Plantae is made of cellulose and at last, they have complex organ systems [61].

2.2.4. Kingdom Fungi

Fungi cells are quite different from both plants and animal cells. Fungi are classified in their own kingdom. Like plants, Fungi have cell-wall-bound cells. Unlike plants, Fungi's cell walls are made from chitin, a polysaccharide containing nitrogen, not from cellulose.

Fungi are eukaryotic and range from being unicellular to multi-cellular, but multi-cellular Fungi do not have cell walls or membranes separating individual cells. Thus, the cytoplasm is continuous among the cells [58].

2.2.5. Kingdom Animalia

Kingdom Animalia are multi-cellular organisms that are capable of locomotion and rely on other organisms to obtain their nourishment. Most animal's bodies are differentiated into tissues. In some animals, tissues form organ systems. All animals have cells that lack rigid cell walls (like those found in plant cells) [58].

2.3. Prokaryotic cells

Prokaryote cells do not have a membrane-bound nucleus and instead of having chromosomal DNA, their genetic information is in a circular loop called a plasmid. These cells have few internal structures that are distinguishable under a microscope. Cells in the monera kingdom such as bacteria and cyan bacteria are prokaryotes [60].

Bacterial cells are very small, roughly the size of an animal mitochondrion (about 1-2 μm in diameter and 10 μm long). Prokaryotic cells feature three major shapes: rod shaped, spherical, and spiral [60].

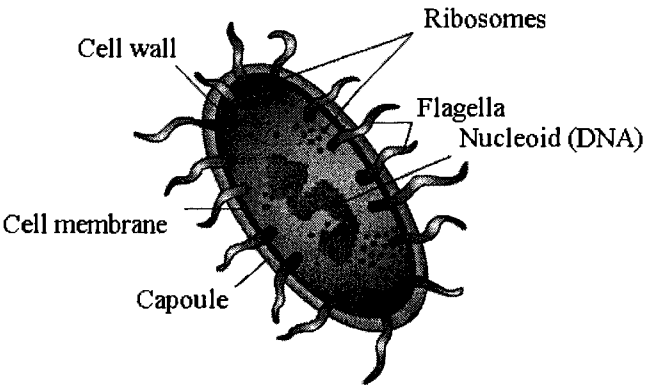

Figure 2.2 -- Diagram of a prokaryotic cell [59]

2.4. Eukaryotic cells

Eukaryotic cells comprise all of the life kingdoms except Monera. They can be easily distinguished through a membrane-bound nucleus. Eukaryotic cells also contain many internal membrane-bound structures called organelles. These organelles such as the mitochondrion or chloroplast serve to perform metabolic functions and energy conversion. Other organelles like intracellular filaments provide structural support and cellular motility [60].

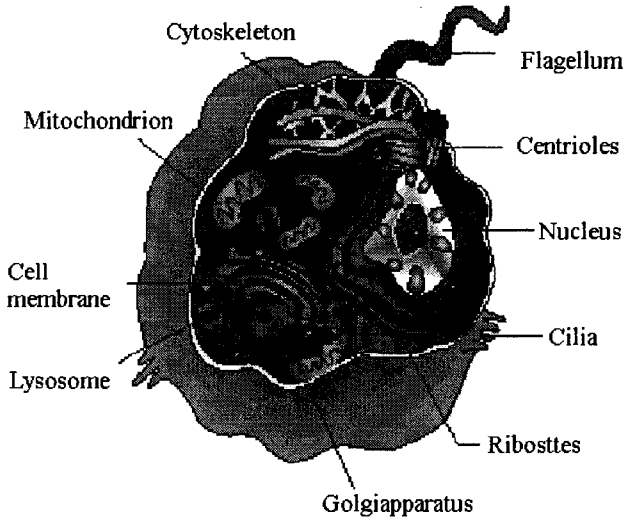

Figure 2.3 -- Diagram of an animal cell [59]

Another important member of the eukaryote family is the plant cell. They function essentially in the same manner as other eukaryotic cells, but there are three unique structures, which set them apart. Plastids, cell walls, and vacuoles are present only in plants [60].

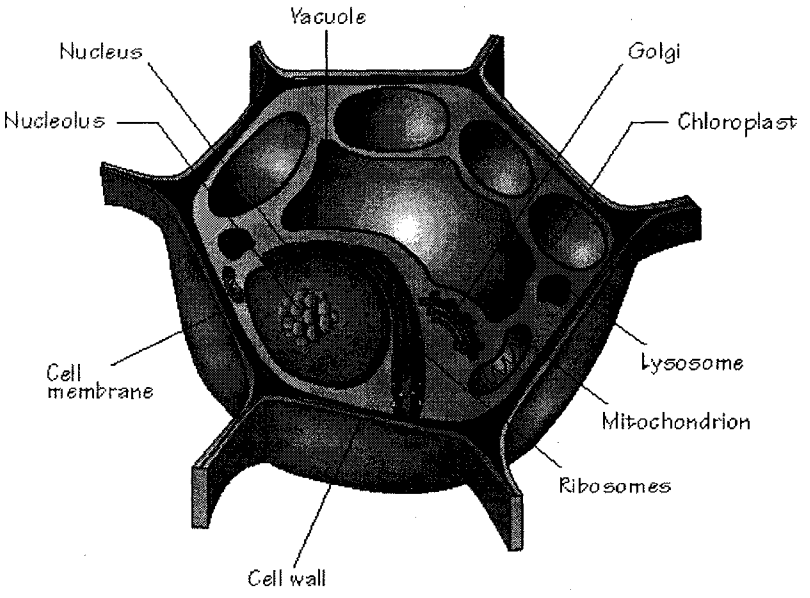

Figure 2.4 -- Diagram of a plant cell [59]

Below are pictures of eukaryotic cells from the animalia, plantae, Fungi, and Protista kingdoms.

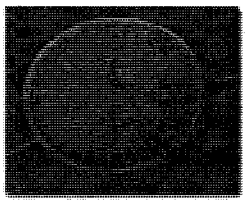

Picture of a Centric Diatom (from the Protista kingdom)

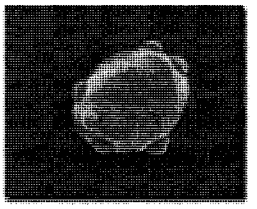

Picture of a Bread Yeast - S. cerevisiae (from the Fungi kingdom)

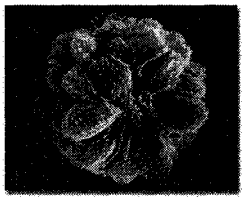

Picture of Golden Colonia Alga - Synura (from the Protista kingdom)

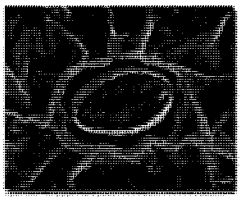

Picture of a Pea Leaf Stomata (from the Plantae kingdom)

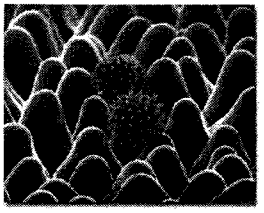

Sunflower Petal and Pollen Grains - Helianthus (from the Plantae kingdom)

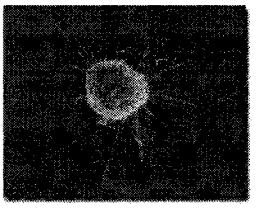

Human Breast Cancer Cell (from the Animalia kingdom)

Human Red Blood Cells, Platelets, and T-lymphocytes (from the Animalia kingdom)

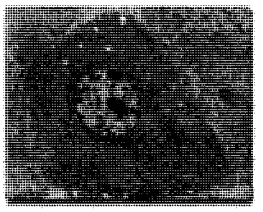

Human Liver Cell (from the Animalia kingdom)

Figure 2.5 -- Cell kingdoms [59]

As mentioned before even though all cells are quite small, not all cells are alike. They differ in size, shape and function (how they work). Figure 2.6 shows different shape of human body cells.

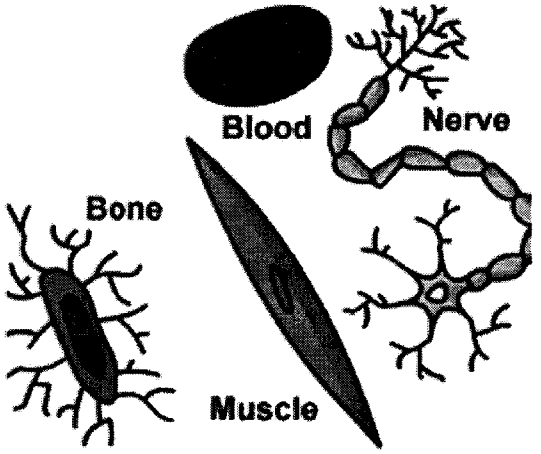

Figure 2.6 -- Cell different shapes in human body [56]

As it is clear, the bone cells differ from blood cells and nerve cells differ from muscle cells. Each one is designed to do a different job. Red blood cells carry oxygen throughout the body. Nerve cells carry electrical signals to and from our brains to muscles all over our bodies. Bone cells, which are very rigid, form the skeleton that gives our bodies shape. Muscle cells contract to move these bones to help us get around. Stomach cells secrete an acid to digest food. Special cells in intestines absorb nutrients from the food. Many of these cells change food. Cells are packed tightly together. They combine to form tissues, like skin and muscle. Tissues combine to form organs. Muscle cells combine to form muscle tissues. Muscle tissues combine to form organs like heart [58].

2.5. Cell structure

Figure 2.7 shows a generic animal cell. Typical animal cell shows the characteristic organelles and cellular inclusions. The arrangement of the intracellular features and the shape of the cell vary from cell to cell. The outer boundary, or cell membrane, forms a compartment that is biochemically distinct from the outside environment [62].

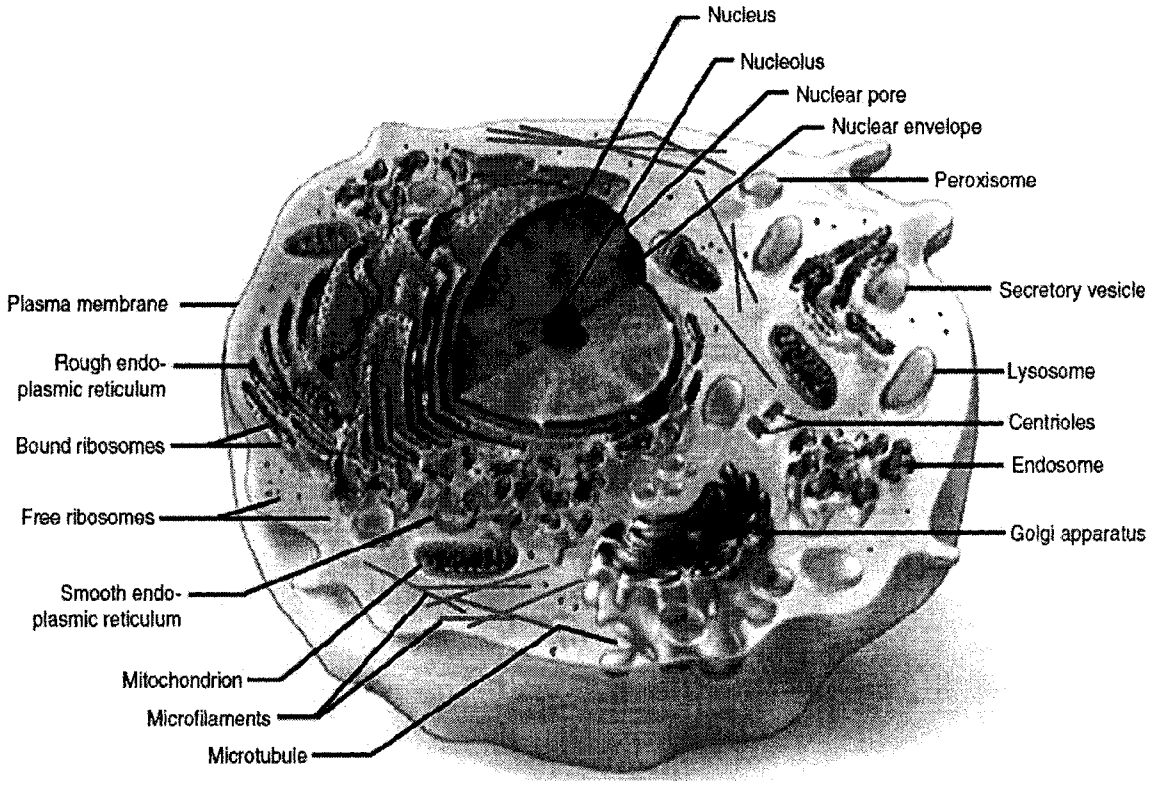

Figure 2.7 -- Typical animal cell [62]

The main structural components of cells are membrane, cytoplasm and nucleus. A brief explanation of other structural components is in appendix I.

2.5.1. Membrane

From the early days of the microscope, the cell has been differentiated as having an outer boundary membrane (the cell or plasma membrane) containing a heterogeneous soup (cytoplasm) and a nucleus.

While the plant cell has a rigid cell wall, an animal cell membrane is a flexible lipid bilayer. The plasma membrane performs several functions for the cell. It gives mechanical strength, provides structure, helps with the movement and controls the cells volume and its activities by regulating the movement of chemicals in and out of the cell. The plasma membrane is composed of phospholipids interspersed with protein and cholesterol [58].

Membrane is important in regulating the internal environment of the cell and in creating and maintaining concentration gradients between the internal cell environment and the extracellular environment.

Consider a simple model cell that consists of a plasma membrane and cytoplasm. The cytoplasm in this model cell contains protein that cannot cross the plasma membrane and water, which can. At equilibrium, the total osmolarity inside the cell must equal the total osmolarity outside the cell. If the osmolarity inside and the osmolarity outside of the cell are out of balance, there will be a net movement of water from the side of the plasma membrane where it is more highly concentrated to the other side until equilibrium is achieved [62].

The plant cell wall is a remarkable structure. It provides the most significant difference between plant cells and other eukaryotic cells. The cell wall is rigid (up to many micrometers in thickness) and gives plant cells a much-defined shape. While most cells have an outer membrane, none is comparable in strength to the plant cell wall. The cell wall is the reason for the difference between plant and animal cell functions. Because the plant has evolved this rigid structure, they have lost the opportunity to develop nervous systems, immune systems, and most importantly, mobility [62].

2.5.2. Cytoplasm

In eukaryotic cells, there are large numbers of organelles, which perform specific tasks. Eukaryotic cells contain a nucleus that is separated from the cytoplasm by a double membrane structure. The cytoplasm contains the rest of the organelles such as the endoplasmic reticulum and the mitochondria, each necessary for the cell's survival.

The area of the cytoplasm outside of the individual organelles is called the cytosol. The cytosol is the largest structure in the cell. It composes 54% of the cells total volume. The cytosol contains thousands of enzymes that are responsible for the catalyzation of glycolysis and gluconeogenesis and for the biosynthesis of sugars, fatty acids, and amino acids. The cytosol takes molecules and breaks them down, so that the individual organelles can use them. For example, in order for respiration to occur, glucose is ingested and broken down into pyruvate in the cytosol, for use in the mitochondria [62].

The cytosol also contains a skeletal structure, called the cytoskeleton. This structure gives the cell its shape and allows it to organize many of the chemical reactions that occur in the cytoplasm. Additionally, the cytoskeleton can aid in the movement of the cell[62].

Eukaryotic cells have a wide variety of distinct shapes and internal organizations. Cells are capable of changing their shape, moving organelles and in many cases, move from place to place. This requires a network a protein filaments placed in the cytoplasm known as the cytoskeleton[63].

Current understanding shows the cytoplasm, which is mostly water, contains a variety of solutes. Many ions such as calcium, sodium, and potassium ions are found in the cytoplasm and engage in initiating and terminating cellular functions. In fact, the cytoplasm is a semifluid because of the volume and characteristics of its components. In some portions of the cell, the cytoplasm is gelatinous, in other portions, watery. Additionally, numerous compounds including proteins, carbohydrates, and lipids are distributed in the cytoplasm [62].

Contributions by e.g., Pollack [63] suggest that cytoplasm has a gel-like structure with cross-linked cellular polymers such as proteins and polysaccharides forming a matrix holding the solvent (water). Analyses of the material properties of cytogels reveal a viscoelastic material behavior.

2.5.3. Nucleus

The nucleus is the cellular control center and exists only in eukaryotes. The nucleus contains the genetic information for the cell, in the form of DNA and RNA. The genetic information is surrounded by a two-layer nuclear envelope and it is generally found at the center of the cell. The nucleus is responsible for communicating with other organelles in the cytoplasm (the gel-like space surrounding the nucleus) [58]. Messages from inside the nucleus travel through pores on the nuclear envelope to enter the cytoplasm.

2.6. Summary

In this chapter different kinds of cells was reviewed. There was five-cell kingdom which any cell belongs to on of the five kingdoms. The cell structure is briefly described. The main structural components of cells are membrane, cytoplasm, and nucleus. Membrane is important in regulating the internal environment of the cell and in creating and maintaining concentration gradients between the internal cell environment and the extracellular environment. Cytoplasm, which is mostly water, contains a variety of solutes and it is a semi fluid because of the volume and characteristics of its components. Nucleus, which contains the genetic information, is surrounded by a two-layer nuclear envelope and it is generally found at the center of the cell.

Since the biological condition of the cell is associated with the balance among various properties and exchange with the surrounding media of nutrients and toxins, the biological condition of the cell might be associated with the frequency of the natural phenomenon of oscillation.

Chapter 3 - Modeling of living cell and validation of the model

3.1. Introduction

The nanomechanical properties of cell membranes play a significant role in many important biological processes such as metastasis potential, signaling pathways, and viability of the cell [65, 66].

Saccharomyces Cerevisiae commonly known as baker's yeast or budding yeast is one of the major model organisms that have been under intense study for many decades. Yeasts are single cell (unicellular) Fungi, a few species of which are commonly used to leaven bread, ferment alcoholic beverages and even drive experimental fuel cells. A few yeasts, such as Candida Albicans, can cause infection in humans (Candidiasis). More than one thousand species of yeasts have been described. The most commonly used yeast is Saccharomyces Cerevisiae, which was domesticated for wine, bread, and beer production for thousands of years. Figure 3.1 shows the spherical shape of Saccharomyces Cerevisiae.

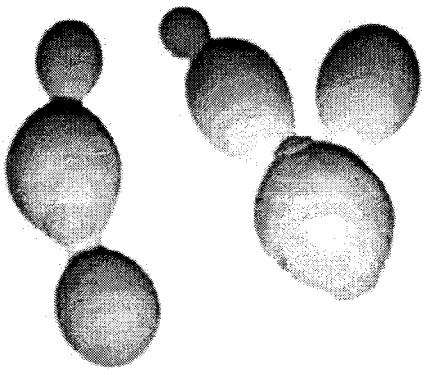

Figure 3.1 -- Saccharomyces Cerevisiae [67]

Saccharomyces Cerevisiae are 3–15 μm in diameter with a cell wall thickness of 100–1000 nm [32]. The cell membrane that is bounded to the cytoplasm inside the cell regulates the transfer of water and ions. Functional protein molecules integrated in the membrane are providing the transport and keep up the transcellular gradients. The cell is filled with cytoplasm, which is a watery solution of enzymes, proteins, and ions. Furthermore, different cell organelles are suspended in the cytoplasm, from which the most important one is the nucleus containing the DNA. Furthermore, a vacuole serving as reservoir of water, lipids or gas is one of the dominant internal parts of the cell besides mitochondria and the endoplasmic reticulum [68, 69].

Saccharomyces Cerevisiae has a similar dynamic behavior as heart cells in terms of vibrating by itself. It is interesting to note that different attempts made by different research groups do not result in the same value of elastic modulus and natural frequency hence they have presented different values.

A critical issue in the study of the natural oscillations of the biological cells is obtaining appropriate and realistic values for the elastic properties of the cells. In experiments, it is difficult to obtain accurate values of the elastic properties of the cell's membrane which are so thin approximately 100–1000 nm thick for cell and 10 nm thick for bacteria. Although this is particularly the case with certain cells and bacterias because these category have a stiff membrane and the established method used for measuring elastic properties of cells like RBCs cannot be applied [56]. Thus, disagreement exists in the literature on the associated values.

Recently, the mechanical behavior of Saccharomyces Cerevisiae has received attention because resonance vibrations of the yeast cell membrane at 0.8 to 1.6 *kHz* have been detected by atomic force microscope (AFM) and the Young's modulus of E=0.75 *MPa* was reported [32]. The reported value of Young's modulus is two orders of magnitude lower than that measured by micromanipulation techniques, E =110 *MPa*, [68, 69, 70]. The natural vibrations of specific bacteria and Saccharomyces Cerevisiae are investigated using a shell model and the natural oscillation of 160 *kHz* and 2.05 *MHZ* are obtained [44].

The corresponding qualities determined from these experiments are different as illustrated in Table 3.1.

Table 3.1 -- Mechanical properties for Saccharomyces Cerevisiae [32, 44, 46, 70]

Approaches	Method	Frequency	Modulus of elasticity
1	Andrew E. Pelling et. al [32]-AFM	0.8 *kHz* - 1.6 *kHz*	0.54 *MPa* - 0.75 *MPa*
2	Alexander E. Smith et. al [70] Micromanipulation Technique	-	107 *MPa* to 112 *MPa*
3	Amirouche et. al [46] F.F.M	16.19 *Hz* – 60.96 *Hz*	-
4	P. V. Zinin et. al [44] Closed Form	160 *kHz* – 2.05 *MHz*	-

Available results on the problem are limited to four reports, which are shown in Table 3.1. The main objective of this work is to establish a spherical model of elastic wall filled with liquid and experiences the resonant frequencies. As clear from Table 3.1, the

available results on the natural frequencies are limited to three papers in the literature. The very much different results reported in the literature naturally lead to the need to validate either of the results.

3.2. Modeling of living cell

A spherical shape of cell is considered because many cells and bacteria have a spherical shape. The thickness of the shell is small as compared with the cell radius and the shell is regarded as a simple elastic membrane. The frequency of the natural oscillations of spherical cell can be obtained by modeling the spherical cell by using finite element method.

In order to describe the mechanical behavior of the cell, we should simplify the complex structure of cell and reduced its model to simple model; containing the relevant structural parts of the cell.

The cell organelles are supposed to have very little signification on the result of the analysis and hence the mechanical behavior of the cell. It is supposed that they do not contribute much to the mechanical behavior of the cell. Membranes around the whole cell, the nucleus and the vacuole are the main parts of the cell that are illustrated in Figure 3.2.

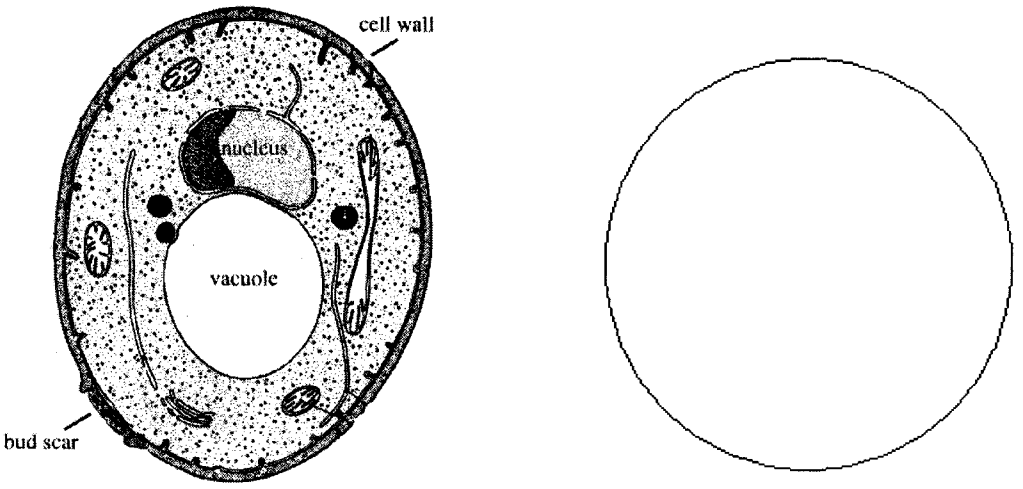

Figure 3.2 -- Structure [67, 68] (a) and (b) Proposed model of the Saccharomyces Cerevisiae

We made the assumption of a spherical membrane model for a biological cell to estimate the natural frequencies of the specific type of cell.

There are some reports on the analytical solutions of fluid filled spherical shell as stated earlier in section 1.4 [47-51]. The solutions have been carried out for several conditions. For compressible fluid spherical shells, a solutions have been presented by Advani et. al [54]. In the literature [54] the equations governing motion of an elastic shell completely filled with an inviscid, compressible fluid using of Hamilton's principle is obtained. Advani et. al [54] have obtained the axisymmetric modal form of the equations of motion. In that model, the free vibration formulation considers the energy associated with the shell- fluid interaction and the strain and kinetic energies of the deformed shell. In addition, the effect of shell transverse shear and rotational inertia are taken in to account.

The frequency equation for fluid filled spherical cell, which satisfy the equation of motions, is reported as [54],

$$c_1\beta_n^6 + c_2\beta_n^4 + c_3\beta_n^2 + c_4 = 0 \tag{3.4}$$

where,

$$\beta = \frac{\Omega_n R}{C_s}$$

$$C_s = [\frac{E}{\rho}(1-\nu^2)]^{\frac{1}{2}}$$

$$c_1 = \varepsilon k_1^2 k_r k_s,$$

$$c_2 = -k_1^2 - \varepsilon k_1[k_r + (k_1 + k_r)k_s]\lambda_n + \varepsilon k_1[2k_r k_s - (1+3\nu)k_r k_s] + \varepsilon k_1 k_r k_s \bar{\gamma}_n,$$

$$c_3 = (1+3\nu)k_1 + k_1\lambda_n - 2\varepsilon k_s[(1+3\nu) + 2(1+\nu)k_r] + \varepsilon[2(1+\nu)k_s k_r + 4k_1\nu k_s - 2k_r$$
$$-(1-\nu)k_1]\lambda_n + \varepsilon(k_1 + k_r + k_1 k_s)\lambda^2 - (k_1 - \varepsilon k_s(1-\nu-\lambda_n)(k_1 + k_r)]\bar{\gamma}_n,$$

and

$$c_4 = 2(1-\nu^2) - 4\varepsilon(1-\nu^2)k_s - (1-\nu^2)\lambda_n - \varepsilon\lambda_n^3 - \varepsilon\lambda_n[(1-\nu^2)^2 - 2(3+2\nu-\nu^2)k_s] +$$
$$\varepsilon\lambda_n^2[3-\nu-2(1+\varepsilon)k_s] - [1-\varepsilon k_s(1-\nu-\lambda_n)](1-\nu-\lambda_n)\bar{\gamma}_n$$

The parameters k_1, k_r are shell inertia and shell rotary inertia constants, k_s is average shear coefficient , ε is shell thickness parameter and is equal to $\frac{1}{12}(\frac{h}{R^2})$ when h is shell thickness and R is radius of curvature of shell middle surface, ν is Poisson's ratio, γ_n is pressure radial displacement constant and λ_n is defined by $\lambda_n = n(n+1)$.

Eigenvalues, β_n are obtained for fluid filled shell by author for a specific fluid and properties and shell dimensions and material constants. The eigenvalues, obtained in this literature are for thick elastic shell that is filled with a compressible fluid, which is not a suitable model for cell.

In another report, the vibration response of fluid filled shell is considered for an elastic, homogeneous and isotropic shell [53]. The motion of an inviscid and irrigational fluid undergoing small oscillation is governed by wave equations. In spherical coordinate, the equation of motions is expressed as [53]:

$$\frac{1}{r^2}\frac{\partial}{\partial r}(r^2\frac{\partial \phi}{\partial r})+\frac{1}{r^2\sin\varphi}\frac{\partial}{\partial \varphi}\times(\sin\varphi\frac{\partial \phi}{\partial \varphi})=\frac{1}{c^2}\frac{\partial^2\phi}{\partial t^2} \tag{3.5}$$

where ϕ is the velocity potential and c represents the speed of sound in the fluid. The equations of motion of fluid filled shell are derived from Hamilton's principle. Two partial differential equations are obtained from substituting the potential energy V, and T, the kinetic energy of the fluid filled shell in the analytical statement of Hamilton's principle [53]. The analytical statement of Hamilton's principle is

$$\delta\int_{t1}^{t2}(T-V)dt=0 \tag{3.6}$$

The obtained two partial differential equations are expressed as,

$$(1+\alpha^2)[-\frac{\partial^2 u}{\partial\varphi^2}-\cot\varphi\frac{\partial u}{\partial\varphi^2}+9(\nu+\cot^2\varphi)u+\alpha^2\frac{\partial^3 w}{\partial\varphi^3}+\alpha^2\cot\varphi\frac{\partial^2 w}{\partial\varphi^2}-$$
$$[\alpha^2(\cot^2\varphi+\nu)+(1+\nu)]\frac{\partial w}{\partial\varphi}+\frac{1-\nu^2}{E}\rho_s a^2\frac{\partial^2 u}{\partial t^2}=0 \qquad (3.7)$$

and

$$\alpha^2\frac{\partial^3 u}{\partial\varphi^3}+2\alpha^2\cot\varphi\frac{\partial^2 u}{\partial\varphi^2}-[(1+\nu)(1+\alpha^2)+\alpha^2\cot^2\varphi]\frac{\partial u}{\partial\varphi}+[\alpha^2\cot^3\varphi+3\alpha^2\varphi\cot\varphi-(1+\nu)$$
$$(1+\alpha^2)\cot\varphi]u-\alpha^2[\frac{\partial^4 w}{\partial\varphi^4}+2\cot\varphi\frac{\partial^4 w}{\partial\varphi^4}-(1+\nu+\cot^2\varphi)\frac{\partial^2 w}{\partial\varphi^2}+(2\cot\varphi+\cot^3\varphi-\nu\cot\varphi)\frac{\partial w}{\partial\varphi}]$$
$$-2(1-\nu)w-\frac{1-\nu^2}{E}\rho_s\alpha^2\frac{\partial^2 w}{\partial\varphi^2}-\frac{1-\nu^2}{Eh}\alpha^2[\rho_f\frac{\partial\phi(a,\phi,t)}{\partial t}-p_e(\varphi,t)=0 \qquad (3.8)$$

Where u and w are the meridional and radial displacement with respect to centre of mass of the system, E is Young's modulus, v is Poisson's ratio, t is time and α^2 is the thickness parameter, which is defined by $h^2/12a^2$, when h is the shell thickness and a is the inner radius of shell.

By introducing the dimensionless variables and using the method of separation of variations and applying the boundary condition, the vibration response of fluid filled shell system is obtained by A.E. Engin [53] as follows,

For n=0

$$[1+f\frac{j_0(\Omega)}{\Omega j'_0(\Omega)}]s^2\Omega^2-2(1+\nu)=0 \qquad (3.9)$$

For n≥1 and $\lambda = n(n+1)$

$$[1+f\frac{j_n(\Omega)}{\Omega j'_n(\Omega)}]s^4\Omega^4 + \{[1+f\frac{j_n(\Omega)}{\Omega j'_n(\Omega)}]\times(1-\nu-\lambda_n)(1+\alpha^2)-2(1+\nu)-$$
$$\alpha^2[\lambda_n^2-\lambda_n(1-\nu)\}s^2\Omega^2-(1+\nu)\{2(1-\nu-\lambda_n)(1+\alpha^2)+\lambda_n[1+\nu-\alpha^2(1-\nu-\lambda_n)]\}$$

$$-\alpha^2(2-\lambda_n)[\lambda_n^2-\lambda_n(1-\nu)]=0 \qquad (3.10)$$

where

$$s=\frac{C}{C_s}$$

and

$$C_s=[\frac{E}{\rho}(1-\nu^2)]^{\frac{1}{2}}$$

The parameter $j_n(\Omega)$ is spherical Bessel function of the first kind, $\Omega=\omega a/c$ is the unknown dimensionless frequency, λ is a constant that is defined by $\lambda=n(n+1)$, s is the speed ratio or c/c_s which c_s is apparent wave speed in the shell.

The aim of author in this paper is a study of various mechanical properties of the head as revealed by its response to pressure wave [53]. The problem have been solved for specific ratio, the ratio of the inner radius of shell a to the outer shell thickness (h); $a/h=20$ which is not applicable for cell [53].

Analytical solution have been obtained for fluid filled spherical cell and natural frequencies have been computed for specific types of spherical cells whose elastic properties of shell have been experimentally measured by P. V. Zinin et. al [44].

A theoretical study of the spectrum of the natural vibrations is based on a simplified cell model to the shell model when the motion of the cell is composed of the motion of three components: the internal fluid, the shell, and the surrounding fluid. The frequencies of the natural oscillations of spherical cell have been obtained by solving the equations of motion of a viscous fluid and the equations of motion of an elastic shell.

The equation of natural oscillations of fluid filled elastic sphere, which is surrounded by external fluid, is reported as follow:

$$\omega_n = \Omega_n - i\alpha_n \tag{3.11}$$

Where Ω_n and α_n are positive real numbers: Ω_n determines the frequency of oscillations and α_n the rate of their decay. The decaying oscillations may is characterized by another variable, called the quality of oscillation given by the equation

$$Q_n = \frac{\Omega_n}{2\alpha_n} \tag{3.12}$$

The other form of solution is presented by P. V. Zinin et. al [44] is in the form of

$$\omega_n = \Omega_n(1 - \frac{i}{2Q_n}) \tag{3.13}$$

The natural vibrations of specific bacteria and Saccharomyces Cerevisiae are reported by this analytical solution [41] and the natural oscillation of Saccharomyces Cerevisiae is reported.

All the investigated models for obtaining natural frequencies of fluid filled spherical shells are simplified and the model assumptions may not be suitable with the small size of the cell when solutions are sought. As stated earlier the results with the experimental measurements for natural frequency of spherical cell do not agree with the analytical approach. All of these resulted in adopting the Finite Element Method (FEM) as the best theoretical tool for analyzing the problem. In the following chapter, we presented a finite element analysis to determine the value of the natural frequency of spherical cell.

3.3. Summary

In this chapter, a spherical shape of the cell is considered because many cells and bacteria have a spherical shape. Saccharomyces Cerevisiae commonly known as baker's yeast or budding yeast is one of the major model organisms that have been under intense study for many decades. Saccharomyces Cerevisiae, which have spherical shape, is 3–15 μm in diameter with a cell wall thickness of 100–1000 nm [32]. Resonance vibrations of the Saccharomyces Cerevisiae membrane at 0.8 to 1.6 kHz have been detected by atomic force microscope (AFM) and the Young's modulus of E=0.75 MPa was reported. The reported value of Young's modulus is two orders of magnitude lower than that measured by micromanipulation techniques, E =110 MPa and the value reported for resonance

frequency is too different from two other reports for natural frequency of spherical cell which are about 160 *kHz* and 16.19- 60.96 *Hz* in two different reports. The available values for natural frequency are limited to three papers in the literature. The very much different results reported in the literature naturally lead to the need to validate either of the results. There are some reports on the analytical solutions of fluid filled spherical shells. The solutions have been carried out for several conditions for instance; solutions have been obtained for fluid filled shells, which the fluid is compressible or the analysis have been done considering thick shell theories.

All the investigated models are solved for special conditions and the model assumptions may not be suitable with the small size of the cell when solution is sought. All of these resulted in adopting the Finite Element Method (FEM) as the best theoretical tool for analyzing the problem

Chapter 4 - Modal analysis for cells

4.1. Three-Dimensional modal analysis for in vacuo spherical cell

Numerical methods prove extremely useful though they involve approximation. In this work, we have used the finite element method, which is one of the most popular numerical methods in use.

4.1.1 FEA using ANSYS

A comprehensive finite element analysis is carried out using ANSYS 11 (For more information please refers to the Appendix II).

Based on available literatures, we have considered the following assumptions for membrane.

1. Linear elastic material following the Hooke's law

2. Homogeneous material

3. Isotropic material

A Three-dimensional model of spherical cell is created. The parametric model is generated with the help of APDL programming feature of ANSYS (ANSYS Parametric Design Language) [64], with the radius (R), Young's modulus (Ya), the thickness of the membrane (Tk), density (Ro) and Poisson's ratio (Nu) for the membrane.

The proposed model has a radius 3 μm, thickness 0.1 μm and the related mechanical properties are shown in Table 4.1.

Table 4.1 -- Mechanical properties of the model

Cell property	Unit	
Young's modulus (E)[32]	*MPa*	0.75
Density (ρ)	kg/m^3	1000
Poisson's ratio (nu)	*1*	0.4999

There are two element are suitable for analyzing thin shell structures; SHELL181 and SHELL 41. SHELL 181 element which is suitable for thin to moderately thick shells has the option of being a "membrane only" element (Key opt 1, 1) while SHELL41 is a 3-D element which has membrane properties.

Element Shell 41, which is the most suitable element for a structural analysis of thin shells and membranes, is considered for meshing the modeling. This element can be used effectively for satisfying the needs of this research. It is actually intended for shell structures where bending of the elements is of secondary importance. The element has freedom in the x, y, and z nodal directions. Figure 3.3 shows the spherical cell model that is created in ANSYS.

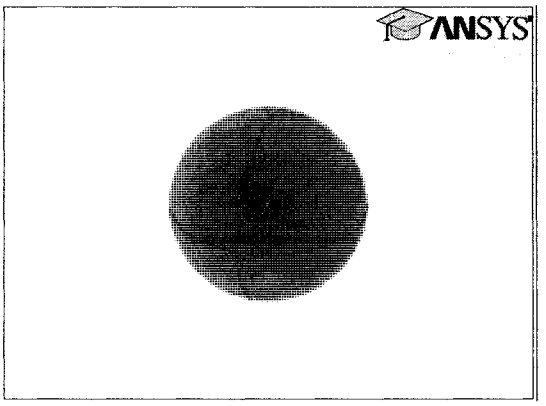

Figure 4.3 -- Spherical cell model

After creation of all the areas, an automatic meshing process is performed. Boundary conditions should be specified after defining element type and meshing. The only loads valid in a typical modal analysis are zero-value displacement constraints. If applied load is a nonzero displacement constraint, the program assigns a zero-value constraint to that DOF instead. Other loads can be specified, but are ignored. The mesh shape and boundary conditions for this model are shown in the Figure 4.4. All degrees of freedom are constrained at the bottom of cell.

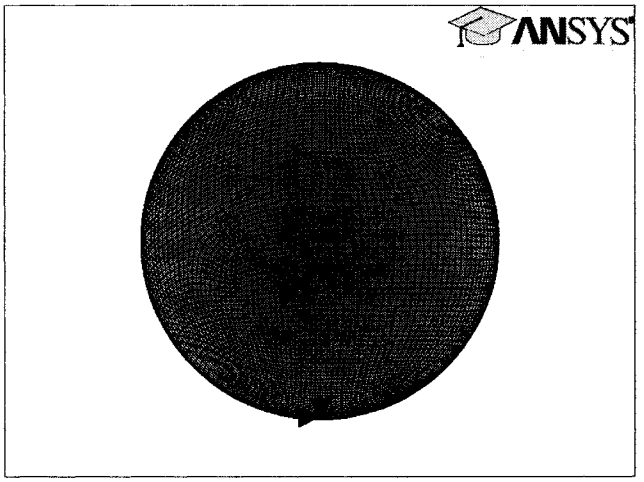

Figure 4.4 -- Mesh shape and boundary conditions

ANSYS is used to perform modal analyses. Using a high-frequency modal analysis in 3-D, it can perform tasks such as finding the resonant frequencies and mode shapes for a structure.

Modal analysis in the ANSYS family of products is a linear analysis. Any nonlinearities, such as plasticity are ignored even if they are defined.

Natural frequencies and mode shapes are obtained for in vacuo spherical cell and are illustrated in Figure 4.5 to 4.8. As shown in Figure 4.5 the first mode shape has lateral movement.

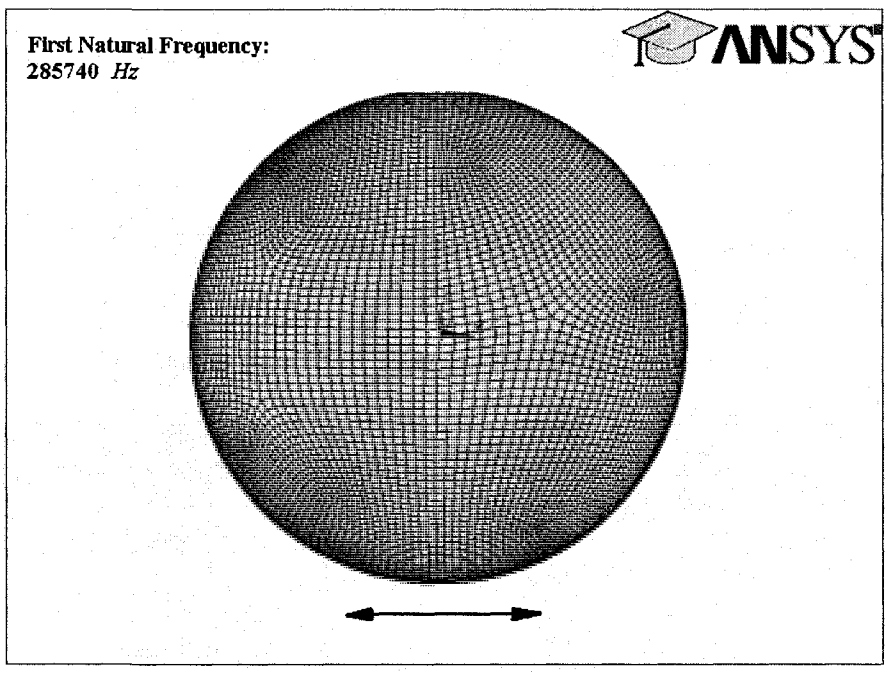

Figure 4.5 -- First natural frequency and its mode shape of in vacuo spherical cell

The second mode shape indicates the vertical motion as shown in Figure 4.6.

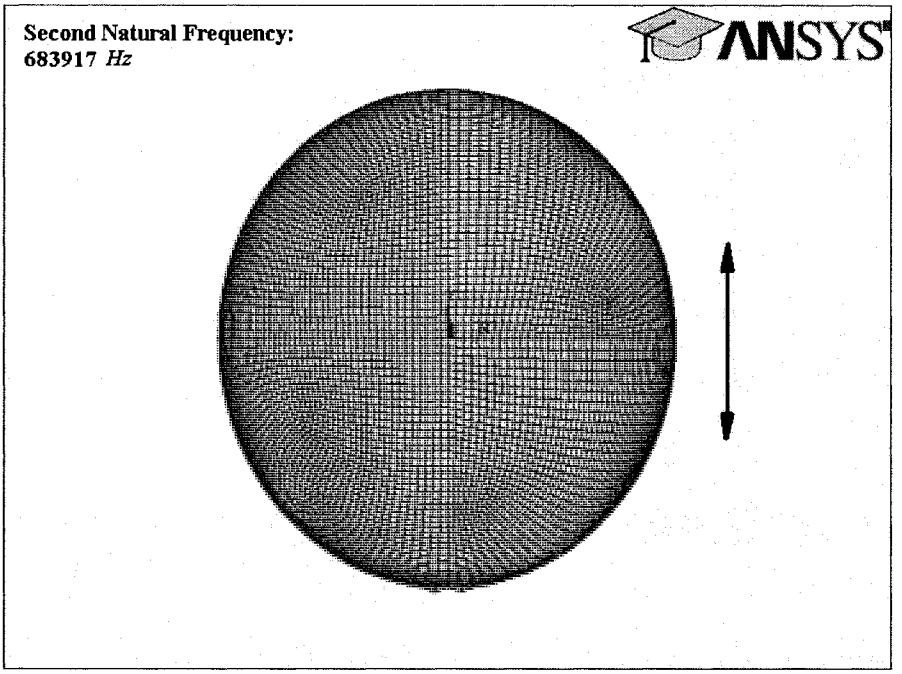

Figure 4.6 -- Second natural frequency and its mode shape of in vacuo spherical cell

Figures 4.7 and 4.8 show the third and forth modes and the mode shape respectively.

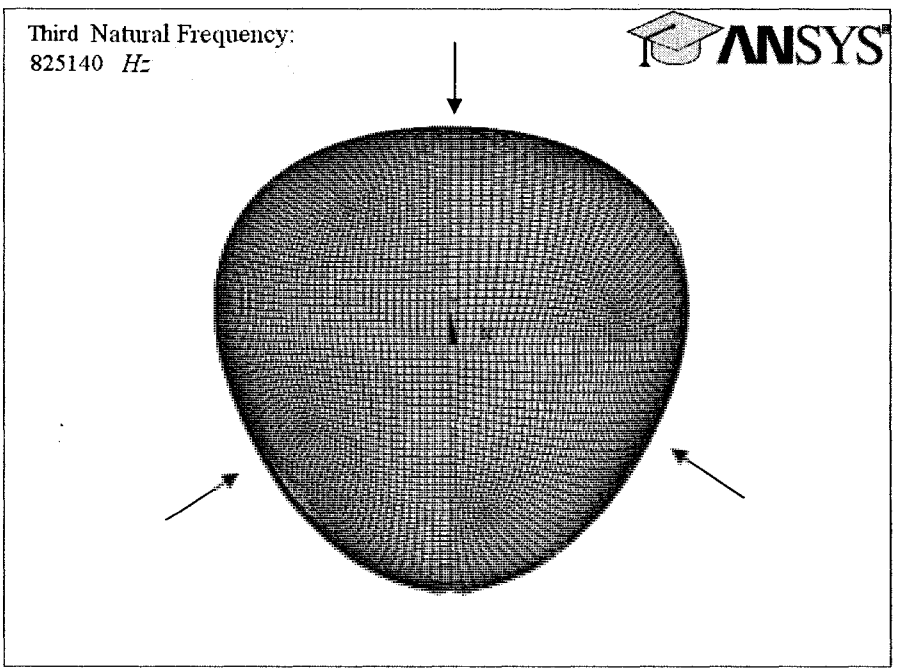

Figure 4.7 --Third natural frequency and its mode shape of in vacuo spherical cell

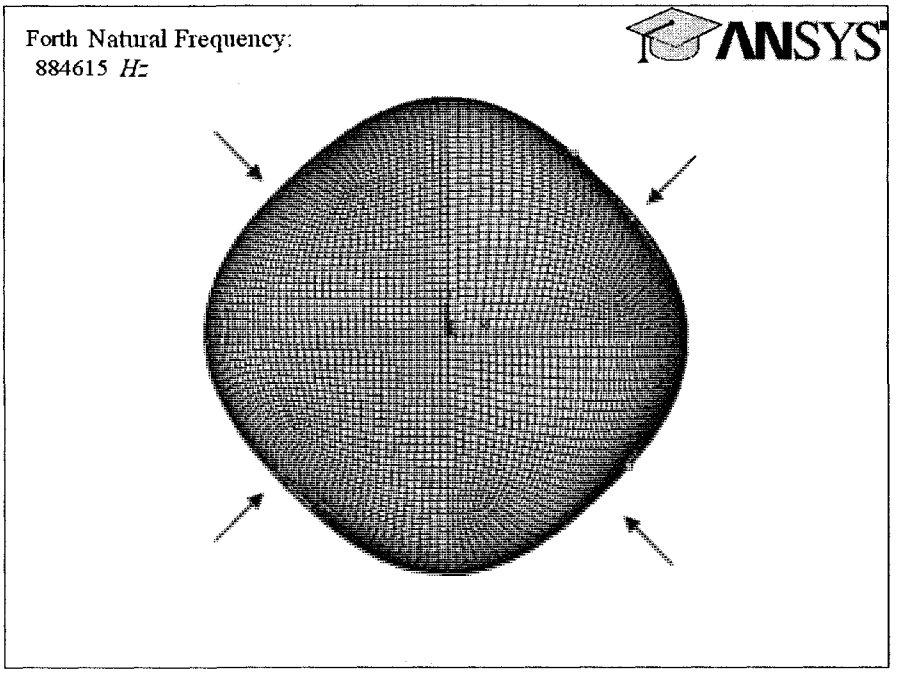

Figure 4.8 -- Forth natural frequency and its mode shape of in vacuo spherical cell

4.1.2. FEA using COMSOL (FEMLAB)

A three-dimensional model of spherical cell is created in COMSOL to validate the previous analysis in ANSYS. The proposed model, as previous model in ANSYS, has the properties according to Table 4.2

Table 4.2 -- Dimensional and mechanical properties of the model

Cell property	Unit	
Young's modulus (E)	*MPa*	0.75
Density (ρ)	kg/m^3	1000
Poisson's ratio (nu)	*1*	0.4999
Radius	*m*	3e-6
Thickness	*m*	0.1e-6

All degrees of freedom are constrained at the bottom same as in the ANSYS model. The element type used for the numerical analysis for this model is Argyris shell (simple but sophisticated 3-node triangular element for computational simulations of isotropic and elastic shells). Figure 4.9 shows the spherical cell model.

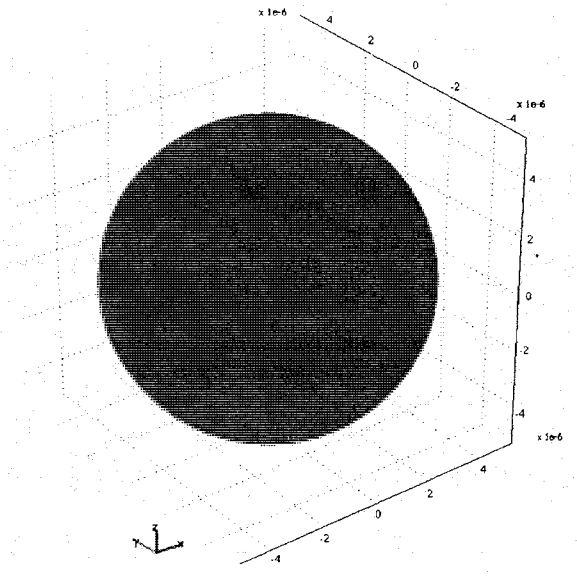

Figure 4.9 -- Spherical cell model

The boundary conditions and mesh shapes for this model are shown in the Figure 4.10. As mentioned earlier, all degrees of freedom are constrained at the bottom.

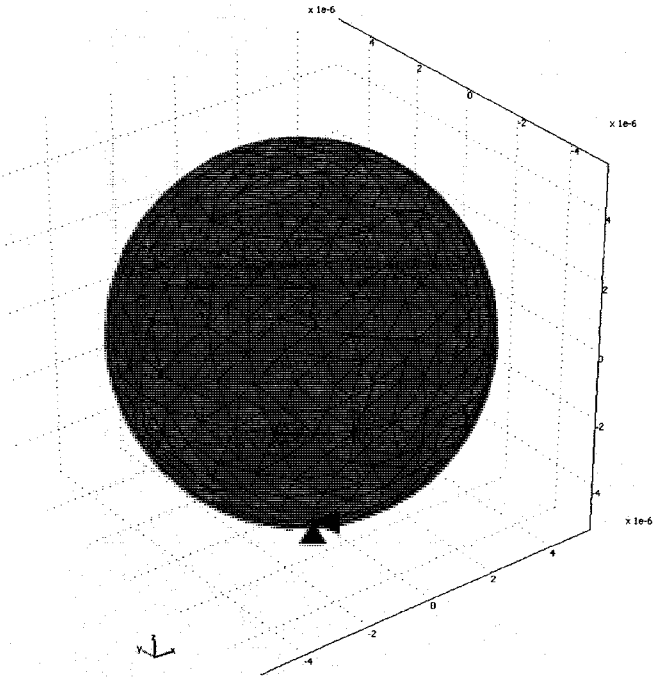

Figure 4.10 -- Boundary conditions and mesh shape

The modal analysis is done with COMSOL and natural frequencies are obtained. Figure 4.11 shows the first corresponding natural frequency ant its mode shape. The lateral movement of sphere is clear from Figure 4.11.

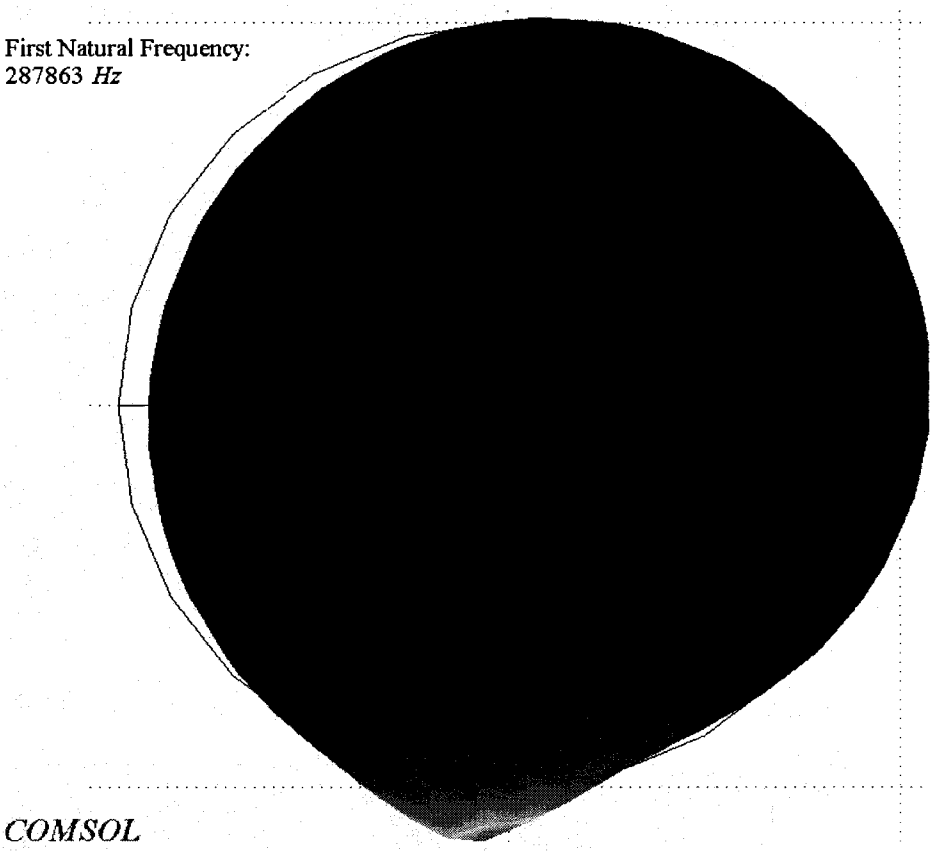

Figure 4.11 -- First natural frequency and mode shape of in vacuo spherical cell.

The corresponding values of natural frequencies of empty shell for second, third and forth modes of vibration in COMSOL are 635691 *Hz*, 757823 *Hz* and 772996 *Hz* as well. Table 4.3 shows the natural frequencies for in vacuo spherical cell obtained form both FE software ANSYS and COMSOL.

Table 4.3 – Comparison of the natural frequencies obtained by ANSYS and COMSOL

Mode number	FEA using ANSYS	FEA using COMSOL	Difference %
First mode	285740	287863	0.7
Second mode	683917	635691	7
Third mode	825140	757823	8
Forth mode	884615	772996	12.6

Comparison of the results shows that the values of natural frequencies for the empty spherical cell using COMSOL with respect to the natural frequencies obtained by ANSYS have average error of 7%. The results show that the FE approaches using ANSYS and COMSOL agree with each other with a very good range. The difference between two analyses should be due the differences in element types in two analyses. The element that is used in FEA using COMSOL has the properties of an elastic shell while the element SHELL 41 is used in FEA using ANSYS is an element with membrane properties. In section 4.2, Three-Dimensional finite element modal analysis for fluid filled spherical cells is carried out using ANSYS.

4.2. Three-Dimensional FE model for fluid filled spherical cell

A Three-Dimensional simplified model of yeast cell is created in ANSYS 11. The following assumptions have been considered for membrane and cytoplasm:

1. Linear elastic material following the Hooke's law

2. Homogeneous material

3. Isotropic material

Although all three assumptions reduce the cell to an elastic sphere filled with a fluid, the attempt provides more meaningful data regarding the resonant frequency of an idealized cell. The size and the elastic properties of the cell are as those of Saccharomyces Cerevisiae and data is collected form the literatures.

The parametric model is generated with the help of APDL programming feature [64] of ANSYS, with the radius (R), Young's modulus (Ya), the thickness of the membrane (Tk), density (Ro), and Poisson's ratio (Nu) for the membrane. The parametric symbols, which are defined for cytoplasm, are elasticity modulus (mo), radius (R), and density (Po). In order to describe the mechanical behavior of the cell, we should simplify the complex structure of the cell and reduced it to cell membrane and cytoplasm .We have neglected the effect of the other parts of cell like nucleus and other relevant structural parts of the cell. Other cell organelles are assumed to have minimum importance for the result analyses and mechanical behavior of the cell.

The three dimensional finite element analyses is done based on the spherical model of cell for two different elastic modulus that is reported for cell membrane in the literatures [32, 44, 68, 69, 70].

The elastic modulus of the yeast cells reported by Pelling et. al [32], E=0.75 *MPa* and that measured by Alexander E. [70] and is also obtained from other literatures; E =110 *MPa* [68, 69]. The difference between the two reported values is significant.

The result that are obtained form E=0.75 *MPa,* E=0.6 *MPa* and E =110 *MPa* are compared with the natural frequencies for Saccharomyces Cerevisiae, reported by Pelling et. al [32] and the value reported by P. V. Zinin et. al [44] .

4.2.1. FE model for fluid filled spherical cell using Pelling's data (AFM method) [32]

A sphere shell with elastic modulus of E=0.75 *MPa* and radius 4.5 μm is considered. The thickness of the sphere is 0.1 μm. Both sphere and shell are modeled as linear elastic materials. The elastic modulus of membrane is kept constant at 0.75 *MPa*. The Poisson's ratio of 0.499 [44] is considered for the membrane and all degrees of freedom are constrained at the bottom.

The mechanical properties for membrane and cytoplasm are shown in Table 4.4.

Table 4.4 -- Properties of spherical cell (Saccharomyces Cerevisiae) [32]

Parameter	Value
Radius of the yeast cell	4.5 μm
Membrane density	1000 *kg/m3*
Density of the fluid inside the sphere	1000 *kg/m3*
Membrane Young's modulus[32]	0.75 *Mpa*
Membrane thickness	0.1 μm
Membrane Poisson's ratio [44]	0.499

The spherical cell model is same as the model illustrated in Figure 4.3. The element type used for this model, is for the membrane, is SHELL 41. As mentioned before this element is the most suitable element for a structural analysis of shells and membranes [64]. It is intended for shell structures where bending of the elements is of secondary importance. In addition, the mode shapes that can be obtained by this element were the most accurate

shapes. SHELL 41 elements can be used effectively for satisfying the needs of this research. The cytoplasm has a gel-like appearance and it is composed mainly of water. The element that is defined for the inner sphere or the cytoplasm is SOLID 187. This element can be used as fluid when the stiffness decrease and the damping of the model increase as well.

A node-to-surface contact elements is used between the spherical shell target surface (meshed with TARGE 70) and the contact surface (meshed with CONTA 175). CONTA 175 is used to represent contact and sliding between 3-D target surfaces (TARGE 170) and a deformable surface, defined by this element. The element is applicable to 3-D structural and contact analyses [64].

After defining element type and meshing, the boundary conditions are applied on the model. The only loads valid in typical modal analyses are zero-value displacement constraints. The boundary condition for this model is shown in the Figure 4.12. All degrees of freedom are constrained at the bottom.

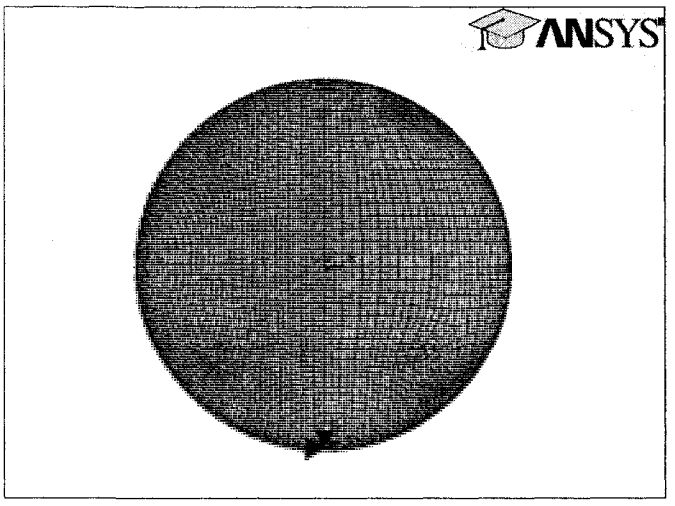

Figure 4.12 -- Boundary condition-constraint on all DOF in one point.

The modal analysis is performed and natural frequencies are obtained and shown in Figure 4.13 and 4.14.

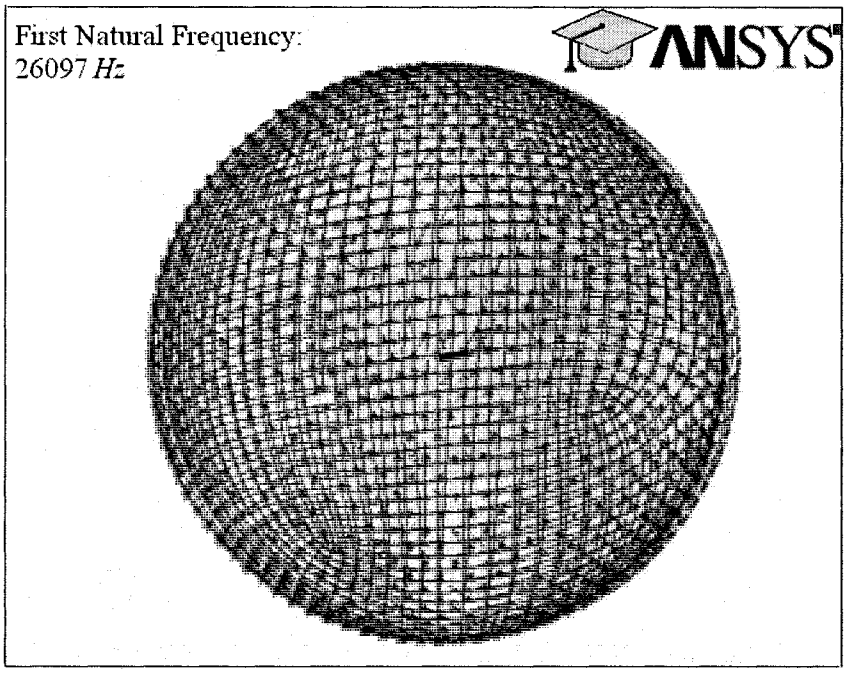

Figure 4.13 -- First natural frequency and mode shape of Saccharomyces Cerevisiae with radius of 4.5 *μm* and Young's modulus of 0.75 *MPa*

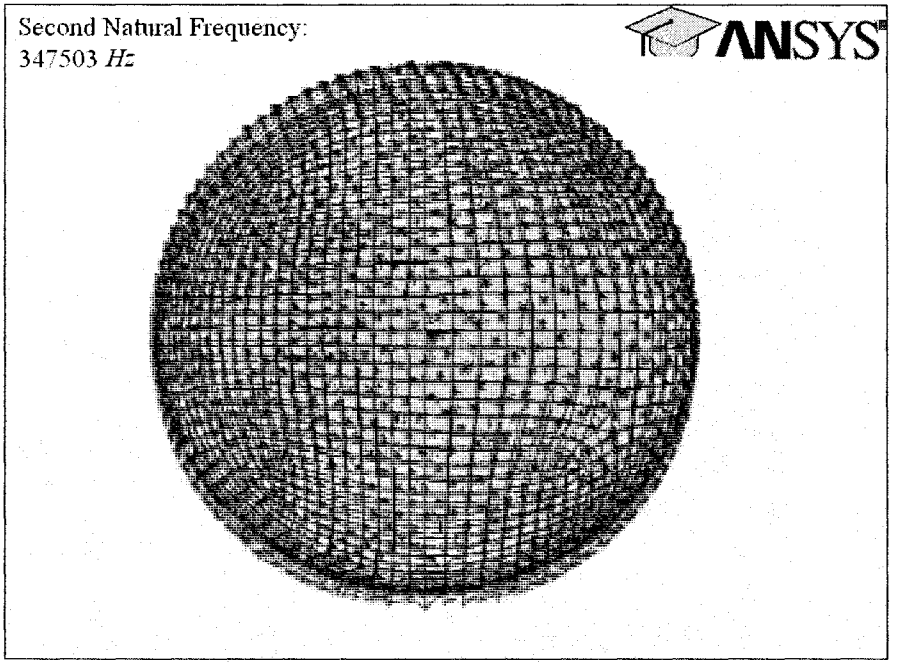

Figure 4.14 -- Second natural frequency and mode shape Saccharomyces Cerevisiae with radius of 4.5 *μm* and Young's modulus of 0.75 *MPa*

As shown in Figure 4.13 and 4.14, the first natural frequency of the spherical cell is about 26 *kHz* and second natural frequency of 347 *kHz*. The third and forth natural frequencies are about 561 *kHz* and 1.3 *MHz*. The obtained values for natural frequencies of Saccharomyces Cerevisiae are far from the result reported by Pelling et. al [32], which is 0.8 to 1.6 *kHz* for the same condition of cell. Pelling et. al [32], in their work have recorded nanoscale motion for a time period of 15 seconds and they have provided evidence for amplitude modulation and frequency modulation over time. The cell wall motion displayed frequencies in the range of 0.8 to 1.6 *kHz* and amplitudes in the range of 1 to 7 *nm*.

4.2.2. FE model for fluid filled spherical cell using Zinin et. al's data [44]

To verify the validity of the results reported by P. V. Zinin et. al [44], the sphere with radius 4.5 μm is considered for the next analysis. Two elastic modulus of E =0.6 *MPa* and E=110 *MPa* and radius of 4.5 μm is considered as is shown in Table 4.5. The thickness of the shell of the sphere is 0.1 μm. Both sphere and shell are modeled as linear elastic materials. The problem is solved for two elastic modulus of membrane .The Poisson's ratio of 0.499 is considered for the membrane. Table 4.5 shows the properties of the model.

Table 4. 5 -- Properties of spherical cell

Parameter	Value
Radius of the yeast cell	4.5 μm
Membrane density	1000 *kg/m3*
Density of the fluid inside	1000 *kg/m3*
Membrane Young's modulus[44]	0.6 *MPa*
Membrane Young's modulus [70]	110 *MPa*
Membrane thickness	0.1 μm
Membrane Poisson's ratio	0.499

Mesh shape and boundary condition are the same as mentioned in 4.2.1. All degrees of freedom are constrained at the bottom of cell. The spherical cell is analyzed for the elastic modulus of 0.6 *MPa*.

In this section, Three-Dimensional finite element modal analysis for fluid filled spherical cells is done two times; one time considering the elastic modulus of 0.6 *MPa* and the second time considering the elastic modulus of 110 *MPa* for cell membrane.

The first and second natural frequencies are shown in Figure 4.15 and 4.16 for the spherical cell with the elastic modulus of 0.6 *MPa* for the membrane.

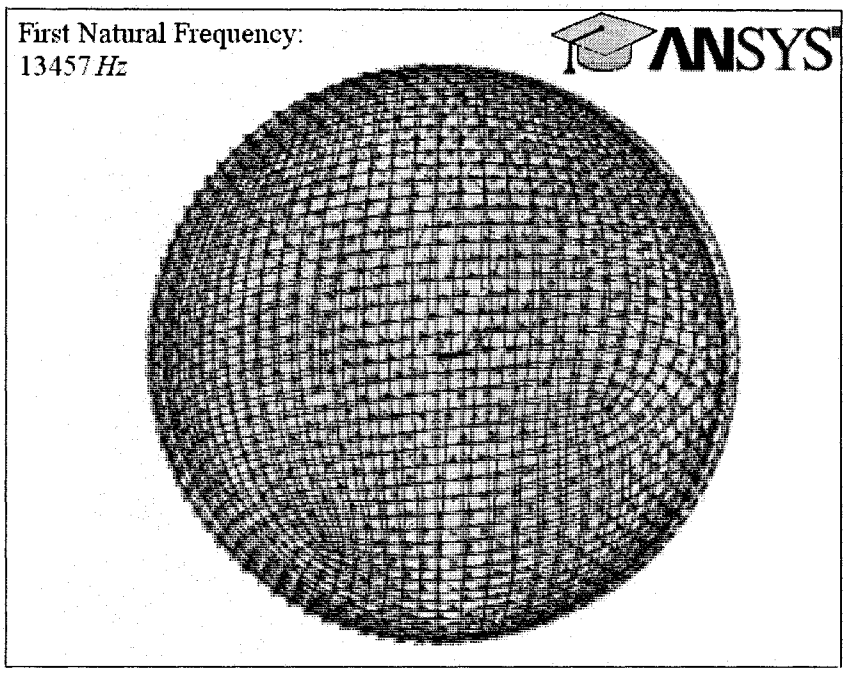

Figure 4.15 -- First natural frequency and mode shape Saccharomyces Cerevisiae with radius of 4.5 *μm* and Young's modulus of 0.6 *MPa*

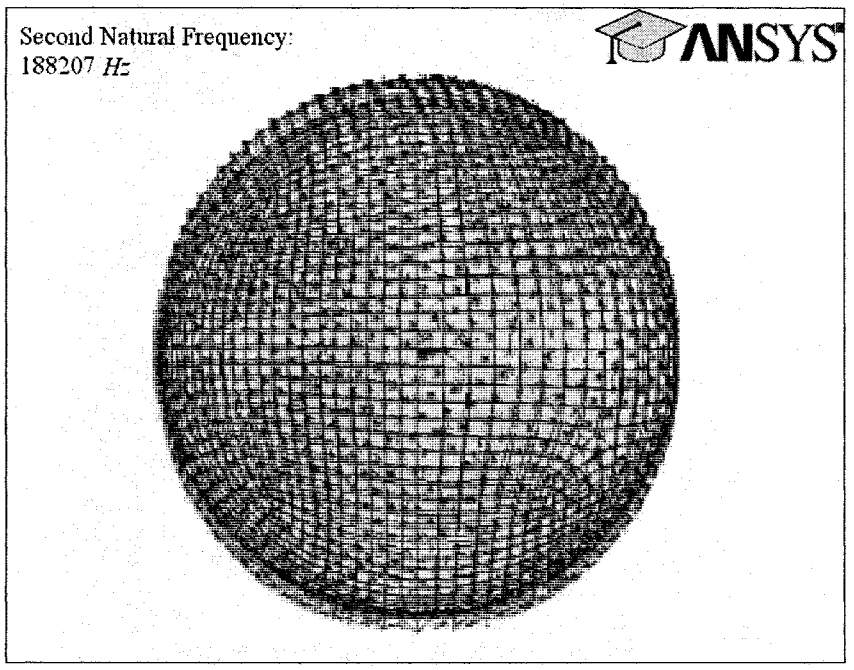

Figure 4.16 -- Second natural frequency and mode shape Saccharomyces Cerevisiae with radius of 4.5 *μm* and Young's modulus of 0.6 *Mpa*

The third and forth natural frequencies are about 396 *kHz* and 996 *kHz*.

Figure 4.17 and 4.18 show the corresponding first and second natural frequencies for the spherical cell with the elastic modulus of 110 *MPa* for the membrane.

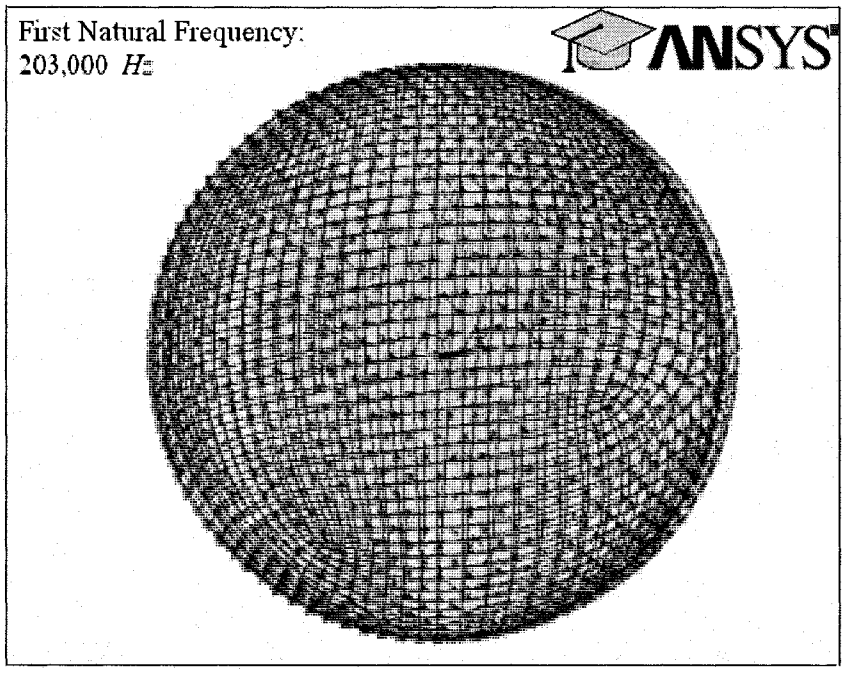

Figure 4.17 -- First natural frequency and mode shape Saccharomyces Cerevisiae with radius of 4.5 *μm* and Young's modulus of 110 *MPa*

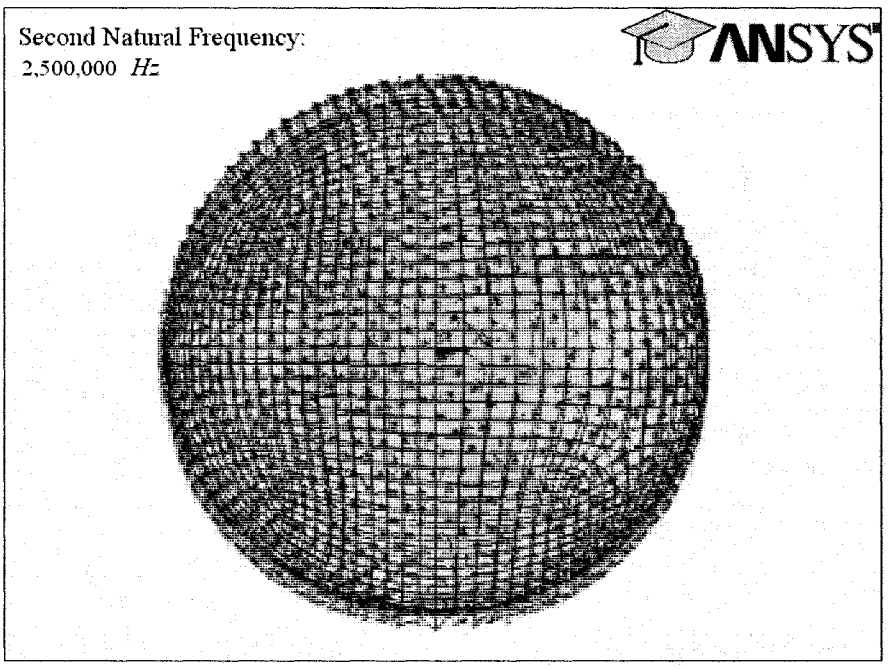

Figure 4.18 -- Second natural frequency and mode shape Saccharomyces Cerevisiae with radius of 4.5 *μm* and Young's modulus of 110 *MPa*

The comparison of the results yield by our model with the results reported by Zinin et. al [44] , which is shown in Table 4.6, shows that there is a reasonable agreement between both analyses.

Table 4.6 -- Natural frequencies Ω_n vibrations for different types of yeast cell (n=2)

Cell Type	Module of elasticity (*MPa*)	Natural frequency (*MHz*) Zinin [44]	Natural frequency (*MHz*) FEA (ANSYS)
Yeast cell [44]	0.6	0.16	0.18
Yeast cell [70]	110	2.06	2.5

All computations for natural frequencies by P.V. Zinin were done for the mode n=2 which is thought to be the most important in drop breakup according to P. L. Marston explorations on shape oscillations [71].

4.3. Summary

In this chapter, a spherical shape of the cell was considered for this analysis. Three-Dimensional finite element modal analysis for empty and fluid filled spherical cells was carried out using ANSYS and COMSOL (FEMLAB). Comparison the results showed that the corresponding values for the empty spherical cell using COMSOL were corresponds to an average error of 7%. The results showed that the FEA approaches using ANSYS and COMSOL agree with each other with a very good range. Three-Dimensional finite element modal analysis for fluid filled spherical cells was done for three different modulus of elasticity, E=0.75 *MPa*, E=0.6 *MPa* and E=110 *MPa* for cell membrane to compare with the reported natural frequencies of Saccharomyces Cerevisiae by Pelling [32] and P.V. Zinin [44]. Three-Dimensional finite element modal analysis of was done with elastic modulus of E=0.75 *MPa* to obtained values for natural frequencies of and compare with the results reported by Pelling et. al [32]. The results were far from the result reported by Pelling et. al [32].

A Three-Dimensional finite element modal analysis for Saccharomyces Cerevisiae was done two times for the spherical cell; one time considering the elastic modulus of 0.6 *MPa* and the second time considering the elastic modulus of 110 *MPa* for cell membrane. The natural frequencies obtained considering 0.6 *MPa* Young modulus, started from 13 *kHz* for the first and 0.18 *MHz* for the second mode. Natural frequencies were obtained for elastic modulus of 110*MPa* as well. For this value of elastic modulus, first natural frequency was 0.2 *MHz* and the second was 2.5 *MHz*.

P.V. Zinin has reported the value of second natural frequency of cell, which relates the natural frequency of 0.16 *MHz* for the cell wall with Young modulus of 0.6 *MPa* and second natural frequency of 2.05 *MHz* for the cell wall with young modulus of 110 *MPa* [44]. The comparison of our results with these values shows a reasonable agreement between the second natural frequencies.

Chapter 5 - Experimental works and results

5.1. Experimental analysis

Since measurement of alive cells is a very challenging task and it needs very sophisticated and specialized equipments that were not available for this work and due the fact that direct measurement of the resonant frequency of alive cells is not part of this work, some scaled up models of cell are considered for modal analysis using experimental methods. Experimental tests are performed on four typical elastic spheres full filled with different dimensions and the results are compared with those obtained from FE analysis. The main objective of testing the spheres with different fluid and different dimensions is to determine their natural frequencies based on their size and fluid properties and use these results to validate the FE analysis of the cell. Although this is a very linear approach that would not really match the biomaterials with non-linear behaviors, the approach of scaled up model was used since measurement of such systems is easy and really available in the laboratory. Table 5.1 shows the specification of different specimens used for test.

Table 5.1 -- Specification of different specimen used for test.

	Specimen1 - filled with water	**Specimen2 - filled with water**	**Specimen3 - filled with water**	**Specimen4 -filled with fluid**	**Specimen5 -containing inner sphere**
Radius*(mm)*	29	37	43	37	37
Density (kg / m^3)	970	970	970	1200	970

5.1.1. Experimental setup

The experimental setup is shown in Figure 5.1. As seen in the Figure 5.1, a shaker unit, which provides the sinusoidal displacement, is used to create frequency sweep from 1 *Hz* to 100*Hz*. A Laser Vibrometer detects the magnitudes of the vibration and the transformation to the frequency domain of the time domain and data will yield the frequencies of the specimen. The cursor values are saved from signal analyzer.

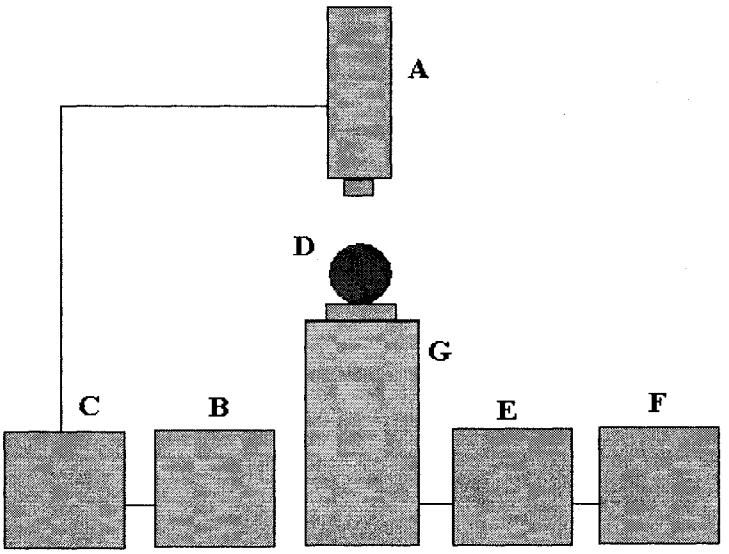

A- Laser Vibrometer
B- Signal Analyser Unit (BK 2035)
C- Power Supply
D- Specimen
E- Power Amplifier
F- Signal Generator
G- Shaker

Figure 5.1 -- Schematic diagram of experimental setup

A signal generator that generated a sinusoidal wave motion with sweep time 12 *Sc* and sweep frequency from 1 to 100 *Hz* drove the shaker. This sweep was transferred to the samples through the shaker.

The magnitude of the specimen frequencies is measured using a Helium Neon Laser Vibrometer from the vertical and lateral positions. The generated frequencies by all of the specimens are measured and monitored on the signal analyzer.

The natural frequencies obtained from Signal Analyzer are displayed on a monitor as illustrated in Figure 5.2.

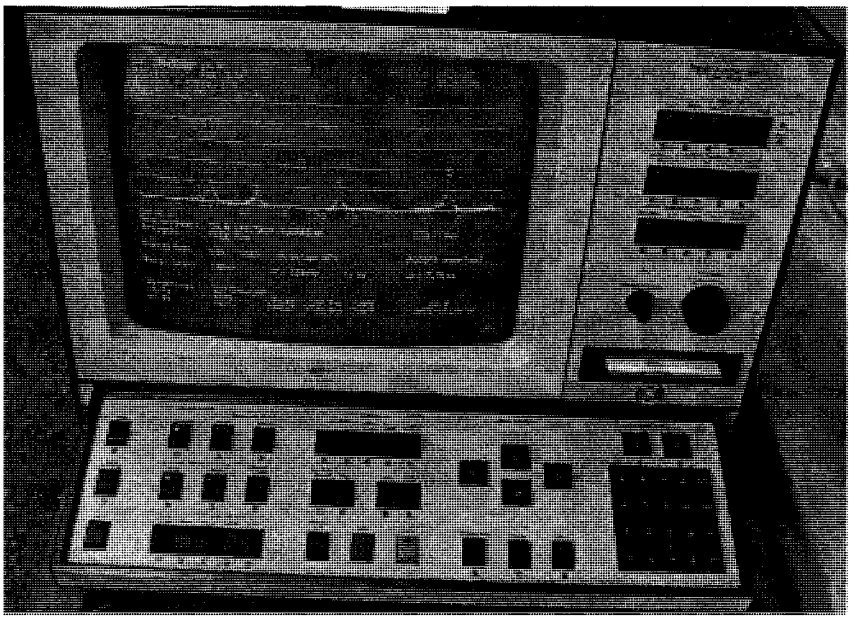

Figure 5.2 – Natural frequencies in Signal Analyzer

The equipment and their specifications used in the experimental set up are listed as follows:

- Power Amplifier:
  Amplification gain: 0-10
  Range: 3-1-30 V
  Current Limit: 0-24 amperes
  Displacement limit pk-pk: 0.2-2 inches

- Signal Generator: Agilent 33220A
  20MHz Function/Arbitrary Waveform Generator

- Shaker: 4812 s/n 342330 made by Büel & Kjær.
  Useful frequency range: 5 ~ 13000Hz;
  Displacement Limit: 12.7;
  Current Limit: 0-22 amperes
  Bolt torque: 0.35 kg m;

- Power Supply: Type 2815. made by Büel & Kjær
  Amplifier factor: 10mv/lbf

- Dual Tracking Power Supply : Model GPC-3030D
  Useful Amplifier factor: 1V/lbf

- Signal Analyser Unit
  Range: 0-50 Hz
  Resolution: 125 mHz
  Amplitude: 100 mV (pk-pk)
- Helium Neon Laser -Class 2

The complete experimental set up with all the electronic components and the display unit is shown in the Figure 5.3.

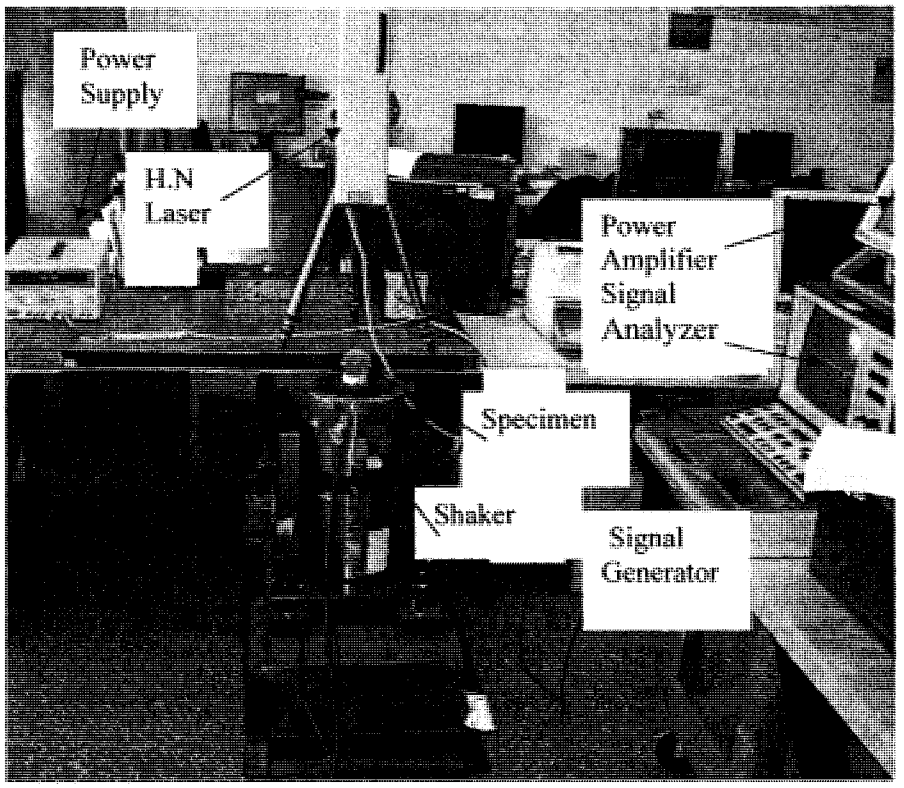

Figure 5.3 -- Photograph of the complete setup

The specimens are placed on the rigid stand on the shaker. A sinusoidal wave shape dynamic motion is applied by the shaker, which is activated by the signal generator. The output from the Helium Neon Laser Vibrometer is sent to signal analyzer. The data is further post processed on a desktop computer.

5.1.2. Tests and results

Different specimens are used for test. Natural frequencies are obtained from top or vertical and from side or lateral as shown in Figure 5.4 and 5.5.

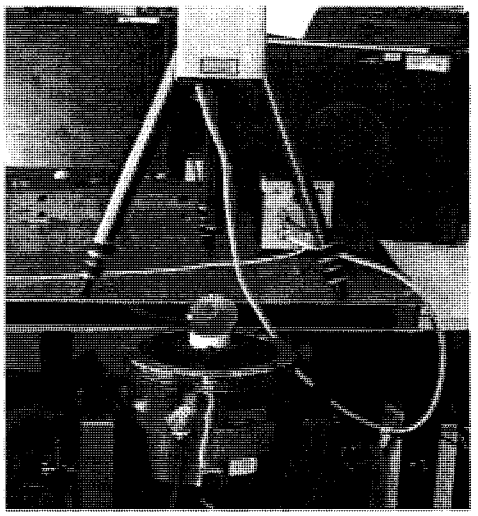

Figure 5.4 -- Measuring natural frequency from top

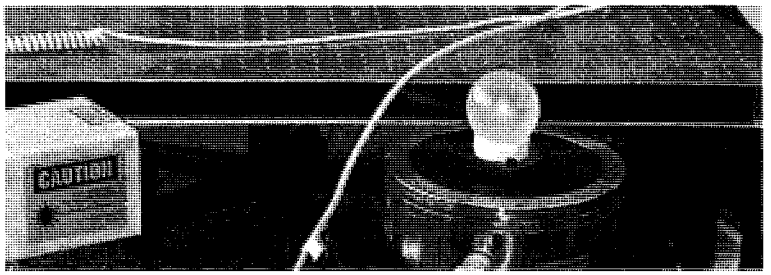

Figure 5.5 -- Measuring natural frequency from side

The effect of radius on natural frequency is studied. For this purpose, three different sizes of specimens filled with water are used. The radiuses of the specimens are 29 *mm,* 37 *mm* and 44 *mm* respectively.

In Figure 5.6, the obtained data corresponding to four natural frequencies of the specimen filled with water are shown. The radius of the specimen is 29 *mm*.

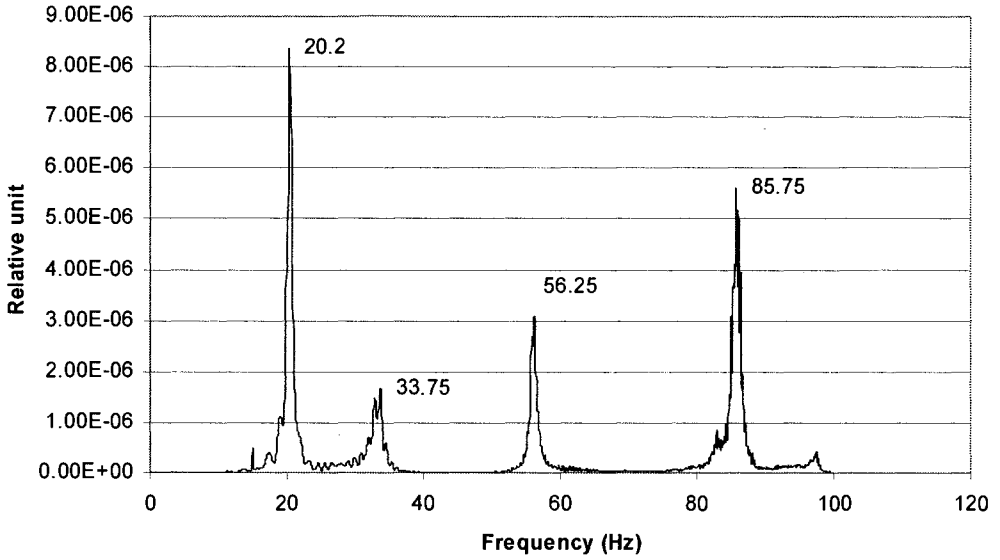

Figure 5.6 -- Natural frequencies detected from top for the radius of 29 *mm* specimen filled with water

As mentioned before, the natural frequencies are obtained from two directions. Figure 5.7 shows the natural frequencies measured laterally.

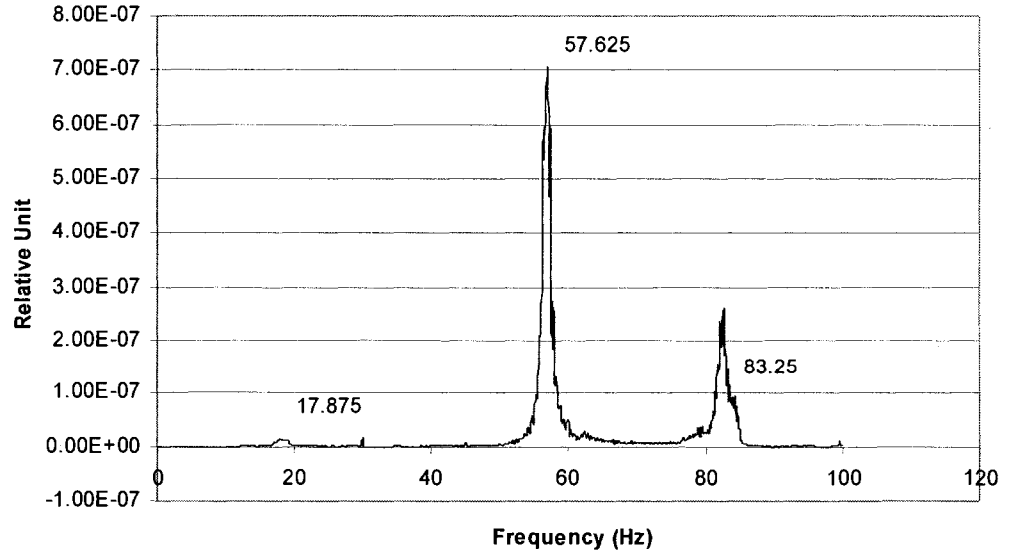

Figure 5.7 -- Natural frequencies detected from side for the radius of 29 *mm* specimen filled with water

Figure 5.8 and 5.9 show the frequencies measured from two directions. The specimen is filled with water with radius of 37 *mm*.

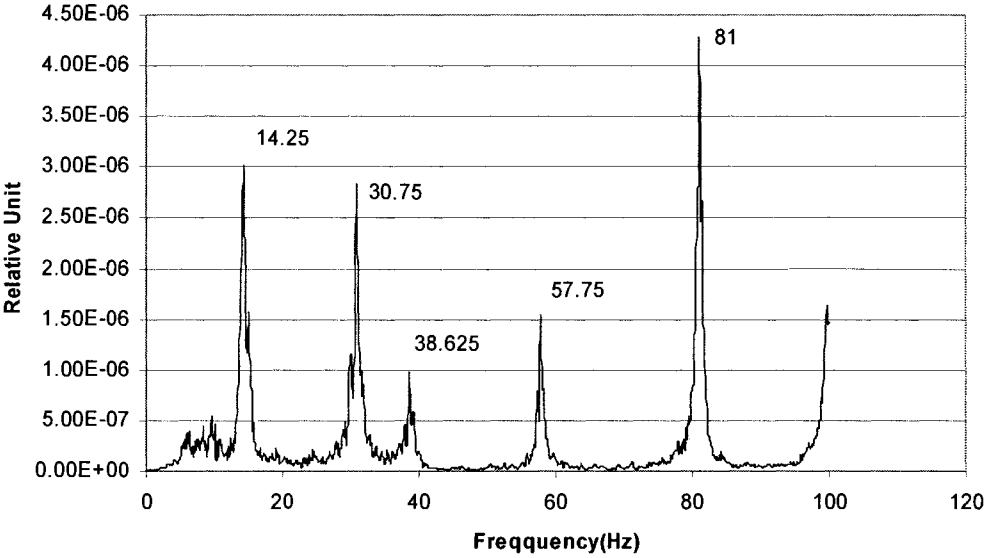

Figure 5.8 -- Natural frequencies detected from top for the radius of 37 *mm* specimen filled with

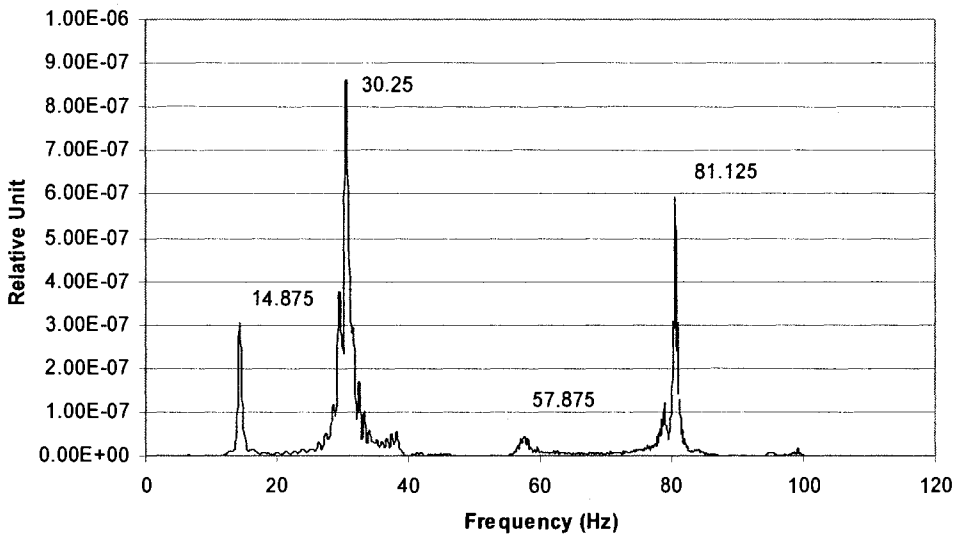

Figure 5.9 -- Natural frequencies detected from side for the radius of 37 *mm* specimen filled with water

The last specimen, which is filled with water, has the radius of 44 *mm*. The corresponding natural frequencies for two directions are shown in Figure 5.10 and 5.11

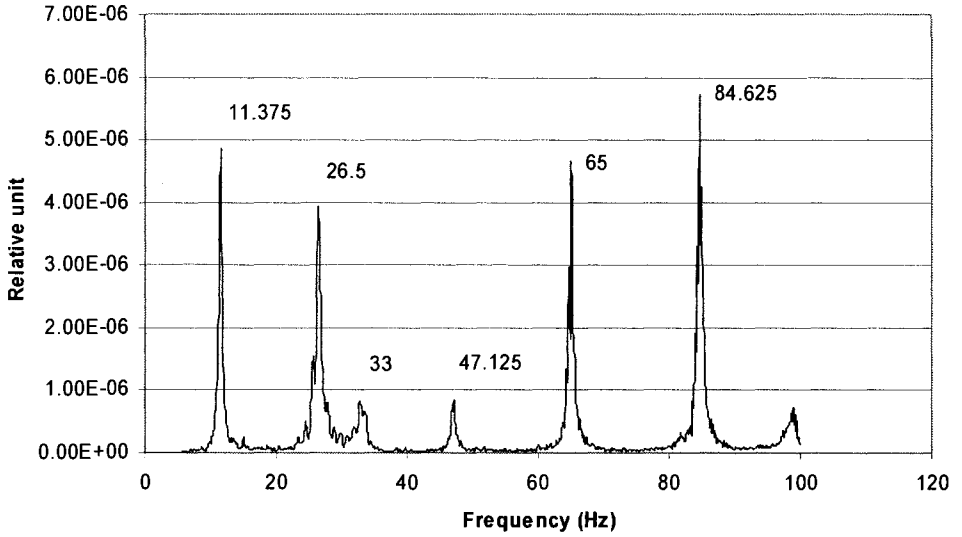

Figure 5.10 -- Natural frequencies detected from top for the radius of 44 *mm* specimen filled with water

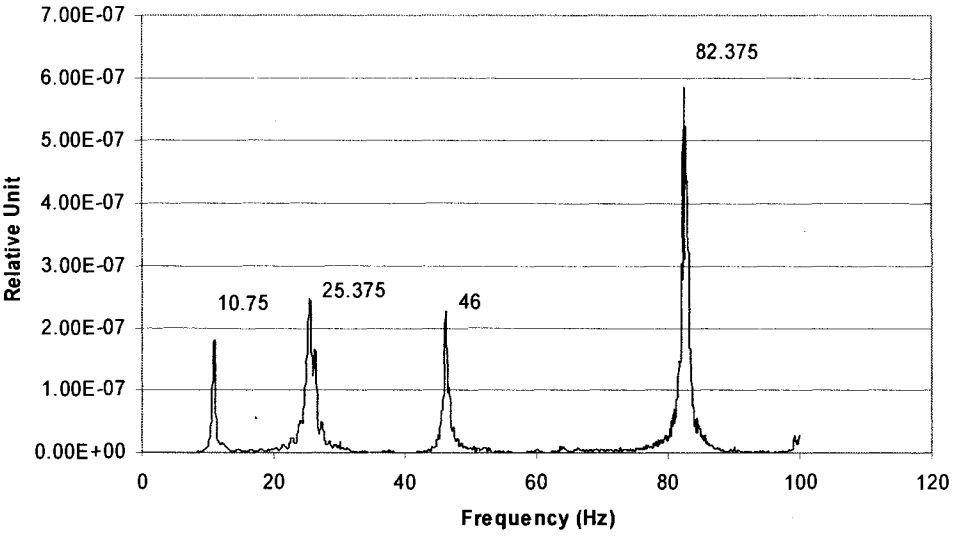

Figure 5.11 -- Natural frequencies detected from side for the radius of 44 *mm* specimen filled with water

To find out the effect of fluid density on the natural frequencies; the specimen has been filled with a fluid with the density higher than water. The radius of specimen is 37 *mm,* the same as second specimen filled with water. The obtained frequencies are shown in Figure 5.12 and 5.13

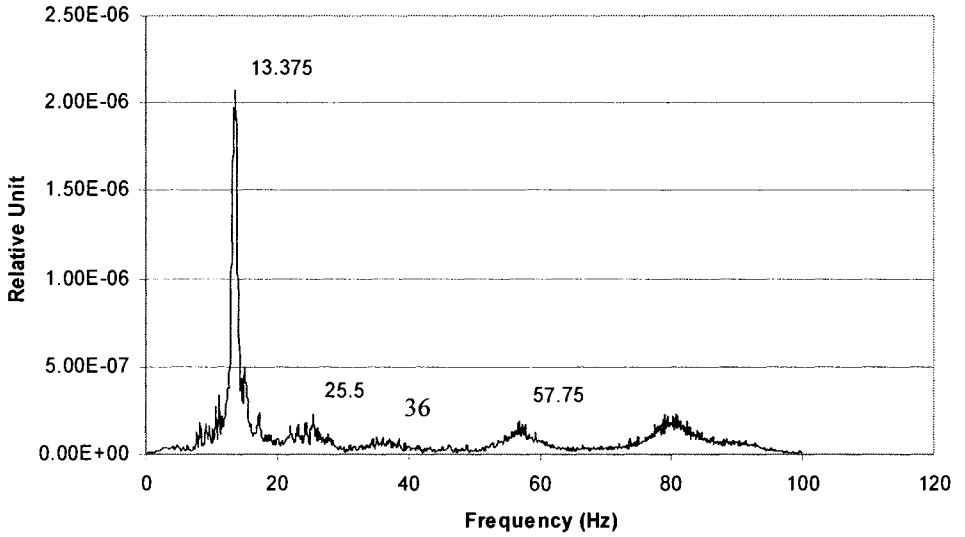

Figure 5.12 -- Natural frequencies detected from top for the specimen filled with fluid with density of 1200 *Kg/m3* and radius of 37 *mm*

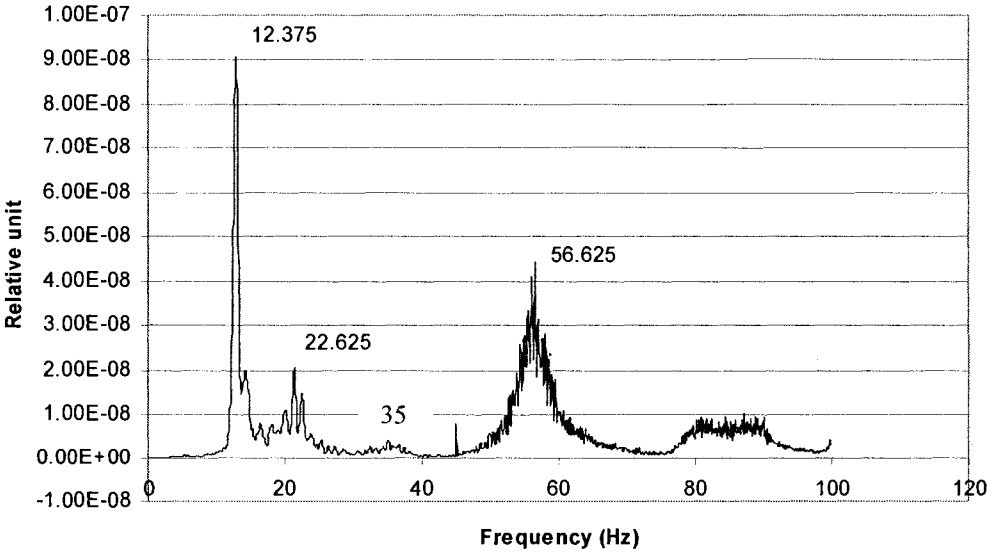

Figure 5.13 -- Natural frequencies detected from side for the specimen filled with fluid with density of 1200 *Kg/m3* and radius of 37 *mm*

Since the fluid with more density will increase the damping of the system because more viscous media and large mass, reduce the resonance frequency. Figure 5.14 shows how natural frequencies decrease as the effect of increasing density.

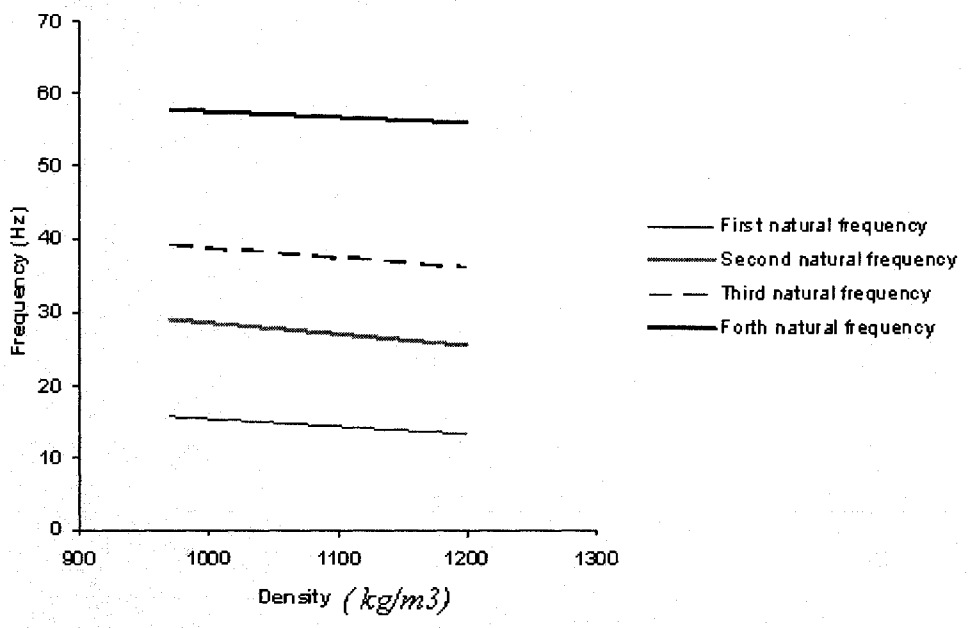

Figure 5.14 -- Comparison natural frequencies of specimen with the radius of 37 *mm* filled with water and fluid with density of 1200 *Kg/m3*

The values of natural frequencies decrease as the radius of specimens increase. This is due to increasing the mass of the system. Figure 5.15 shows the values of natural frequencies of specimens from the first to the forth-natural frequencies of specimens with radius of 29*mm*, 37 *mm* and 44 *mm*.

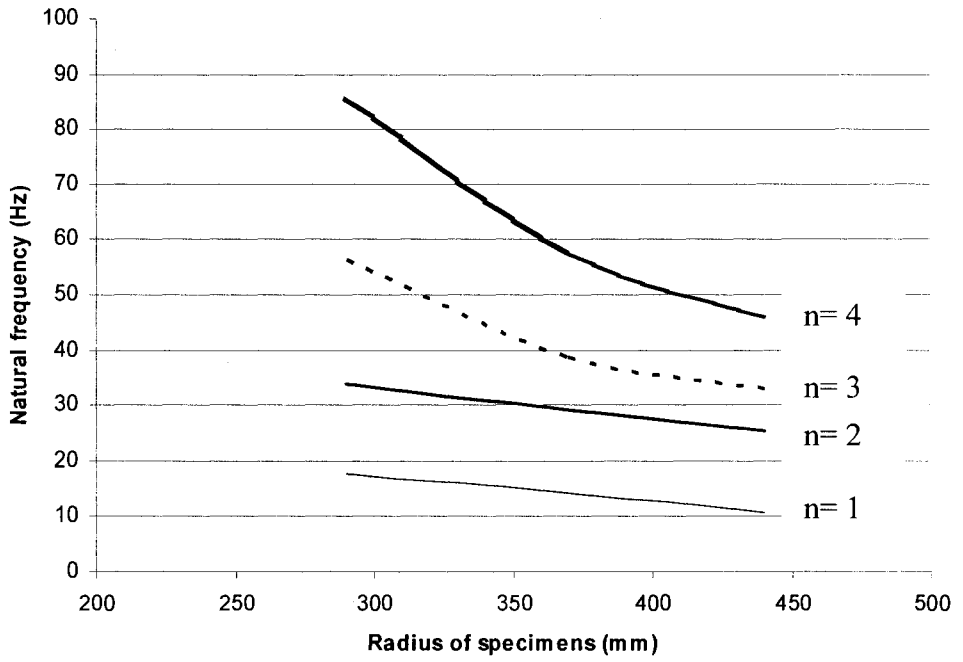

Figure 5.15 -- Comparison natural frequencies of specimens with the radius of 29 *mm*, 37 *mm* and 44 *mm*

To observe the effect of having inner sphere or nucleus in natural frequencies of the specimen, we located a water-filled sphere inside another sphere that is filled with water. Figure 5.15 shows the specimens that are used in experiment also the floating Inner sphere (nucleus) inside one of the specimens.

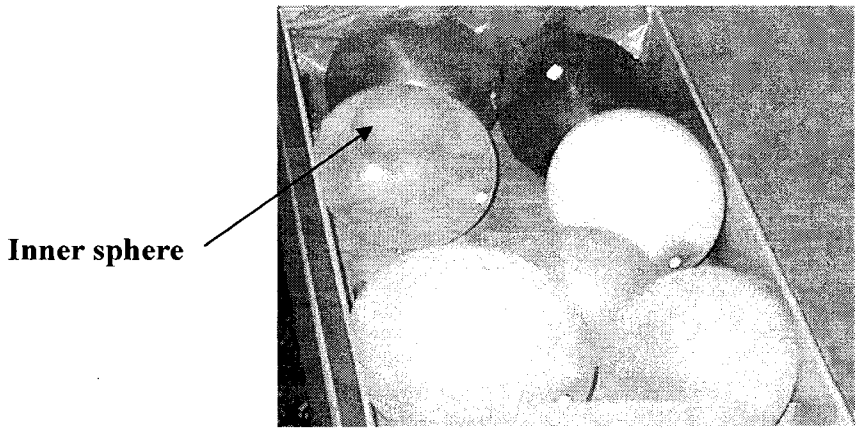

Figure 5.16 -- Specimens and inner sphere inside the specimen

The corresponding natural frequencies for two directions are shown in Figure 5.17 and 5.18

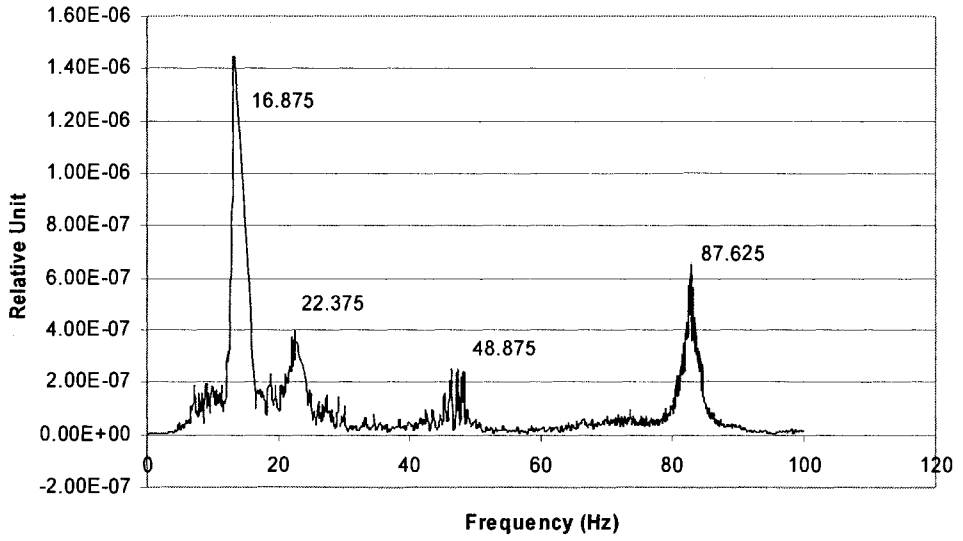

Figure 5.17 -- Natural frequencies detected from top of specimen with radius of 37 *mm* containing the inner sphere.

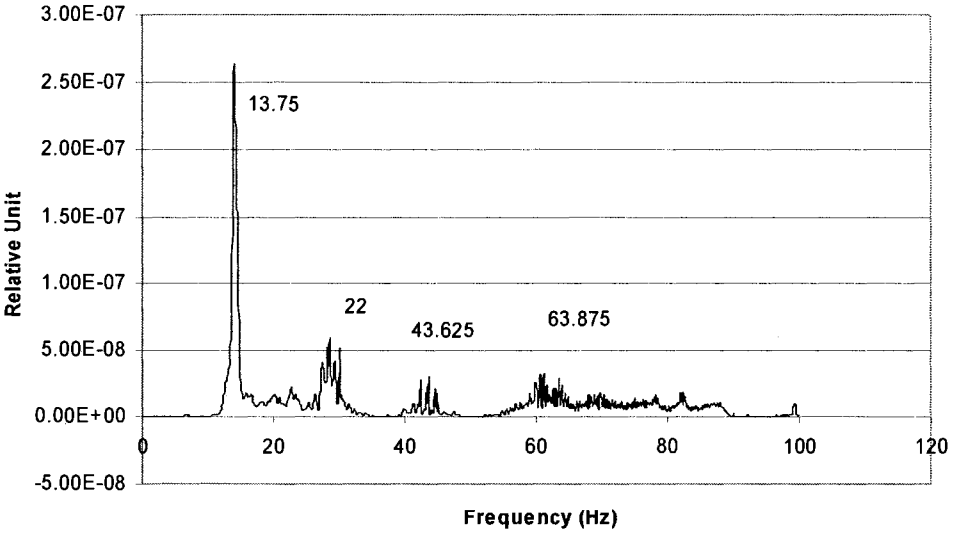

Figure 5.18 -- Natural frequencies detected from side of specimen with radius of 37 *mm* containing the inner sphere.

Table 5.2 allows direct comparison of the frequency shifts associated with inner sphere.

Table 5.2 -- Comparison of natural frequencies by experiment for water filled scaled up model of cell with and without the inner sphere (radius = 37 *mm*)

Natural frequencies	First mode *Hz*	Second mode *Hz*	Third mode *Hz*
Elastic sphere Without inner sphere	14.25	30.75	38.62
Elastic sphere containing inner sphere	13.75	22	43

The attitude of a smaller sphere (nucleus like) in the large sphere (cell like) indicates a reduction in the first resonant frequency is about 3.5%. The second resonant frequency also is lower by 28.5 %. However, the third resonant frequency comes higher by 11.3%, which clearly indicates a very non- linear behavior of the system.

5.2. FEA of fluid filled spheres

Four specimens are used throughout the finite element simulations to compare with the results obtain form experiment.

For each of the above specimens, values of natural frequencies are obtained by post-processing the ANSYS results.

The problem is solved for three scaled up models of cell with different radius; 29 *mm*, 37 *mm* and 43 *mm*, filled with water and for a specimen filled with a fluid with the density higher than the density of water and the radius of 37 *mm*. The thickness of the specimen in stretch mode is about 80 μm.

The elastic modulus of membrane has been measured and is kept constant a 1.9 *MPa*. The Poisson's ratio of 0.45 is obtained for the membrane. The model created in ANSYS is the same as illustrated on Figure 4.3.

The element type used for the analysis for this model as described in chapter 4 is SHELL 41 for the membrane and SOLID187 for the inner sphere or fluid. A node-to-surface contact elements has been used between the spherical membrane or target surface (meshed with TARGE 170) and the contact surface or the inner sphere (meshed with CONTA 175).

At the experimental test, as shown is Figure 5.19, the specimen is placed on a rigid stand on the shaker.

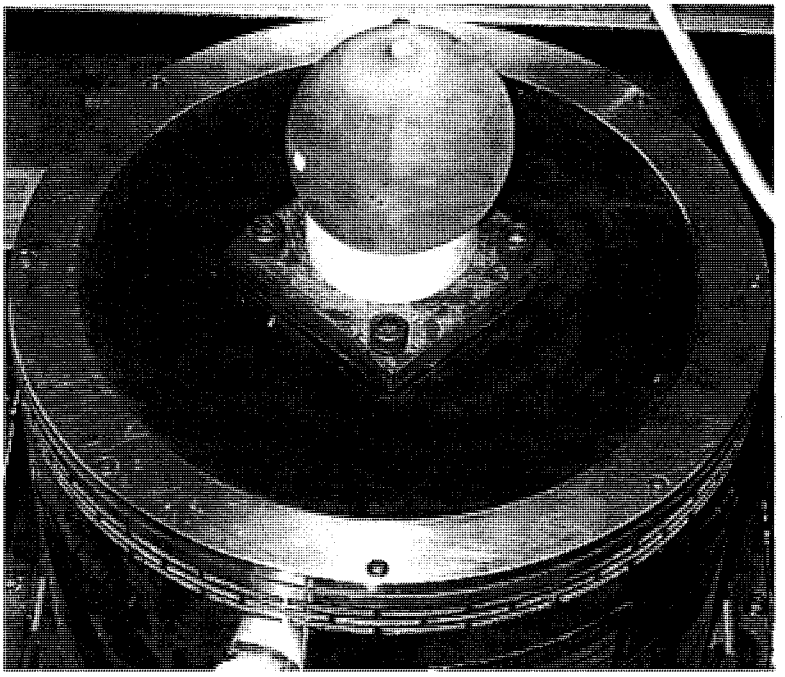

Figure 5.19 -- Fluid filled scaled up model of cell

The same boundary condition is applied for the scaled up models of cell. Figure 5.20 shows the boundary condition considered for the scaled up model of cell.

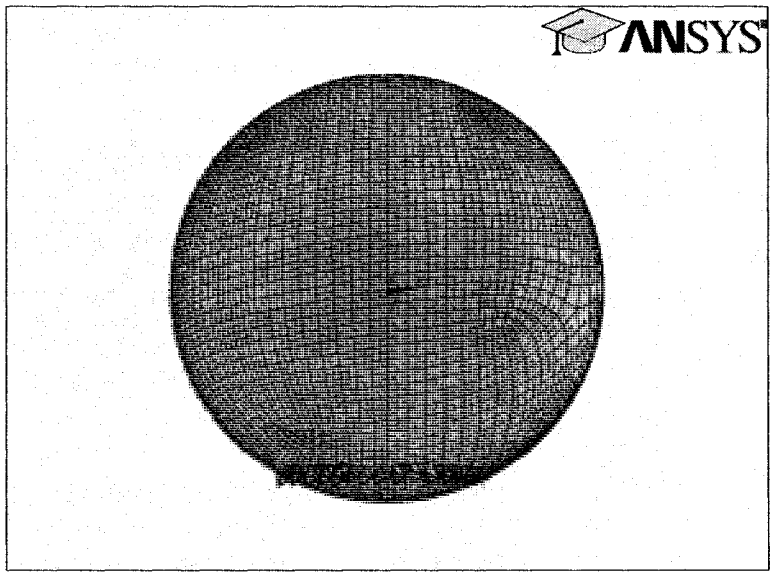

Figure 5.20 -- Boundary conditions for fluid filled scaled up model of cell

Figures 5.21 and 5.22 show the first and second natural frequencies and mode shapes for scaled up model of cell with radius of 29 *mm*.

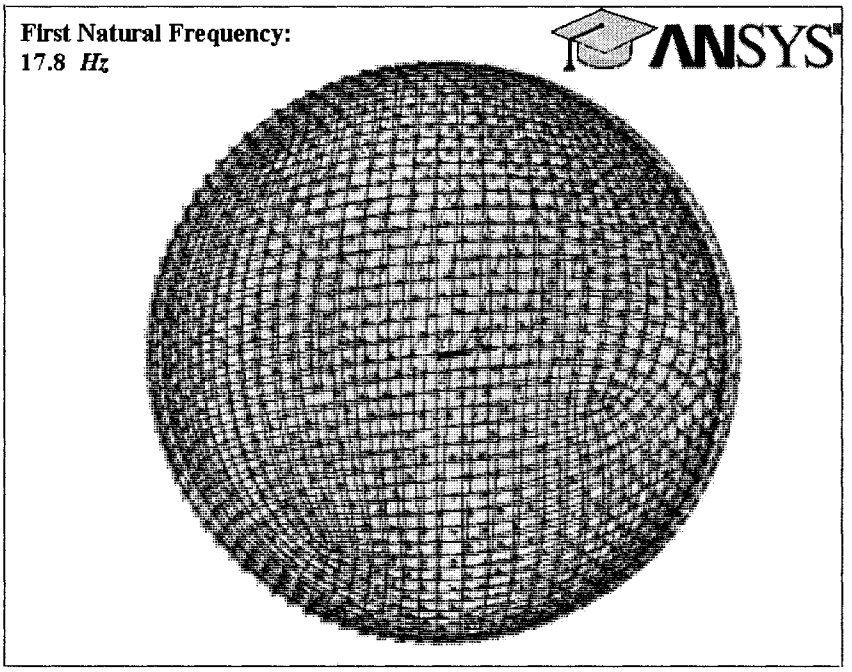

Figure 5.21 -- First natural frequency for the radius of 29 *mm* specimen filled with water

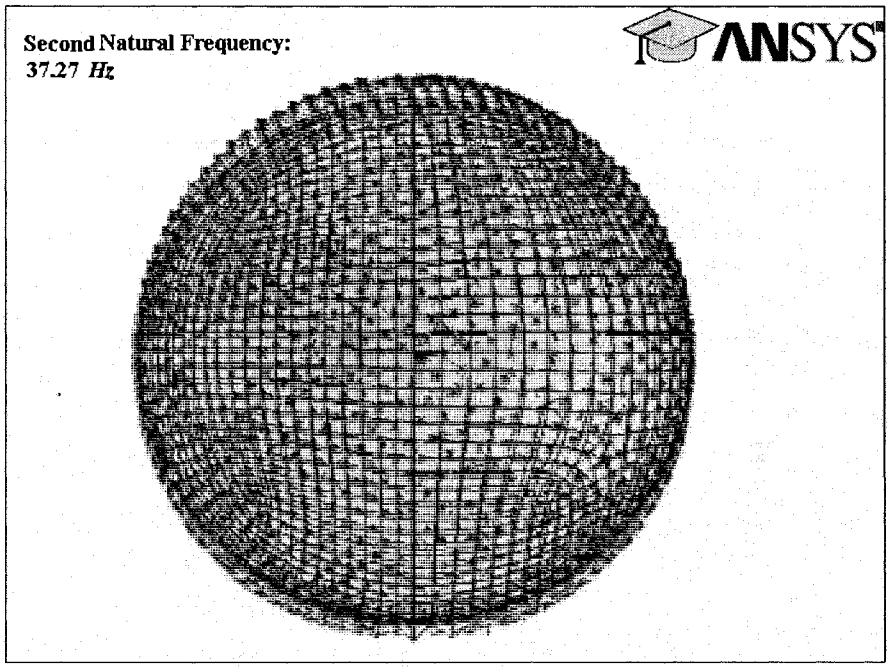

Figure 5.22 -- Second natural frequency for the radius of 29 *mm* specimen filled with water

The following table shows the first and second natural frequencies obtained by FEA for the specimen with radius of 29 *mm* and the corresponding natural frequencies, which are obtained experimentally.

Table 5.3 -- Comparison of natural frequencies obtained by FEA and experimental works for water filled scaled up model of cell (radius = 29 *mm*)

Natural frequencies	Numerical (FEA) *Hz*	Experimental *Hz*	Difference (%)
First natural frequency	17.8	17.875	0.4
Second natural frequency	37.27	33.75	15.5

The FEA further is done for the rest of specimens with radius of 37 *mm* and 44 *mm*. The FEA results as compare with the results, which are obtained experimentally. The results for both FEA and experiment are given in Table 5.4 for the specimen with radius of 37 *mm*.

Table 5.4 -- Comparison of natural frequencies obtained by FEA and experimental works for water filled scaled up model of cell (radius = 37 *mm*)

Natural frequencies	Numerical(FEA) *Hz*	Experimental *Hz*	Difference (%)
First natural frequency	14.25	14.875	4.2
Second natural frequency	32.56	30.75	5.8

Table 5.5 shows both the FEA and the experimental results for the specimen with radius of 44 *mm*.

Table 5.5 -- Comparison of natural frequencies obtained by FEA and experimental works for water filled scaled up model of cell (radius = 44 *mm*)

Natural frequencies	Numerical(FEA) *Hz*	Experimental *Hz*	Difference (%)
First natural frequency	12.789	10.75	18.9
Second natural frequency	24.80	26.5	6.4

To determine the effect of fluid inside the specimens on the natural frequency, one of the specimens is filled with a fluid with density higher than water. The results obtained by FEA for fluid with high-density regarding the density of water and the results, which are obtained experimentally, are shown in Table 5.6. Density of fluid is 1200 *kg/m3*.

Table 5.6 -- Comparison of natural frequencies obtained by FEA and experimental works for the scaled up model of cell filled with a fluid with density of 1200 *Kg/m3* (radius = 44 *mm*)

Natural frequencies	Numerical(FEA) *Hz*	Experimental *Hz*	Difference (%)
First natural frequency	13.57	12.375	9.6
Second natural frequency	29.851	25	19.4

Since the fluid with more density will increase the damping of the system because more viscous media and large mass, reduce the resonance frequency.

5.3. Summary

In this chapter, to verify the results obtained form FEA, some scaled up models of cell are considered for modal analysis using both FEA and experimental methods.

Testing the scaled up models of cell with different dimensions was used to determine their natural frequencies based on their size and fluid properties. In parallel, the numerical method that was used for cell modal analysis was employed to determine the natural frequencies of scaled up models of cell to show the agreement between the finite element and experimental analysis. The differences between the results obtained from FEA and experimental analyses were in reasonable band. This indicates a reasonable good agreement between the finite element and experimental analyses.

Chapter 6 - Conclusion and proposed future works

This chapter is devoted to the summary of the work and conclusions of this study and to some proposed future works.

6.1. Summary of work

Both finite element and experimental modal analyses on scaled up models of cell are employed to determine the mechanical properties of the living cells. Since many cells have a spherical shape, a spherical shape of the cell is considered for this analysis. The natural frequencies and corresponding mode shapes are determined for specific types of cells whose elastic properties of the membrane have been experimentally measured. To validate the numerical analysis, an experimental set up designed to measure the natural frequencies of scaled up models of cell. Tests are carried out on the specimens with various diameters and fluids to investigate the effect of these parameters on the natural frequencies. In parallel, the numerical method that was used for cell modal analysis is employed to determine the natural frequencies of scaled up model of cell to show the agreement between the finite element and experimental analysis. The results obtained from the finite element modal analysis of cell are compared to the latest reports in the literatures on the values of natural frequencies of cell.

6.2. Conclusions

In Chapter 3, we considered a spherical model for biological cells using numerical method (FEA) to determine the natural frequencies of the specific types of biological cells. The main objective of this chapter was to verify the correctness of the FEA for this analysis through two different commercial FEM software and gain confidence.

Modal analysis was carried out for an empty spherical cell with both FE softwares ANSYS and COMSOL in Chapter 4.1. The software COMSOL was used to validate the data obtained form ANSYS. Comparison of the results shows that the values for the natural frequencies of empty spherical cell using COMSOL with respect to FEA using ANSYS have an average error of 7%. The difference between two analyses would be due to the differences in element types in two analyses. The element that is used in FEA using COMSOL has the properties of an elastic shell while the element SHELL 41, which is employed in FEA using ANSYS, is an element with membrane properties. The results show that the FE approaches using ANSYS and COMSOL agree with each other in a reasonable band. The research is continued with FE approaches using ANSYS to create a Three-Dimensional model for fluid filled spherical cells. To our knowledge, there is only one experimental observation (using AFM) of the resonances for spherical cells, which Pelling et. al [32] reports the natural frequencies in the range of 0.8-1.6 *kHz* for Saccharomyces Cerevisiae. The natural frequencies are obtained by FEA considering Young's modulus of 0.75 *MPa* reported by Pelling et. al [32], start from 26 *kHz* for the first and 0.34 *MHz* for the second mode of vibration. Comparison of the results obtained from our FE modal analysis of cell with elastic modulus of 0.75*MPa* shows that the

frequency of the resonance oscillations of the yeast cells is much higher than 0.8-1.6 *kHz*, which is detected by Pelling et. al [32]. It is believed that the resonances detected by Pelling et. al [32] using AFM are not related to the mechanical resonances of cell vibration. The AFM cantilever beam and the cell might be coupled and the overall frequency reduces to the value measured by Pelling et. al [32].

Because of the fact that the value of Young's modulus reported in the literatures are so different (0.6 *MPa* and 110 *MPa*), in Chapter 4.2 a Three-Dimensional finite element modal analysis for fluid filled spherical cells were carried out for two different Young's modulus for cell wall. The natural frequencies obtained considering 0.6 *MPa* Young modulus, start from 13 *kHz* for the first and 0.18 *MHz* for the second natural frequency. Natural frequencies were obtained for elastic modulus of 110*MPa* as well. For this value of Young's modulus, first natural frequency was 0.2 *MHz* and the second was 2.5 *MHz*.

Latest report on the values of second natural frequency of cell relates the natural frequency of 0.16 *MHz* for the cell wall with Young's modulus of 0.6 *MPa* and second natural frequency of 2.05 *MHz* for the cell wall with young's modulus of 110 *MPa* [44]. The comparison of our results with these values shows a reasonable agreement between the second natural frequencies.

In Chapter 5, the FEA program used to perform the modal analysis of the Saccharomyces Cerevisiae was employed to some scaled up models of spherical cell, which their natural frequencies were measured from two normal directions experimentally. The scope of this work was to validate the FEA code. The differences between the results obtained from FEA and experimental analysis was reasonable and had an average error 9 %. This error should be due to inaccuracies in measuring the specimen's mechanical properties for

instance Young's modulus and Poisson's ratio and the assumptions that were considered for the FEA. The assumption such as ignoring the fluid surface interaction element, which was neglected in the model since this kind of element was not available in the available ANSYS version, and considering the element SOLID 187 instead of appropriate fluid element for the fluid or the cytoplasm inside cell. However, comparison of the results indicates a reasonable good agreement between the finite element and experimental analysis. This indicates that the FEA approach used to model the Saccharomyces Cerevisiae with the aim of obtaining natural frequencies is the most appropriate and accurate model for spherical cells.

6.3. Proposed future works

There are investigations that could not be included in this thesis which, however, would provide better understanding and will be useful.

1- This work did not consider the effects of other cell organelles like nucleus; an assumption that the role of the organelles is negligible was made. For more precise results, this should be taken into account in future works. Through more detailed models, however, the commercial version of ANSYS may be needed for this simulation.

2- The ANSYS software available was the educational version and particular limitations in terms of the maximum number of elements (16,000) and/or nodes (32,000). Work with the other version of ANSYS with possibility of having number of element more than 16,000 may be required to achieve more accurately the mode shapes for third and forth natural frequencies.

3- The fluid surface interaction element was not available in the available ANSYS version and such interaction was neglected. More works is required to define the cytoplasm as a fluid and define the fluid surface interaction element between fluid and shell to achieve results that are more accurate.

4- Another main aspect of the simulation of the cell is to consider the effect of fluids on cell because, in reality, cells interact with fluids inside the body.

5- Cell membrane is a flexible lipid bilayer and the thickness of membrane is variable. In this work, the number of layers considered for the membrane is one because of lacking the mechanical properties of each layer and problems in mesh generation. More work is also required to achieve better results with having that properties and successful meshing through designing an appropriate type of element that is not available in the present version of ANSYS.

References

1. Goldmann W. H, "Mechanical aspects of cell shape regulation and signaling", Cell Biology International, 26, pp. 313-317, 2002.
2. Christopher Moraes, Craig A. Simmons, and Sun Ya., "Cell mechanic meet MEMS" CSME Bullten SCGM , Fall 2006.
3. Bao G., and Suresh S., "Cell and molecular mechanics of biological materials", J. Nature Materials, Vol. 2, pp. 715-725, 2003.
4. Hochmuth R. M., "Micropipette aspiration of living cells", J. Biomechanics, Vol. 33, pp. 15–22, 2000.
5. Secomb T. W., "Red-blood-cell mechanics and capillary blood rheology", Cell Biophysics, Vol. 8, pp. 231–51, 1991.
6. Hochmuth R. M., Ting-Beall H. B., Beaty B. B., Needham D., and Tran-Son-Tay R., "Viscosity of passive human neutrophils undergoing small deformations", J. Biophysical, Vol. 64, pp. 1596–601, 1993.
7. Sato J., Levesque M. J., and Nerem R. M., "Micropipette aspiration of cultured bovine aortic endothelial cells exposed to shear stress", J. Arteriosclerosis, Vol. 7, pp. 276–86, 1987.
8. Vliet K. J., Bao G., and Suresh S. "The biomechanic toolbox: experimental approach for living cell and biomolecules", J. Acta Materialia , Vol. 51, pp. 5881-5905, 2003.
9. Lehenkari P. P., Charras G. T., Nesbitt S. A., and Horton M. A., "New technologies in scanning probe microscopy for studying molecular interactions in cells", Expert Rev. Mol. Med., pp. 1–19, 2000.

10. Hansma H. G., Kim K. J., Laney D. E., Garcia R. A., Argaman M., Allen M. J., and Parsons S. M., "Properties of biomolecules measured from atomic force microscope images", J. Struct. Biol., Vol. 119, pp. 99–108, 1997.

11. Binnig G., and Quat C. F., "Atomic force microscope", Physical Review Letters, Vol. 56, pp. 930–934, 1986.

12. Radmacher M., Tillmann R. W., Fritz M., and Gaub H. E., "From molecules to cells: Imaging soft samples with the atomic force microscope", Science, Vol. 257, pp. 1900–1905, 1992.

13. Bowen W. R., Lovitt R. W., and Wright C. J., "Application of atomic force microscopy to the study of micromechanical properties of biological materials", Biotechnology Letters, Vol. 22, pp. 893–903, 2000.

14. Fritz M., Kacher C. M., Cleveland J. P., and Hansma P. K. ,"Measuring the viscoelastic properties of human platelets with the atomic force microscope", Department of Physics, University of California, Santa Barbara 93106, USA.

15. Horton M., Charras G., and Lehenkari P., "Analysis of ligand-receptor interactions in cells by atomic force microscopy", J. Recept. Signal Transduct, Vol. 22, pp. 169–190, 2002.

16. Lehenkari P. P., and Horton M. A., "Single integrin molecule adhesion forces in intact cells measured by atomic force microscopy", J. Biochem. Biophys, Vol. 259, pp. 645–650, 1999.

17. Pesen D., and Hoh J. H., "Micromechanical architecture of the endothelial cell cortex", J. Biophys, Vol. 88, pp. 670–679, 2005.

18. Lehenkari P. P., Charras G. T., Nykanen A., and Horton M. A., "Adapting atomic force microscopy for cell biology", J. Ultramicroscopy, Vol. 82, pp. 289–295, 2000.

19. Radmacher M., "Measuring the elastic properties of biological samples with the AFM", IEEE Eng. Med. Biol. Mag., Vol. 16, pp. 47–57, 1997.

20. Rotsch C., Jacobson K., and Radmacher M., "Dimensional and mechanical dynamics of active and stable edges in motile fibroblasts investigated by using atomic force microscopy", Proc. Natl. Acad. Sci. U. S. A., 96, pp. 921–926, 1999.

21. Shroff S. G., Saner D. R., and Lal R., "Dynamic micromechanical properties of cultured rat atrial myocytes measured by atomic force microscopy", J. Physiol, Vol. 269, pp. 286–292, 1995.

22. Rotsch C., and Radmacher M., "Drug-induced changes of cytoskeletal structure and mechanics in fibroblasts:an atomic force microscopy study", J. Biophys, Vol. 78, pp. 520–535, 2000.

23. Haga H., Sasaki S., Kawabata K., Ito E., Ushiki T., and Sambongi T., "Elasticity mapping of living fibroblasts by AFM and immunofluorescence observation of the cytoskeleton", J. Ultramicroscopy, Vol. 82, pp. 253–258, 2000.

24. Matzke R., Jacobson K., and Radmacher M., "Direct, high-resolution measurement of furrow stiffening during division of adherent cells", J. Cell Biol, Vol. 3, pp. 607–610, 2001.

25. Rotsch C., Braet F., Wisse E., and Radmacher M.," AFM imaging and elasticity measurements on living rat liver macrophages", Cell Biol. Int., 21, pp. 685–696.

26. Puntheeranurak T., Wildling L., Gruber H. J., Kinne R. K., and Hinterdorfer P., "Ligands on the string: singlemolecule AFM studies on the interaction of antibodies

and substrates with the Na+ glucose co-transporter SGLT1 in living cells", J. Cell Sci, Vol. 119, pp. 2960–2967, 2006.

27. Sharma A., Anderson K. I., and Muller D. J., "Actin microridges characterized by laser scanning confocal and atomic force microscopy", J. FEBS Lett., Vol. 579, pp. 2001–2008, 2005.

28. Spudich A., and Braunstein D., "Large secretory structures at the cell surface imaged with scanning force microscopy", Proc. Natl. Acad. Sci. U. S. A. 92, pp. 6976–6980, 1995.

29. Parpura V., Haydon P. G., and Henderson E., "Three-dimensional imaging of living neurons and glia with the atomic force microscope", J. Cell Sci., Vol. 104, pp. 427–432, 1993.

30. Bowen W. R., Iilal N., Lovitt R. W., and Wright C. J.," Direct measurement of interactions between adsorbed protein layers using an atomic force microscope", J. Colloid Interface ,Vol. 197, pp. 348–352, 1998 .

31. Thie M., Rospel R., Dettmann W., Benoit M., Ludwig M., Gaub H.E., and Denker H.W., "Interactions between trophoblast and uterine epithelium: monitoring of adhesive forces", Human Reproduction, Vol. 13, pp. 3211–3219, 1998.

32. Andrew E. Pelling, Sadaf Sehati, Joan S. Valentine, and James K. Gimzewski , "Local Nanomechanical Motion of the Cell Wall of Saccharomyces cerevisiae", J. Science, Vol. 305, pp.1147-1150, 2004.

33. Guck, R. Ananthakrishnan, T. J. Moon, C. C. Cunningham, and J. Käs, "The Optical Stretcher - A Novel, noninvasive tool to manipulate biological materials", J. Biophys., Vol. 81, pp. 767-784, 2001.

34. Bausch, A. R., Ziemann, F., Boulbitch A., Jacobson K., and Sackmann, E., "Local Measurements of Viscoelastic Parameters of Adherent Cell Surfaces by Magnetic Bead Microrheometry", J. Biophysical, Vol. 75, pp. 2038-2049, 1998.

35. Basso N., and Heersche J.N.M., "Characteristics of in vitro osteoblastic cell loading models", J. Bone, Vol. 30, pp. 347-351, 2002.

36. DePaola N., Gimbrone M. A., and Davies P. F., "Vascular endothelium responds to fluid shear stress gradients", J. Arterioscler Thromb, Vol.12, pp. 1254–1257,1992.

37. You L., Cowin S. C., Schaffler M. B., and Weinbaum S.You L., "A model for strain amplification in the actin cytoskeleton of osteocytes due to fluid drag on pericellular matrix", J. Biomechanics, Vol. 34, pp. 1375-1386 , 2001.

38. Lu H., Koo L. Y., Wang W. C. M., Lauffenburger D. A., Griffith L. G., and Jensen K. F., "Microfluidic shear devices for quantitative analysis of cell adhesion", Anal. Chem., Vol. 76, pp.5257-5264, 2004.

39. Dennis E. Discher, Paul Janmey, and Yu-li Wang, "Tissue Cells Feel and Respond to the Stiffness of Their Substrate", J. Science, Vol.310, pp. 1139-1143, 2005.

40. Ackerman E., "Resonances of Biological Cells", J. Bull Math. Biophysics, Vol.13, pp. 93-106, 1951.

41. Ackerman E., "Cellular fragilities and resonances observed by means of sonic vibrations", J. Cellular and Comparative Physiology, Vol.39, pp. 167 – 190, 2005.

42. E. Ackerman, "Biophysical Science", Prentice-Hall, Engelwood Cliffs, N. J.,1962.

43- Zinin P. V., Levin V. M, and Maev R. G., "Self-oscillations of biological microbodies", J. Biofizika, Vol. 32, pp. 185-191, 1987.

44. Zinin P. V., Allen J. S., and Levin V. M., "Mechanical resonances of bacteria cells", J. Physical review, Vol. 72, pp. 1539-3755, 2005.

45. Andrew E. Pelling, Sadaf Sehati, Gralla B., and James K. Gimzewski, "Time dependence of the frequency and amplitude of the local nanomechanical motion of yeast" J. Nanomedicine: Nanotechnology, Biology, and Medicine, Vol.1, pp. 178–183, 2005.

46. Farid Amirouche, "Mechanical Testing and Finite Element Simulation", Mechanics of Cell, UIC Department of Mechanical Engineering, 842 West Taylor Street , Chicago, Illinois 60607, www.uic.edu/labs/brl/contact.htm.

47. Lamb H., "On the vibrations of an elastic sphere", Proceedings of the London Mathematical Society, No. 13, pp. 189-212, 1882.

48. Chree C., "The equations of an isotropic elastic solid in polar and cylindrical coordinates, their solution and application", transactions of the Cambridge Philosophical Society, Vol.14, pp. 250-269, 1889.

49. Sato Y., and Usami T., "Basic study on the oscillation of a homogeneous elastic sphere", Geophysics Magazine, Vol.31, pp.15-24, 1962.

50. Sato Y., and Usami T., "Basic study on the oscillation of a homogeneous elastic sphere", Geophysics Magazine, Vol. 31, pp.25-47, 1962.

51. Jiabg H., Young P. G., and Dichinson S. M., "Natural frequencies of vibration of layered hollow spheres using exact three dimensional elasticity equations" J. Sound and Vibration, Vol. 195, pp.155-162, 1996.

52. Lampwood E. R., and Usami T., "Free Oscillations of the Earth", Cambridge: Cambridge University Press, 1981.

53. Engin A. E., "The axi-symmetric response of a fluid-filled spherical shell to a local radial impulse, a model for head injury", J. Biomechanics, Vol. 2, pp. 325-341, 1969.

54. Advani S. H., and Lee Y. C., " Free vibrations of fluid filled shells", J. Sound and Vibration, Vol. 12, pp. 453-461, 1970.

55. Guarino J. C., and Elger D. F., "Modal analysis of a fluid-filled elastic shell containing an elastic sphere", J. Sound and Vibration, Vol. 156, pp. 461-479, 1992.

56. P. G. Young, "A parametric study on the axisymmetric modes of vibration of multi-layered spherical shells with liquid core of relevance to head impact modeling", J. Sound and Vibration, Vol. 256, pp. 665-680, 2002.

57. Boal D., "Mechanics of cell", Camberidge University press, 2002.

58. Smith C. A., "Cell biology / Smith and Wood", London, Chapman & Hall, 1996.

59. Daniel Kunkel, http://library.thinkquest.orgl.

60. Christopher C. Widnell, and Karl H. Pfenninger, "Essential cell biology", Baltimore, Williams & Wilkins, 1990.

61. Jennifer Bergman, University Corporation for Atmospheric Research (UCAR), University of Michigan, 2000.

62. Gabi Nindl Waite, and Lee R.Waite, "Applied cell and Molecular Biology for engineers", McGraw-Hill Companies, 2007.

63. Michael G. Pollacka, and Richard B. Fairb, "Electrowetting-based actuation of liquid droplets for microfluidic applications", American Institute of Physics, Vol. 77, pp.11, 2000.

64. ANSYS Inc. ANSYS Help document.

65. L. Weiss, "Biomechanical interactions of cancer cells with the microvasculature during hematogenous metastasis", J. Cancer Metastasis, Vol. 11, pp. 227 – 235, 1992.

66. Chen C. S., Mrksich M., Huang S., Whitesides G. M, and Ingber D. E., " Geometric control of cell life and death", J. Science, Vol. 276, pp.1425 -1428, 1997.

67. Cell cycle laboratory, http://www.sb-roscoff.fr/CyCell/Page12.htm.

68. Hartnmann C. H., and Delgado A., "Stress and Strain in a yeast cell under high hydrostatic pressure", Proc. Appl. Math. Mech., No.4, pp.316-317, 2004.

69. Hartnmann C. H., and Delgado A., "Numerical simulation of the mechanics of a yeast cell under high hydrostatic pressure", J. Biomechanics, Vol. 37, pp. 977-987, 2004.

70. Alexander E. Smith, Zhibing Zhang, Colin R., Thomas, Kennith E. Moxham, and Anton P. J. Middelberg, "The mechanical properties of Saccharomyces cerevisiae" Proc. Natl Acad Sci U S A, Vol.97, pp. 9871–9874, 2000.

71. Marston P. L., and Apfel R. E., "Quadrupole Resonance of Drops Driven by Modulated Radiation Stresses - Experimental Properties", J. Acoust. Soc., Vol.67, pp. 27-37, 1980.

Appendix I - Other structural parts of cells

I.1. Phospholipids bilayer

The cell membrane is actually a bilayer composed of phospholipids. Different types of phospholipids are shown in Fig I.1

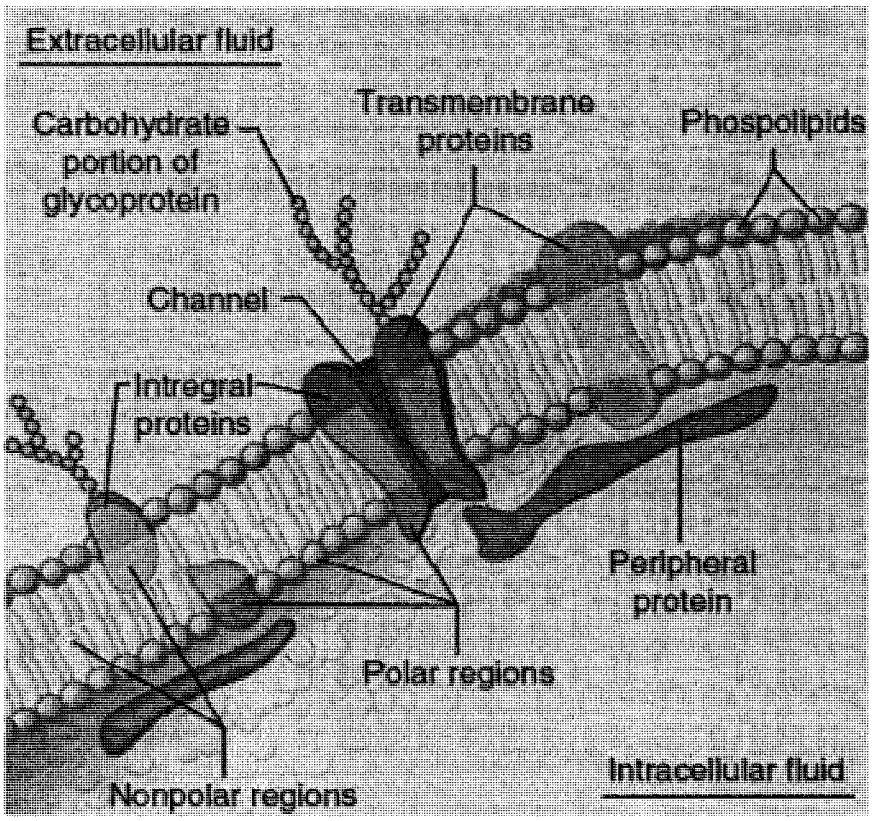

Figure I.1 -- Cell membrane. Membranes are composed of a phospholipid bilayer and associated proteins. Proteins include embedded, or integral proteins, as well as peripheral proteins on a surface of the membrane[62]

Theamphipathic (having two natures) character of phospholipids helps to maintain a hydrophilic (polar or water-soluble) and hydrophobic (no polar or non-water-soluble)

orientation to the cell membrane. This feature of the membrane causes water and other polar (water-soluble) molecules and compounds to stay on one side of the membrane[62].

I.2. Proteins

The phospholipid bilayer of the cell also includes a variety of proteins added to the membrane. The membrane is literally studded with proteins serving a myriad of functions. Membrane proteins fall into two broad categories: integral (incorporated into the membrane) proteins and peripheral (not embedded in the membrane) proteins. Integral proteins are also amphipathic like phospholipids. Integral proteins are not easily extracted from the membrane; however, they can move within the membrane. Peripheral proteins as the name implies are applied to a surface of the membrane though not embedded in the membrane. These proteins are polar like the surfaces of the membrane and found mostly on the intracellular side. These proteins are involved with the cellular skeleton [62]

I.3. Cytoskeleton

Eukaryotic cells have a wide variety of distinct shapes and internal organizations. Cells are capable of changing their shape, moving organelles, and in many cases, move from place to place. This requires a network a protein filaments placed in the cytoplasm known as the cytoskeleton.

The two most important protein filaments are called the actin filaments and the microtubules. The actin is responsbile for contraction (like in muscles) and the microtubules are for structural strength.

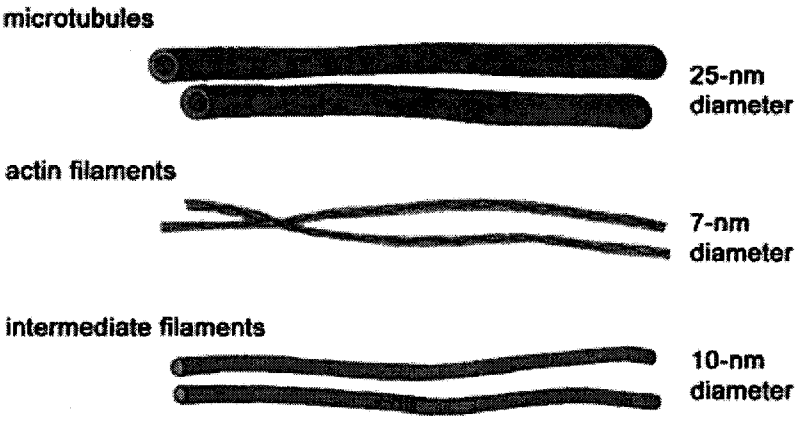

Figure I.2 -- Micro tubes and filaments of cytoskeleton [59]

I.4. Lysosomes

The term "some" means "body" and "lyse" means "destroy," so, a lysosome is a body which destroys. A lysosome is a membrane-bound vesicle (fluidfilled sack) containing enzymes (lysozymes) which can disrupt chemical bonds. The lysosomal membrane keeps enzymes segregated from the rest of the cell contents so that the degradative process is regulated[62].

Appendix II - Analysis in ANSYS

This section discusses details of modeling and analysis. In order to compare the results obtained above from the experimental model; commercially available software can be used, such as, NASTRAN, FEM Lab and ANSYS. The finite element analysis software ANSYS was used in our work with which modal, static and transient analysis can be carried out. With the help of advanced software geometrics, different load sets and materials properties can be analyzed. The ANSYS software used in our research was version 11 and was used to construct a complete geometric model for the living cell and scaled up models of cell to obtain the corresponding natural frequencies.

AII.1. Overview of ANSYS steps

When using ANSYS, all operations are performed using sequential steps. A flow chart, as shown in Figure II.1, is the basic approach to find a solution. We can use ANSYS in two different modes; either the programming mode or graphical mode we have used the programming mode in this work.

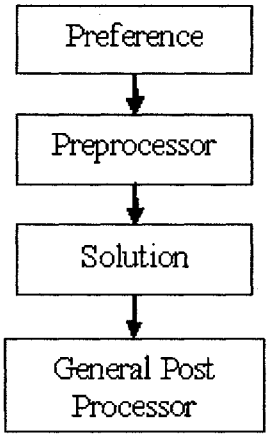

Figure II.1 -- Overview of Ansys steps.

AII.2. Preference

The first step in ANSYS is to describe the nature of problem and to decide the method to be used for solving the problem which, in our case, is of a structural nature. Different modules are available for performing the analysis such as h or p methods. We used the h method for solving our problem.

AII.3. Preprocessor

This is the main body of modeling the problem and defining the element type, materials properties and real constant. In this section, we first defined the element type and its materials properties since the selection of the element is the main process in modeling. The modeling and meshing were performed in the next step. The main operation performed in the preprocessor is given in the flowchart shown in Figure II.2.

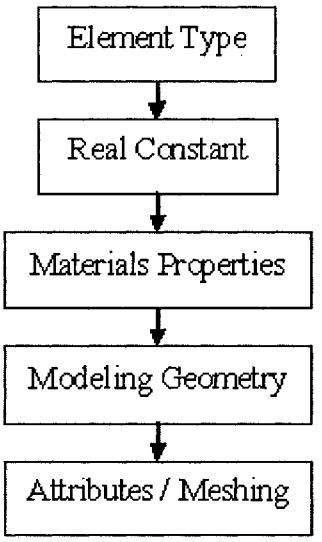

Figure II.2 -- Flow chart of processes in the preprocessor.

AII.4. Solution

In this section, the ANSYS solution of modeled problem is carried out by using the flow chart shown in Figure II.3. The first required entry is to define the analysis types such as static, harmonic, dynamic. Apply loads require entry of boundary conditions that apply to our model. The last step is to solve the meshed model.

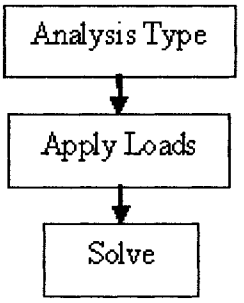

Figure II.3 -- Steps for solving Ansys model.

AII.5. General Post processor

In this section, data obtained as part of the solution section are reviewed using the many options available to see these results. Plot section and list section provide the results in the graphical presentation and numerical values, respectively. Any results such as stresses, strains, reactions at any point can be visualized using graphs.

AII.6. APDL (ANSYS Parametric Design Language)

APDL stands for ANSYS Parametric Design Language, a scripting language permit using automate common tasks or even build the model in terms of parameters (variables). While all ANSYS commands can be used as part of the scripting language, the APDL commands discussed here are the true scripting commands and encompass a wide range of other features such as repeating a command, macros, if-then-else branching, do-loops, and scalar, vector and matrix operations.

AII.6.2. APDL programming to obtain natural frequencies of spherical cell

```
/prep7
!  ---------------     Parameters for shell ------------------
*SET,R,4.5             ! Cell membrane Radius
*SET,Tk,0.1          !cell membrane thickness
*SET,Ro,1000e-18     !cell membrane density
*SET,ya,0.6          !cell membrane Young Modulus
*SET,Nu,0.4999       !cell membrane thickness
*SET,stiff,1
! ------------------------------------------------------------
Et,1,SHELL41
r,1,Tk
mp,ex,1,ya
mp,prxy,1,Nu
mp,dens,1,Ro

CSYS,2
k,12,R,0,0
k,13,R,90,0
k,14,R,0,-90
k,16,R,-90,0
k,18,R,-180,0
k,19,R,0,90
a,19,18,14,13
a,19,13,14,12
a,19,12,14,16
csys,0
arsym,z-z,3,,,,0,0
aglue,1,2,3,4
amesh,all

!  --------------------Parameters for cytoplasm -----------
*SET,R,4.5             ! cytoplasm Radius
```

```
*SET,Po,1000e-18     ! cytoplasm density
*SET,mo,0.0004       ! Elastic moduli
*SET,poi,0.4999      ! Poisson's ratio
!  ------------------------------------------------------------
CSYS,2
Et,2,187
mp,ex,2,mo
mp,prxy,2,poi
mp,dens,2,Po
SPH4,0,0,,R
mshape,1
vmesh,1
EREFINE,all,,1
EREFINE,all,,1

FLST,5,4,5,ORDE,3
FITEM,5,1
FITEM,5,-3
FITEM,5,5
ASEL,S, , ,P51X
ESLA,R
EPLOT
NSLE,R
NPLOT
csys,0
NSEL,R,LOC,Z,4.49999999999
NPLOT
FINISH
/AUTO,1
/REP,FAST
/AUTO,1
/REP,FAST
/SOLU
FINISH
/POST1
FINISH
/SOL
FLST,2,9,1,ORDE,9
FITEM,2,1
FITEM,2,3
FITEM,2,2347
FITEM,2,2527
FITEM,2,3060
FITEM,2,3516
FITEM,2,10432
FITEM,2,10502
FITEM,2,10504
!*
/GO
D,P51X, ,0, , , ,ALL, , , , ,
ALLSEL,ALL
GPLOT
/VIEW,1,,1

/ANG,1
/REP,FAST
/ANG,1
```

```
/REP,FAST
FLST,5,4,5,ORDE,3
FITEM,5,1
FITEM,5,-3
FITEM,5,5
ASEL,S, , ,P51X
ESLA,R
NSLE,R
CM,target,NODE
FINISH

/PREP7
/MREP,EPLOT
ALLSEL,ALL
GPLOT
!*
/COM, CONTACT PAIR CREATION - START
CM,_NODECM,NODE
CM,_ELEMCM,ELEM
CM,_KPCM,KP
CM,_LINECM,LINE
CM,_AREACM,AREA
CM,_VOLUCM,VOLU
/GSAV,cwz,gsav,,temp
MP,MU,1,
MAT,1
MP,EMIS,1,7.88860905221e-031
R,3
REAL,3
ET,3,170
ET,4,175
R,3,,,0.6,0.1,0,
RMORE,,,1.0E20,0.0,1.0,
RMORE,0.0,0,1.0,,1.0,0.5
RMORE,0,1.0,1.0,0.0,,1.0
RMORE,10.0
KEYOPT,4,4,0
KEYOPT,4,5,1
KEYOPT,4,7,0
KEYOPT,4,8,0
KEYOPT,4,9,0
KEYOPT,4,10,2
KEYOPT,4,11,0
KEYOPT,4,12,0
KEYOPT,4,2,0
KEYOPT,3,5,0
!--------------------! Generate the target surface --------------------
NSEL,S,,,TARGET
CM,_TARGET,NODE
TYPE,3
ESLN,S,0
ESURF
CMSEL,S,_ELEMCM
!---------------------! Generate the contact surface -----------------
ASEL,S,,,4
ASEL,A,,,6
CM,_CONTACT,AREA
```

```
TYPE,4
NSLA,S,1
ESLN,S,0
ESURF
*SET,_REALID,3
ALLSEL
ESEL,ALL
ESEL,S,TYPE,,3
ESEL,A,TYPE,,4
ESEL,R,REAL,,3
/PSYMB,ESYS,1
/PNUM,TYPE,1
/NUM,1
EPLOT
ESEL,ALL
ESEL,S,TYPE,,3
ESEL,A,TYPE,,4
ESEL,R,REAL,,3
CMSEL,A,_NODECM
CMDEL,_NODECM
CMSEL,A,_ELEMCM
CMDEL,_ELEMCM
CMSEL,S,_KPCM
CMDEL,_KPCM
CMSEL,S,_LINECM
CMDEL,_LINECM
CMSEL,S,_AREACM
CMDEL,_AREACM
CMSEL,S,_VOLUCM
CMDEL,_VOLUCM
/GRES,cwz,gsav
CMDEL,_TARGET
CMDEL,_CONTACT
/COM, CONTACT PAIR CREATION - END
/MREP,EPLOT

ANTYPE,2
MODOPT,lanb,10,0,10000000
LUMPM,off
Mxpand,10
finish
/solu
solve
finish

/POST1
SET,LIST
```

AII.6.3. APDL programming to obtain natural frequencies of scaled up model of cell (fluid filled specimen with radius of 29 *mm)*.

```
/prep7
!  ---------------      Parameters for outer sphere  ------------------
*SET,R,0.029           ! Outer sphere Radius
*SET,Tk,80e-6          ! Outer sphere thickness
*SET,Ro,1818           ! Outer sphere density
*SET,Ya,1.9e6            ! Outer sphere Young Modulus
*SET,Nu,0.45           ! Poisson's ratio
*SET,stiff,1
! ------------------------------------------------------------
Et,1,SHELL41
r,1,Tk
mp,ex,1,Ya
mp,prxy,1,Nu
mp,dens,1,Ro
CSYS,2
k,12,R,0,0
k,13,R,90,0
k,14,R,0,-90
k,16,R,-90,0
k,18,R,-180,0
k,19,R,0,90
a,19,18,14,13
a,19,13,14,12
a,19,12,14,16
csys,0
arsym,z-z,3,,,,0,0
aglue,1,2,3,4
amesh,all
!AREFINE,all,,1
!  --------------------Parameters for inner sphere--------- -----------
*SET,R,0.029           ! Inner sphere Radius
*SET,Po,970            ! Inner sphere density
*SET,mo,400            ! Elastic moduli
*SET,poi,0.4999        ! Poisson's ratio
!  ---------------------------------------------------------
CSYS,2
Et,2,187
mp,ex,2,mo
mp,prxy,2,poi
mp,dens,2,Po
SPH4,0,0,,R
mshape,1
vmesh,1
EREFINE,all,,1
EREFINE,all,,1

FLST,5,4,5,ORDE,3
FITEM,5,1
FITEM,5,-3
```

```
FITEM,5,5
ASEL,S, , ,P51X
ESLA,R
EPLOT
NSLE,R
NPLOT
csys,0
NSEL,R,LOC,Z,0.026
NPLOT
FINISH
/SOL
FLST,2,17,1,ORDE,17
FITEM,2,537
FITEM,2,1763
FITEM,2,2356
FITEM,2,2383
FITEM,2,2419
FITEM,2,2686
FITEM,2,2953
FITEM,2,2983
FITEM,2,3312
FITEM,2,3443
FITEM,2,3446
FITEM,2,3768
FITEM,2,3899
FITEM,2,3902
FITEM,2,10186
FITEM,2,10245
FITEM,2,-10246
!*
/GO
D,P51X, ,0, , , ,ALL, , , , ,
ALLSEL,ALL
GPLOT
/VIEW,1,,1

/ANG,1
/REP,FAST
FLST,5,4,5,ORDE,3
FITEM,5,1
FITEM,5,-3
FITEM,5,5
ASEL,S, , ,P51X
ESLA,R
NSLE,R
CM,target,NODE
FINISH
/PREP7
/MREP,EPLOT
ALLSEL,ALL
GPLOT
!*
/COM, CONTACT PAIR CREATION - START
CM,_NODECM,NODE
CM,_ELEMCM,ELEM
CM,_KPCM,KP
CM,_LINECM,LINE
```

```
CM,_AREACM,AREA
CM,_VOLUCM,VOLU
/GSAV,cwz,gsav,,temp
MP,MU,1,
MAT,1
MP,EMIS,1,7.88860905221e-031
R,3
REAL,3
ET,3,170
ET,4,175
R,3,,,2e6,0.1,0,
RMORE,,,1.0E20,0.0,1.0,
RMORE,0.0,0,1.0,,1.0,0.5
RMORE,0,1.0,1.0,0.0,,1.0
RMORE,10.0
KEYOPT,4,4,0
KEYOPT,4,5,1
KEYOPT,4,7,0
KEYOPT,4,8,0
KEYOPT,4,9,0
KEYOPT,4,10,2
KEYOPT,4,11,0
KEYOPT,4,12,0
KEYOPT,4,2,0
KEYOPT,3,5,0
!--------------------! Generate the target surface  -------------------
NSEL,S,,,TARGET
CM,_TARGET,NODE
TYPE,3
ESLN,S,0
ESURF
CMSEL,S,_ELEMCM
!--------------------! Generate the contact surface -------------------
ASEL,S,,,4
ASEL,A,,,6
CM,_CONTACT,AREA
TYPE,4
NSLA,S,1
ESLN,S,0
ESURF
*SET,_REALID,3
ALLSEL
ESEL,ALL
ESEL,S,TYPE,,3
ESEL,A,TYPE,,4
ESEL,R,REAL,,3
/PSYMB,ESYS,1
/PNUM,TYPE,1
/NUM,1
EPLOT
ESEL,ALL
ESEL,S,TYPE,,3
ESEL,A,TYPE,,4
ESEL,R,REAL,,3
CMSEL,A,_NODECM
CMDEL,_NODECM
CMSEL,A,_ELEMCM
```

```
CMDEL,_ELEMCM
CMSEL,S,_KPCM
CMDEL,_KPCM
CMSEL,S,_LINECM
CMDEL,_LINECM
CMSEL,S,_AREACM
CMDEL,_AREACM
CMSEL,S,_VOLUCM
CMDEL,_VOLUCM
/GRES,cwz,gsav
CMDEL,_TARGET
CMDEL,_CONTACT
/COM, CONTACT PAIR CREATION - END
/MREP,EPLOT
ANTYPE,2
MODOPT,lanb,10,0,10000000
LUMPM,off
Mxpand,10
finish
/solu
solve
finish
```

Appendix III - Experimental work for measuring natural frequency of specimens

To find out the effect of the boundary condition on the natural frequencies the experimental analysis is performed the same specimens but with different boundary condition. Figure III.1 shows the high flexible stand for the scaled up model of cell.

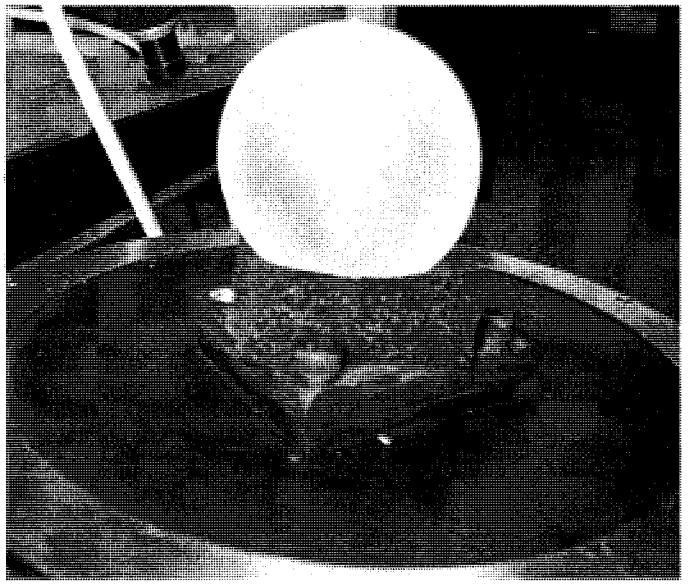

Figure III.1 -- Fluid filled scaled up model of cell and boundary condition.

The complete experimental set up with all the electronic components and is the same setup that is described in section 5.1.1.

The specimens are placed on the flexible stand on the shaker. Figure III.2 shows the corresponding natural frequencies of the specimen filled with water. The radius of the specimen is 29 *mm.*

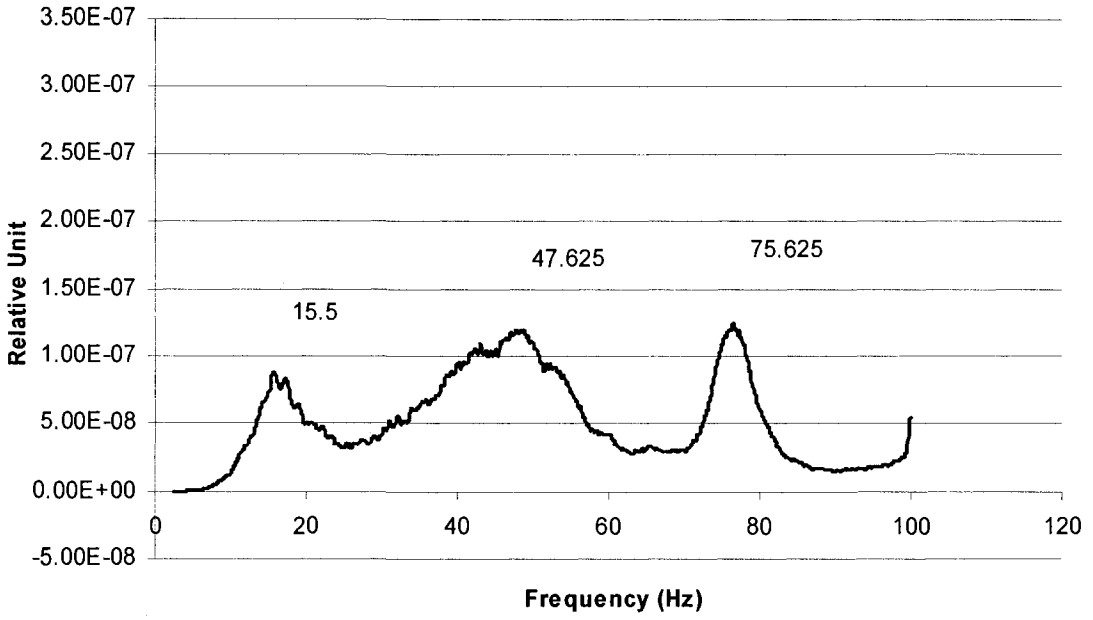

Figure III.2 -- Natural frequencies detected from top of the radius of 29 *mm* specimen filled with water

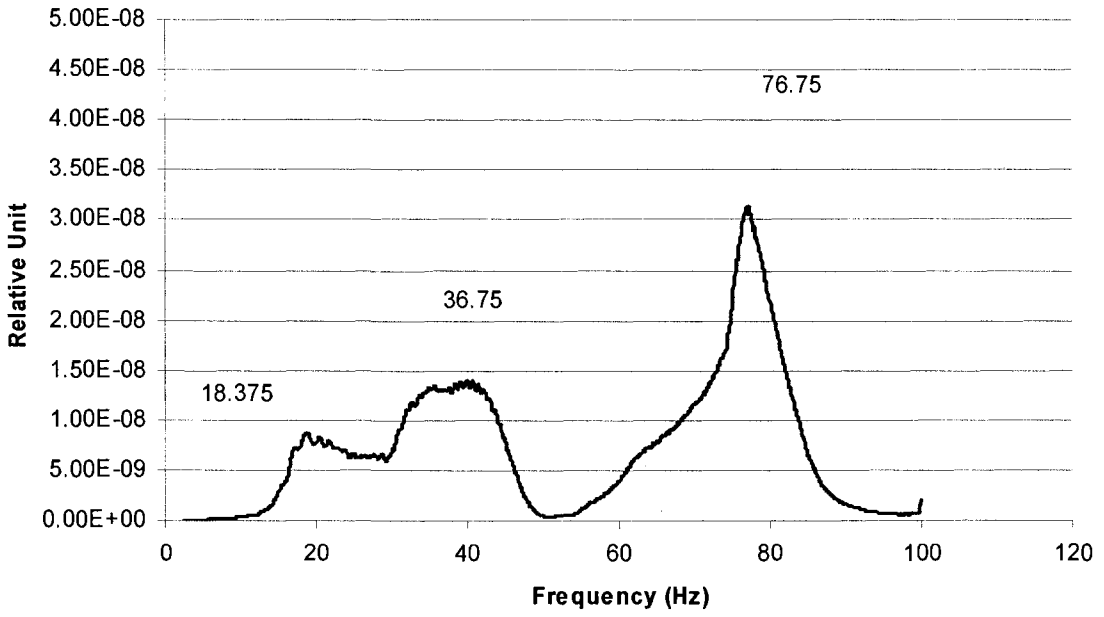

Figure III.3 -- Natural frequencies detected from side of the radius of 29 *mm* specimen filled with water

Figures III.4 and III.5 show the natural frequencies obtained for the samples with diameter 37 *mm*.

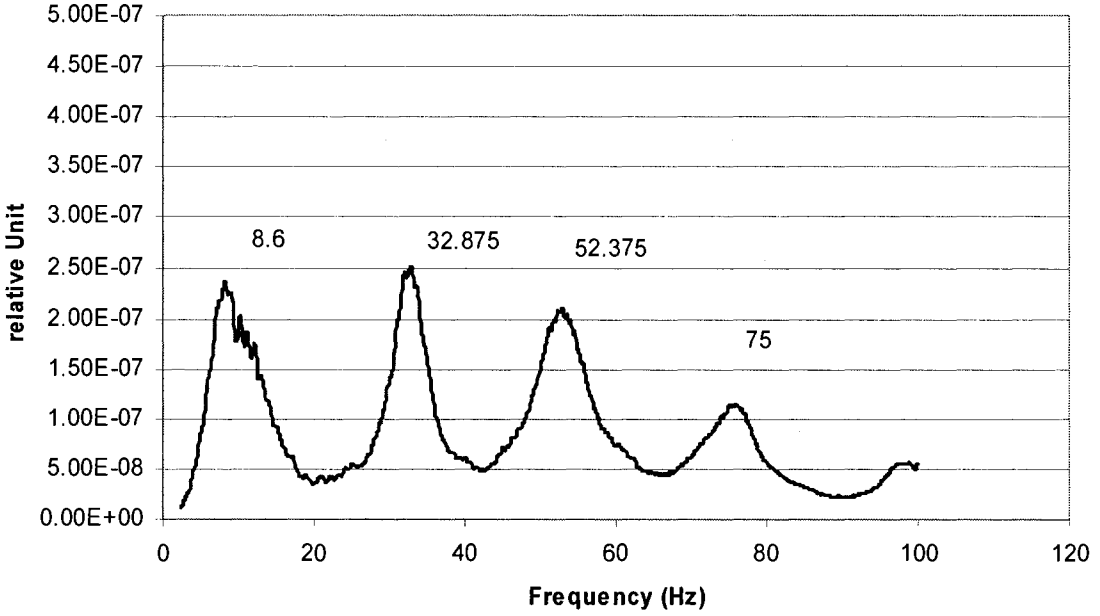

Figure III.3 -- Natural frequencies detected from top of the radius of 37 *mm* specimen filled with water

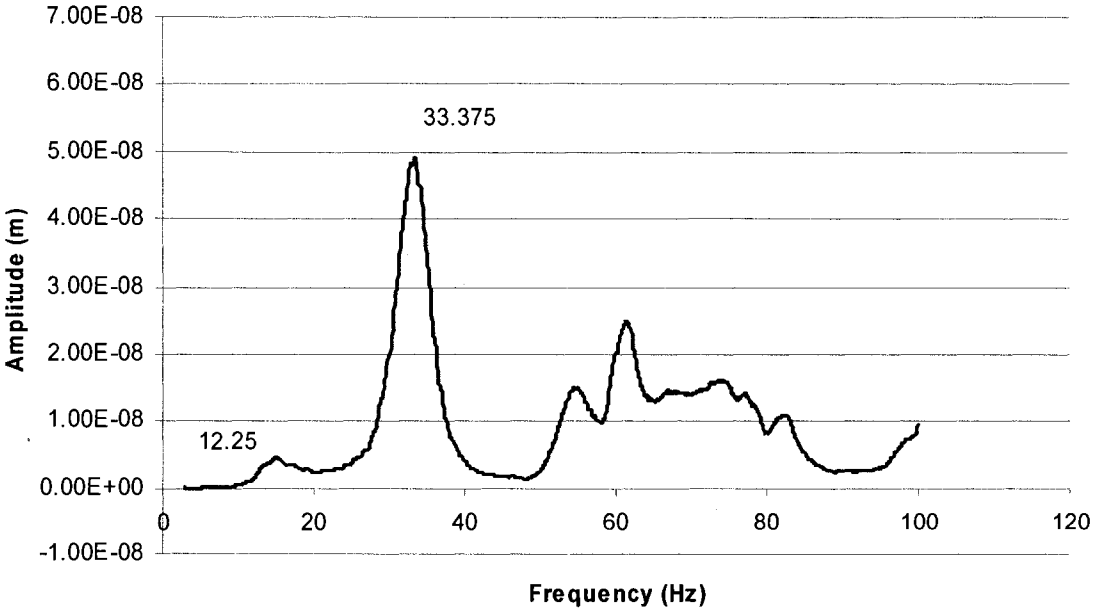

Figure III.4 -- Natural frequencies detected from side of the radius of 37 *mm* specimen filled with water

The last sample that is filled with water has the diameter of 44 *mm*. Figure III.5 and III.6 shows the corresponding natural frequencies.

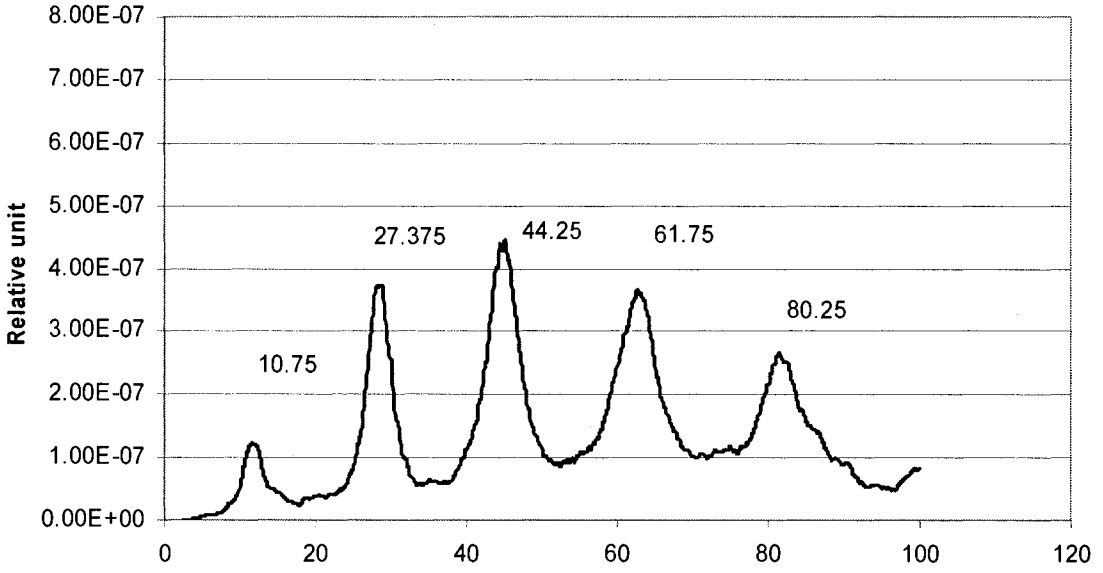

Figure III.5 -- Natural frequencies detected from top of the radius of 44 *mm* specimen filled with water

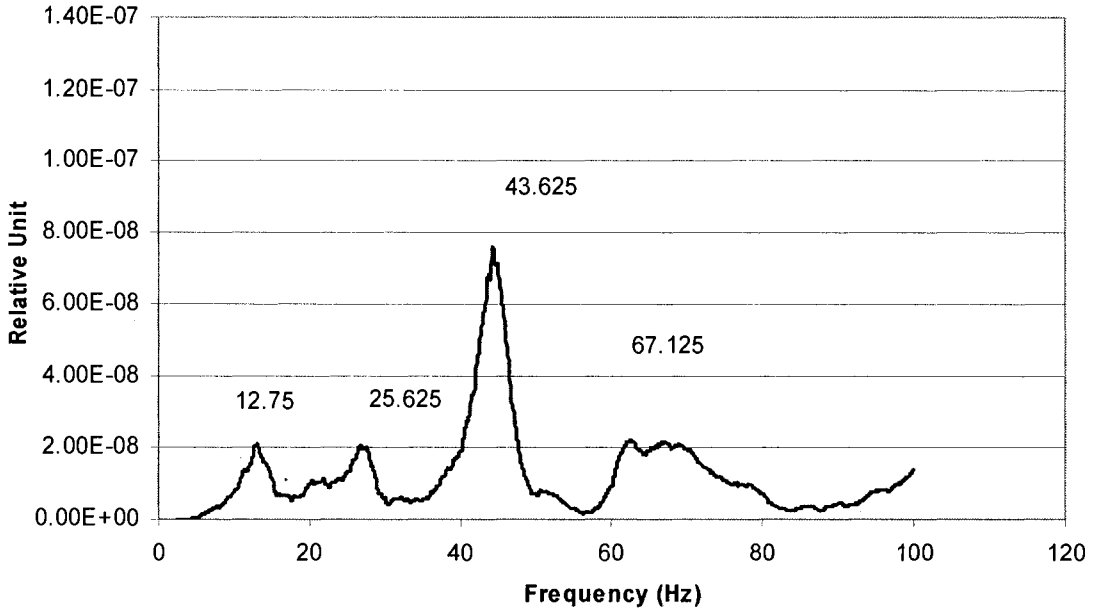

Figure III.6 -- Natural frequencies detected from top of the radius of 44 *mm* specimen filled with water

Effects of the inner sphere on the natural frequency of physical system are found by locating a fluid filled sphere inside a sphere filled with water. To determine the effect of boundary condition on this model, Figure III.7 and III.8 give values of the frequency shifts associated with inner sphere.

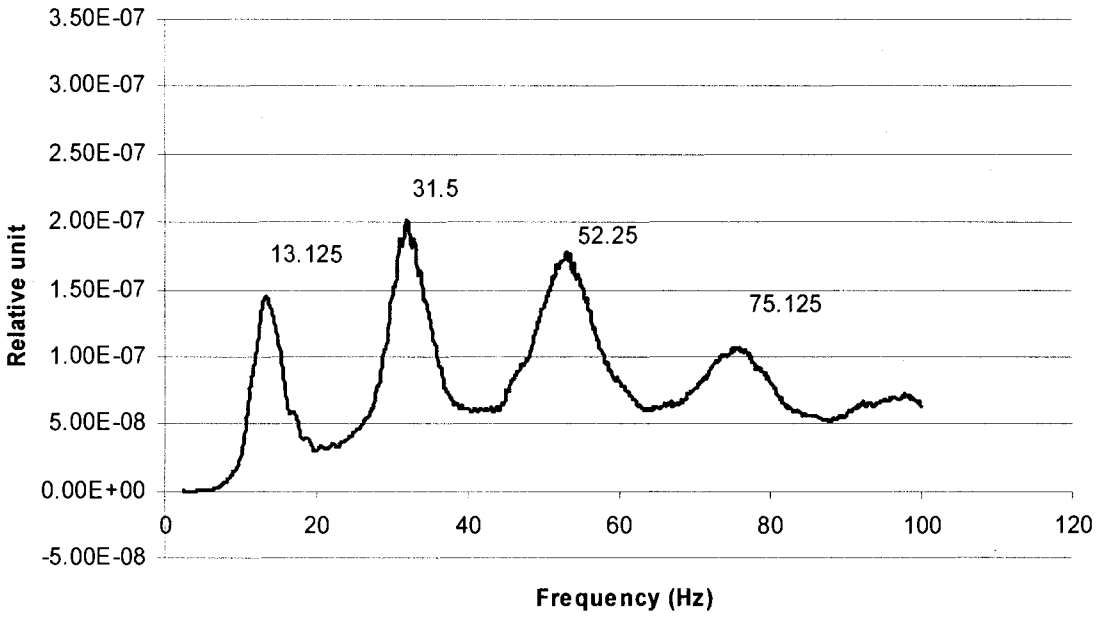

Figure III.7 -- Natural frequencies detected from top of the radius of 37 *mm* specimen filled with water containing inner sphere

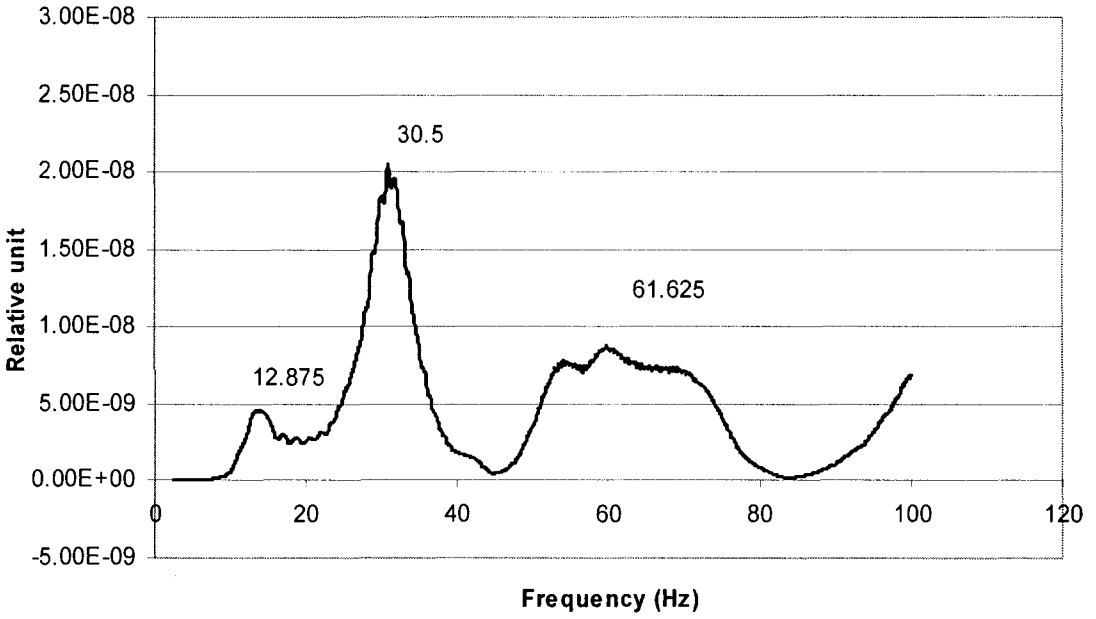

Figure III.8 -- Natural frequencies detected from top of the radius of 37 *mm* specimen filled with water containing inner sphere